UNIVERSIDADE DE LISBOA
FACULDADE DE CIÊNCIAS
DEPARTAMENTO DE BIOLOGIA ANIMAL

Understanding the Gene Regulatory Networks Involved in Sensory Hair Cell Differentiation: How Gfi1 Modulates Cell Differentiation

Catarina Romão Galego

Mestrado em Biologia Evolutiva e do Desenvolvimento

Dissertação orientada por:
Dr Sally Lowell
Professora Solveig Thorsteinsdottir

2019

ACKNOWLEDGEMENTS

I want to express my gratitude to Dr Sally Lowell for the opportunity and guidance through the whole period I developed the project presented here, especially for the patience and time with me during the writing phase. Without the confidence that she put on me, I would not have had the performance that I did. Thank you for letting me to work with you and for all the positive feedback.

Lowell's laboratory group was a key factor in everything that happened in the making of this project. I want to thank Guillaume Blin, Mattias Malaguti, Rosa Portero Migueles, Karolina Punovuori, Darren Wisniewski, Chandrika Rao and Julia Watson for welcoming me as a peer and for all the experiment discussions that also guided me during this process and for helping me a lot with practical situations. I am grateful I took part in the processes involved in the lineage decisions of pluripotent cells projects. A special thanks to Guillaume and his unique sense of humor and wisdom, and to Rosa and her companionship. Thank you for the friendship and all the teaching, motivation and cake sharing. I cannot forget all the supervision made by Aida Costa that introduced the project to me and taught me everything so I could be independent in the laboratory. I also want to thank to those in the MRC Centre for Regenerative Medicine who helped me in times of crisis with technical situations, always with a smile, making me feel part of the family.

Last but not least I want to express my gratitude to my friends and family. I am grateful for all the effort of my family so I could have lived the opportunity of realizing my MSc project in Edinburgh, that added so much to my life. Finally, without any particular order, I especially want to thank to those friends I cannot get rid of and insist of pushing me forward every day.

To the Parkside Terrace OG's, together we shared all the experience of taking a master degree abroad. Matteo, I will miss all your life stories that could have been told in five minutes, and yet you could talk for an all evening. I will always cherish that. Telma and Livia, thank you for all the garlic bread, burger, brownies, pizza, fries, wine and cheese and bossy nights and Arthur's seat singing evenings. To my Grace, you witnessed all my highs and lows and for that I cannot love you more. I am sure you will continue to succeed and buy us our house by the beach where we will sing 'Da Weasel' and maybe have our business. I am also grateful that you shared with me all your highs and lows. To my serotonin impersonated into an ukulele sister "such is the way of the world, you can never know just where to put all your faith and how will it grow. Gonna rise up, burning black holes in dark memories. Gonna rise up, turning mistakes into gold". I will always be there for you!

I cannot think about my master course without thinking of you, Zé and Mira. Thank you for all the hours shared of talks, non-talks, study and lab sessions or just your company. Bernardo, I did not share this journey with you, but I did not forget your companionship and your support, especially to put up with these two. You three are by far among the most intelligent and genuine people I know. Never change!

To Lullu and Fotone, your companionship is something I will take for the rest of my life. Grazie mille, cucciolotto!

Miguel, Ana and Sara, you have been with me since our adventure in Lisbon began, back in 2012. I have no words for our bond. It is beyond places, personalities or interests. I am at home with you.

To Inês and Maria, you are my family! I would not change our time spent together for nothing. Our friendship will never perish.

These acknowledgements would definitely not be written without these people present in my life.

"Knowledge speaks, but wisdom listens".

RESUMO

O ouvido interno pode dividir-se em duas partes distintas: o sistema vestibular, responsável pela detecção do movimento e posição, e o sistema auditivo, responsável pela audição. Um dos aspetos mais importantes do ouvido interno é a existência de um padrão celular tipo "tabuleiro de xadrez" nos seus epitélios sensoriais compostos por células ciliadas, no estrato apical, rodeadas basal e lateralmente por células de suporte. As células ciliadas são os mecanorrecetores primários dos nossos sentidos de audição e de equilíbrio, nos vertebrados, transformando os estímulos vibratórios em impulsos elétricos que são transmitidos ao cérebro.

No sistema auditivo encontra-se apenas um epitélio sensorial, o órgão de Corti, com uma estrutura celular altamente organizada e precisa, responsável pela capacidade da cóclea detetar e distinguir sons. No entanto, estas células são facilmente destruídas e não existe um mecanismo de regeneração espontâneo em mamíferos, ao contrário de outros vertebrados não-mamíferos. A destruição das células ciliadas é um processo frequente e irreversível que conduz a uma perda de audição definitiva.

A perda de audição afecta milhões de pessoas em todo o mundo e é principalmente causada pela perda das células sensoriais ciliadas do ouvido interno. Apesar de no período da infância a medicina regenerativa oferecer soluções terapêuticas para a maioria das perdas de audição, os outros casos ficam limitados ao uso de aparelhos prostéticos que apresentam uma ajuda insuficiente. Sendo que se estima que a perda de audição venha a aumentar devido à poluição sonora e envelhecimento da população, é crescente a necessidade do desenvolvimento de terapias que promovam a regeneração das células ciliadas.

Para induzir a regeneração destas células temos que, primeiro, compreender os mecanismos moleculares que regulam a sua diferenciação. Atoh1 é a molécula que tem recebido mais atenção devido à sua capacidade de converter células do ouvido interno não-especializadas em células sensoriais ciliadas. Contudo, a capacidade regenerativa da célula, conferida pela expressão do Atoh1, é ineficaz em cócleas mais envelhecidas/adultas. Investigações recentes permitiram identificar outros factores de transcrição fundamentais para o desenvolvimento destas células. Um dos factores de transcrição é o Gfi1, que parece desempenhar um papel importante na capacidade do Atoh1 promover o desenvolvimento de células ciliadas. Na sua ausência, Atoh1 é determinante para um destino celular neuronal. Para além do Atoh1, Gfi1 também revelou ser decisivo para que o factor de transcrição Pou4f3 mude a sua actividade de determinante para uma diferenciação neuronal para determinante para uma diferenciação em células sensoriais ciliadas. O Gfi1 parece funcionar como um "interruptor" que ativa o programa de diferenciação das células ciliadas.

Nesta tese, exploramos o papel central que o Gfi1 desempenha na modelação da atividade dos outros dois fatores de transcrição, Atoh1 e Pou4f3, e sugerimos que o faz, possivelmente, de duas maneiras distintas: através da repressão da diferenciação neuronal induzida pelo Atoh1 e Pou4f3, e pela promoção da alteração na especificidade do Atoh1 e Pou4f3, permitindo que estes fatores ativem os genes específicos para a diferenciação das células sensoriais ciliadas. Mas, é desconhecido o mecanismo pelo qual o Gfi1 controla este processo.

Neste projeto, foi pretendido identificar os mecanismos pelos quais o Gfi1 altera a função do Atoh1 e Pou4f3. Para tal, foi estudada a importância da ligação do Gfi1 com o ADN ou com fatores de transcrição, como o Atoh1 e Pou4f3 e/ou outros co-fatores, cujo recrutamento seja mediado por diferentes regiões do Gfi1. Para tal, foi usada uma nova estratégia *in vitro* desenvolvida por Aida Costa para a produção de células ciliadas. Esta estratégia envolve a expressão da combinação dos três fatores de transcrição Gfi1-Pou4f3-Atoh1, para programar os progenitores em diferenciação (derivados das células estaminais embrionárias) diretamente em células ciliadas. A ativação conjunta destes fatores *in vitro* mostrou resultar numa indução de células ciliadas, que expressam marcadores específicos e apresentam estruturas morfologicamente semelhantes aos estereocílios mecanorrecetores.

A caracterização *in vitro* das células ciliadas induzidas foi feita a nível transcricional e morfológico, usando três linhas celulares da combinação dos três factores de transcrição, com variações do Gfi1 em diferentes domínios: 1) Gfi1 sem o domínio "zinc finger" que permite a ligação directa com o ADN; 2) Gfi1 com uma mutação no domínio "SNAG" que destrói a sua capacidade repressora; 3) substituição do Gfi1 pelo Gfi1b, que diferem na região intermédia, entre os dois domínios.

Esta caracterização foi feita recorrendo a imuno-citoquímica nas amostras das linhas transgénicas e PCR quantitativo em tempo real, para detetar a expressão de marcadores das células ciliadas e/ou marcadores neuronais. A análise da expressão foi feita comparando as amostras com a linha transgénica contendo um Gfi1 intacto (linha selvagem). De um modo geral, verificou-se que é preciso um Gfi1 intacto para que os marcadores de células ciliadas sejam expressos tal como na linha selvagem.

Para aprofundar a nossa investigação, recorremos à funcionalidade do Gfi1 como repressor. O Gfi1 é conhecido por atuar noutros tipos celulares através da interação com proteínas reguladoras da cromatina. Estudos hematopoiéticos mostram que o recrutamento de um complexo LSD1/CoRest/HDACs1-2, pelo domínio SNAG, é essencial para um fenótipo selvagem. Da mesma forma, estudos no laboratório de Sally Lowel revelaram que impedindo a ligação do domínio LSD1, impossibilita a atividade do Gfi1 necessária para induzir a diferenciação de células ciliadas, no sistema usado neste projecto. O recrutamento deste complexo pode ser o mecanismo principal (ou pelo menos um dos mecanismos chave) pelo qual determina a diferenciação de células ciliadas.

Usando o mesmo método de análise, foram usados químicos para inibir a função dos domínios LSD1 e HDACs, na linha transgénica selvagem. De um modo geral, observou-se que quanto maior a concentração de inibidor, menor era a expressão de marcadores de células ciliadas. Excepções foram observadas, principalmente nos marcadores específicos para os estereocílios, o que acentua a complexidade dos mecanismos responsáveis por este processo.

Estas experiências tiveram um carácter preliminar, mas que permitem identificar os vários desafios a ultrapassar, bem como para o delineamento de futuras experiências, a fim de identificar os eventos-chave da diferenciação regulada pelo Gfi1.

Em suma, a caracterização da expressão dos marcadores de células ciliadas/ neuronais, utilizando o nosso sistema de linhas transgénicas, é uma abordagem viável para a investigação do

mecanismo de diferenciação das células sensoriais do ouvido interno. Acreditamos que este estudo contribuiu para a aquisição de conhecimentos sobre os processos que possam estar envolvidos no desenvolvimento de células ciliadas.

Palavras-chave: Gfi1; células sensoriais ciliadas; ouvido interno; regeneração; células estaminais embrionárias.

ABSTRACT

In the inner ear, mechanosensory hair cells are the primary receptors of our hearing senses, localized in the auditory system, and balance, in the vestibular system. Damage or loss of hair cells is the leading cause of deafness. Unfortunately, these cells are easily destroyed and spontaneous hair cell regeneration does not occur in mammals (unlike non-mammalian vertebrates) and there is no treatment for their regeneration.

To unlock hair cell regeneration capacity, we first need to gain a deeper understanding of the molecules that control hair cell generation. Gfi1, Atoh1 and Pou4f3 are key transcription factors of the gene regulatory network, driving hair cell fate specification. Gfi1 is a vital player of this network by playing, possibly, two distinct roles: 1) Gfi1 represses neuronal differentiation induced by Atoh1 and Pou4f3; 2) Gfi1 promotes a transcriptional switch for Atoh1 and Pou4f3 allowing them to activate hair cell genes.

The main goal is to identify how Gfi1 influences these transcription factors, whether by binding to DNA or by recruiting other co-factors through the SNAG domain and/or through the intermediary region. To test these, induced hair cells *in vitro* were characterized using variants of Gfi1 knock-in lines (a combination of Gfi1-Atoh1-Pou4f3) that 1) lack the DNA binding domain, 2) have a mutation that enables SNAG domain activity and 3) the Gfi1 intermediary region was replaced. Furthermore, we focused on the recruitment of the epigenetic complex LSD1/CoRest/HDACs1-2 by the SNAG domain that enables Gfi1 to act as a transcription repressor, as a key mechanism for hair cells fate determinant. Chemical inhibitors of the LSD1 and HDACs domains were administered on the wild type cell line (with an intact Gfi1).

The characterization was done by detecting hair cell and neuronal markers, by immunocytochemistry and qPCR. Our analysis identified that an intact Gfi1 is required for a proper hair cell program. Similarly, the inhibition of the epigenetic complex lead to hair cell differentiation impairments.

The characterization and analysis of the selected Gfi1 cell lines allowed us to examine the molecular mechanisms by which Gfi1 modulates hair cell formation. In addition, it provides tools for the delineation of further experiments at determining the function of these and other co-factors during inner ear development.

Keywords: Gfi1; sensory hair cells; inner ear; regeneration; embryonic stem cells.

INDEX

LIST OF FIGURES

LIST OF TABLES

ABBREVIATIONS LIST

Atoh1 – atonal homolog 1

bHLH – Basic helix-loop-helix

BrdU - Bromodeoxyudirine

C-terminus – Carboxyl-terminus

Casp3 – Caspase 3

Cdh23 – Cadherin 23

cDNA – Complementary deoxyribonucleic acid

ChIP – Chromatin immunoprecipitation

CIP/KIP – CDK interacting protein/Kinase inhibitory protein

cm – Centimeters

Co-IP – Co-immunoprecipitation

CO_2 – Carbon dioxide

CoRest – Corepressor of RE1 silencing transcription factor

Ct – Cycle quantification value

DAPI – 4',6-diamidino-2-phenylindol

Dcx – Doublecortin

DMEM – Dulbecco's modified Eagle's medium

DMSO – Dimethyl sulfoxide

DNA – Deoxyribonucleic acid

DNase – Deoxyribonuclease

dNTP – Deoxynucleotide triphosphate

Dox – Doxycycline

DTT – 1,4-Dithiothreitol

EBs – Embryoid bodies

EDTA – Ethylenediaminetetraacetic acid

ES cells – Embryonic stem cells

Espn – Espin

F – Forward strand

FACS – Fluorescence-activated cell sorting

FBS – Fetal bovine serum

FCS – Fetal calf serum

FDS – Fetal donkey serum

g – Relative centrifugal force, given as acceleration of gravity

Gfi1 – Growth factor independent 1

Gfi1b – Growth factor independent 1B

Gfi1DZF6 – Gfi1 lacking the zinc finger domain

Gfi1P2A – Gfi1 with a mutation proline to alanine at amino acid 2

GFP – Green fluorescent protein

GFP+ – Green fluorescent protein positive

Gl – Glutamine

GMEM – Glasgow minimum essential medium

GPA – Gfi1-Pou4f3-Atoh1 transcription factors combination

GPS – Gfi1/PAG-3/SENS family of zinc finger transcription factors

Gy – Gamma irradiation

h - Hours

H3-K4 – Lysine 4 residues on histone 3

H3-K9 – Lysine 9 residues on histone 3

HC – Hair cell

HDACi – Histone deacetylase inhibitor

HDACs – Histone deacetylases

ICC – Immunocytochemistry

iMEFs – inactivated mouse embryonic fibroblasts

Lhx3 – LIM homeobox 3

LIF – Leukemia inhibitor factor

LSD1 – Lysine-specific histone demethylase 1

LSD1i – Lysine-specific histone demethylase 1 inhibitor

MEFs – Mouse embryonic fibroblasts

mg – Milligram

mL – Milliliter

mm – Millimeter

mM – Millimolar

min – Minutes

mRNA – Messenger RNA

Myo6 – Myosin VI

Myo7a – Myosin VIIa

N-terminus – Amino-terminus

ng – Nanogram

ºC – Degree Celsius

Otof – Otoferlin

P/S – Penicillin/Streptomycin

PBS – Phosphate buffered saline

PFA – Paraformaldehyde

Pou4f3 – POU class 4 homeobox 3

Pyr – Pyruvate

qPCR – real-time quantitative polymerase chain reaction

R – Reverse strand

RNA – Ribonucleic acid

RNase – Ribonuclease

rpm – Revolutions per minute

RT – Room temperature

s – Seconds

Sdha – Succinate dehydrogenase complex, subunit A

SNAG – SNAIL/Gfi1 proteins family domain

TBST – Tris buffered saline ten solution

TSA – Trichostatin A

Tuj1 – Beta III tubulin

Wt – Wild type

vGFP – Yellow fluorescent protein, mutant of green fluorescent protein

µg – Microgram

µL – Microliters

µM – Micromolar

µm – Micrometers

1. INTRODUCTION

1.1. STRUCTURE AND DEVELOPMENT OF THE MECHANOSENSORY HAIR CELL

In the inner ear, mechanosensory hair cells, supporting cells and nerve endings constitute the sensory epithelia [1]. Mechanosensory hair cells are produced during embryonic development and convert mechanical stimuli in electric signals. They are the primary receptors of our senses of hearing and balance, which display unique physiological characteristics that are not observed in any other cell types. However these cells are easily destroyed by loud noise, therapeutic drugs or during ageing, leading to permanent hearing loss [2].

In vertebrates the auditory system functions by an epithelial sensory receptor, the hair cell (HC), which lacks an axon and is innervated by non-mechanosensory neurons. HCs are located in the ear's vestibular system, for proprioception, and cochlear organ of Corti, for auditory function [3] (***Figure 1.1***). The ability of the cochlea to detect and distinguish sounds depends on the specific organization of its neurosensory epithelium. Given this complexity it is expected that many genes are required for the development of the vertebrate inner ear [4]. The mammalian HCs' mechanotransduction machinery is located in actin-rich extensions, that form the hair bundle, which are modified microvilli called stereocilia (***Figure 1.1***) which have mechanosensitive ion channels, of unknown molecular identity, and are precisely organized to detect sub-nanometer deflections [3, 5, 6]. HCs receive stimuli of different modalities in the form of vibrations or static deformations that stimulate the bending of their hair bundles. HCs respond with a small receptor potential which excite afferent nerve fibers by chemical or electrical synapses [7].

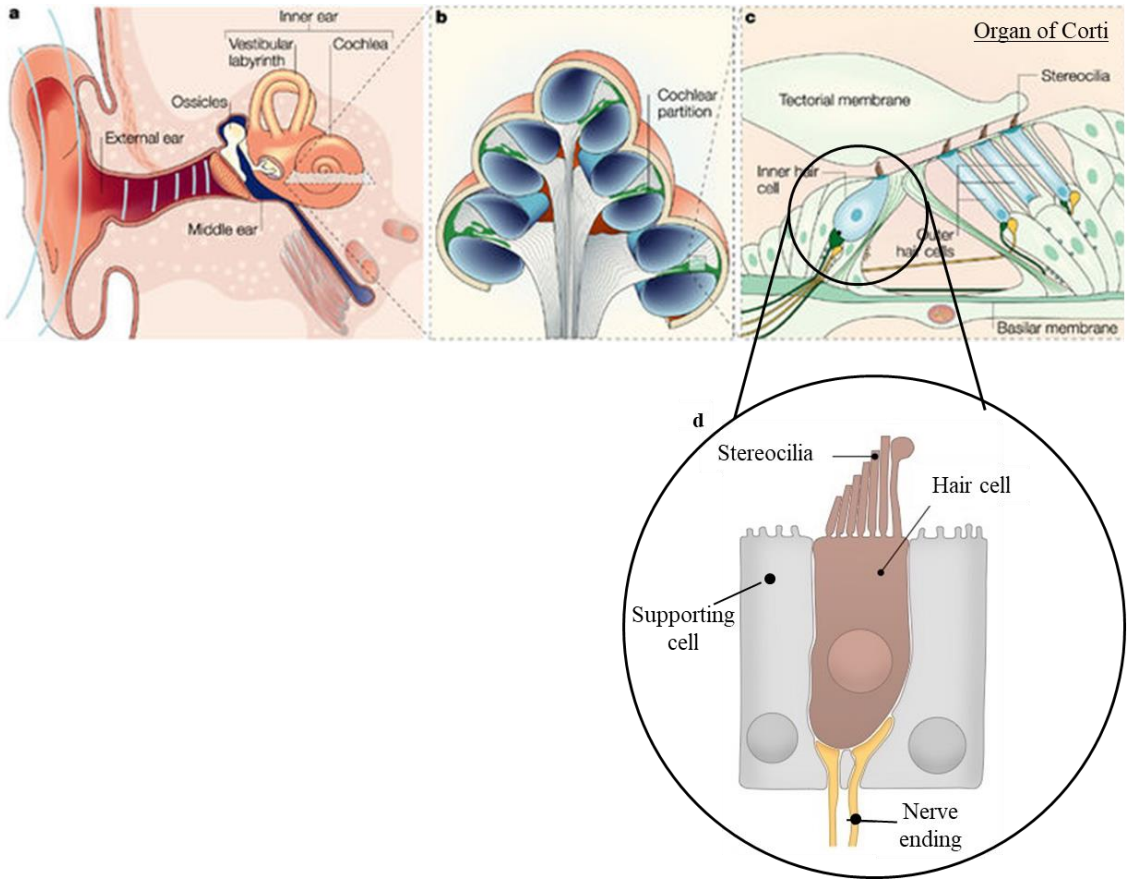

Figure 1.1 - Mammalian ear structure: a) section of external ear and inner ear. The inner ear includes the vestibular and auditory systems; b) section of the cochlea; c) section of a cochlear partition showing the organ of Corti; d) magnification of an inner hair cell. Adapted from Frolenkov et al., 2004.

Stereocilium core contains parallel actin filaments held together by proteins, such as Espin (Espn) [8] and Cadherin-23 (Cdh23) [9]. The filaments are unidirectionally aligned with their barbed end, which is the high-affinity actin polymerization site, and oriented away from the surface of the cell [10]. Studies show that the actin filaments terminate at the base of the stereocilia and only some extend into the body of the cell, predisposing the stereocilium to bend at the base and not at a higher position [11]. To maintain this, a tight control of actin polymerization and depolymerization is required. Myosin VI (Myo6) is located at the base of the hair bundle. It has an actin-binding site and is thought to provide mechanical stability to the apex of the HC [12]. Myosin VIIa (Myo7a) is another protein that interacts with actin, involves in the development and maintenance of the stereocilia [13]. The stereocilia are arranged by height to form a staircase-like pattern. The bundles are directionally sensitive and a precise orientation is essential for a normal auditory perception: deflections towards the tallest stereocilia open the channels and increase the mechanotransduction current whereas deflections in the opposite direction close the channels and decrease the current [14, 15].

The deflection of HC stereocilia opens mechanically gated ion channels that allow cations, primarily potassium and calcium, to enter the cell. This influx of cations depolarizes the cell, resulting in the receptor potential. Consequently, voltage gated calcium channels open. Calcium ions enter the cell and trigger the release of neurotransmitters (glutamate) at the basal end of the cell and diffuse across the space

between the HC and the nerve terminal, where they bind to receptors triggering action potentials in the nerve. In this way the mechanical signal is converted into electrical signal [16]. Cdh23, besides being required for establishing and/or maintaining the proper organization of the hair bundle, takes part in the functional network, that includes Myo7a, that mediates mechanotransduction in cochlear HCs, due its calcium-dependent cell adhesion nature [17]. Also Otoferlin (Otof) interacts in a calcium-dependent manner to trigger exocytosis of neurotransmitters [18].

Myo7a, Myo6, Otof, Cdh23 and Espn genes are all deafness associated, required for proper function of hearing.

Besides the proteins already mentioned, LIM homeobox 3 (Lhx3) is also associated with HCs of the auditory and vestibular system [2]. Although it is expressed in the nucleus of HCs its role in the inner ear has not been thoroughly described. Studies *in vivo* identified a differential regulation of Lhx3 expression in the two systems suggesting that it might be required for normal hearing [19].

1.2. HEARING IMPAIRMENTS: LIMITED THERAPIES

The mammalian inner ear has a very limited capacity to replace lost or damaged HCs [20]. Hearing loss occurs because the hair bundle bends to the point where it is damaged or by cell death. When a HC develops it inhibits its neighboring cells from differentiating into HCs and instead the neighboring cell becomes a supporting cell. Studies in non-mammalian animals (e.g. birds and fish) show that after damaging HCs, supporting cells can divide and produce progeny that can differentiate as HCs or by transdifferentiation the supporting cells change their phenotype and assume a HC identity [21]. In contrast, spontaneous HC regeneration does not occur in humans or other mammals, and there is no treatment to restore cells. There are hearing aids that amplify sound for less severe damage, and cochlear implants that functions as HCs converting sound into electrical impulses. However these systems offer limited help. Therefore understanding the gene regulatory networks that drive HC development will inform about possible therapeutic routes to HC regeneration to reverse hearing loss.

1.3. HAIR CELL DIFFERENTIATION: FACTORS INVOLVED IN THE MECHANISM AND THE USE OF KNOCK-IN LINES

Atoh1 is a basic helix-loop-helix (bHLH) transcription factor that has received much attention because it has a key role in HC differentiation. *In vivo*, Atoh1 is the only transcription factor known to be necessary and sufficient for HC differentiation [1, 22, 23]. It is known that Atoh1 deletion in mice causes HC loss in all inner ear sensory organs [1, 24], whereas its overexpression promotes the generation of ectopic HCs in the developing ear [23, 25, 26]. Atoh1 is also necessary for the specification of various subsets of neurons [27, 28, 29], intestinal secretory cells [30] and Merkel cells [31], implying that Atoh1 acts in combination with different transcription factors to activate lineage-specific differentiation programs. *In vitro*, the overexpression of Atoh1 alone in stem cells induces neuronal rather that HC differentiation, supporting the idea that Atoh1 must work with other transcription factors in order to determine different cell identities in different contexts. During development, diverse intrinsic and extrinsic signals are integrated to result in a specific combinatorial expression of transcription factor binding in many different cell types [32, 33].

Besides Atoh1, the zinc-finger transcription factor Gfi1 and Pou-domain transcription factor Pou4f3 are the only known transcriptional regulators essential for the proper differentiation and/ or

survival of all vestibular and auditory HCs [34, 35]. The expression of Gfi1 and Pou4f3 is initiated in nascent HCs soon after the onset of Atoh1 upregulation [34, 25]. It is possible that Atoh1 acts in combination with these two transcription factors to induce efficient HC generation.

Growth factor independence 1 (Gfi1) is the vertebrate member of the GPS (Gfi1/PAG-3/SENS) family of zinc finger transcription factors. GPS proteins are characterized by the presence of a zinc finger domain frequently found at their C-terminus and a SNAG transcriptional repressor domain also found in the N-terminus of Snail/Slug zinc finger proteins [36]. The intermediary region is everything in between the C- and N-terminus. In vertebrates, Gfi1 is best known as a major regulator of hematopoiesis, playing a prominent role in the development of the myeloid and lymphoid cell lineages. Here it controls diverse developmental processes, such as cell fate determination, differentiation, proliferation and cell survival [37, 38, 39, 40]. Outside the hematopoiesis system, Gfi1 mRNA has been detected in a wide range of other tissues, but expression of Gfi1 protein seems to be restricted to mechanoreceptor cells, such as HCs and Merkel cells, neurons of the cerebellum and retina, and specialized epithelial cells in the gut and lung. Gfi1 plays a key role in the differentiation or survival of these non-hematopoietic cell types [3].

In my host laboratory, using a mouse embryonic stem cell differentiation *in vitro* system developed by Costa A., 2014 [41], there is evidence that support the hypothesis that Gfi1 is a key factor that interacts with Atoh1 in order to enable an efficient HC differentiation program. In this system the overexpression (induced by doxycycline) of the three transcription factors, Gfi1, Pou4f3 and Atoh1 is able to program HC identity, whereas the overexpression of Atoh1 or Pou4f3 and Atoh1 leads to neuronal differentiation (***Figure 1.2***). These results imply that Gfi1 promotes HC differentiation by repressing neuronal differentiation induced by Atoh1 and Pou4f3 and promoting a switch in the specificity of Atoh1 and Pou4f3 allowing these transcription factors to activate HC genes (unpublished). Gfi1 also allows Atoh1 or Pou4f3 singly to upregulate some HC markers (***Figure 1.2***) like Myo7a, but not others such as Lhx3 and Espn. There is also some *in vivo* evidence that support this hypothesis: Gfi1 knockout mice aberrantly express neuronal markers in their cochlear HCs and exhibit severe morphological defects in all types of HCs [34, 42]. Yet, nothing is known about the mechanism by which Gfi1 represses neuronal identity and promotes HC identity.

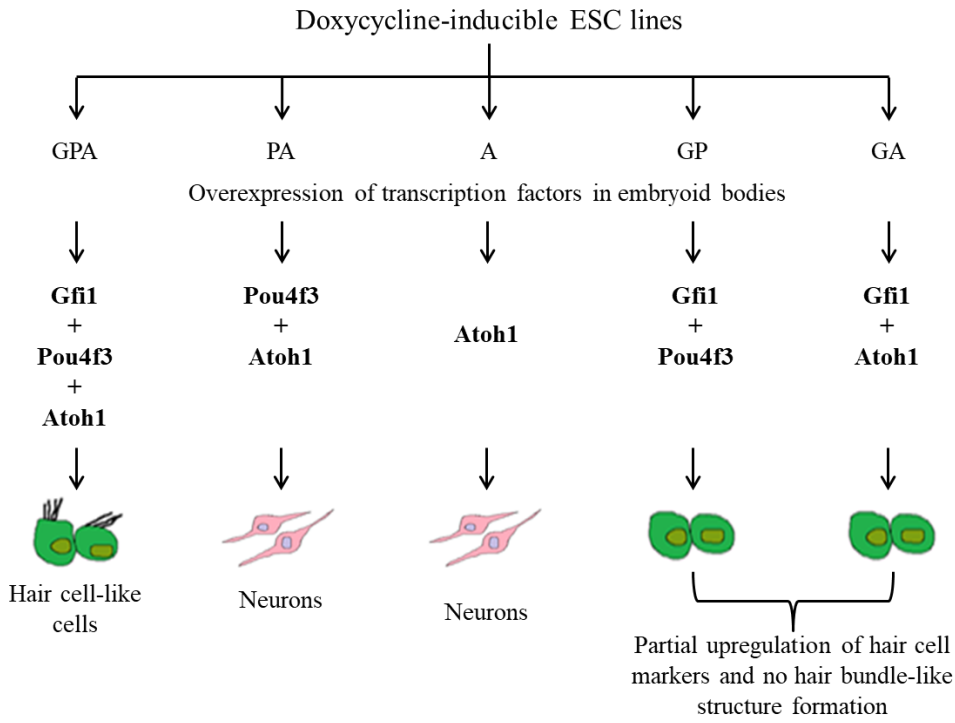

Figure 1.2 - Gfi1 is a key factor in HC differentiation program: results obtained with the *in vitro* system generated by Costa. A, using doxycycline-inducible ESC lines. It shows that the presence of Gfi1 directs the HC differentiation fate (unpublished).

Gfi1 has six zinc fingers and their presence suggests that it functions as a DNA binding transcription factor. Nevertheless, of the six zinc fingers, only the third, fourth and fifth zinc fingers seem to be required for DNA binding [43]. The role of the other zinc fingers remains unclear but it is possible that they may function as protein-protein interaction domains (***Figure 1.3***). Therefore, Gfi1 might act by binding DNA and/or by recruiting co-factors in order to repress neuronal genes, such as Neuron-specific class III beta-tubulin (Tuj1) and Doublecortin (Dcx), or activate HC genes.

Clues from the hematopoietic system tell us that Gfi1 functions as a transcriptional repressor, recruiting a chromatin-regulating complex, LSD1/CoRest/HDACs1-2, that applies repressive epigenetic marks to critical regulatory genes [44]. In mice with a proline to alanine mutation at amino acid 2 in Gfi1's SNAG repressor domain, Gfi1 fails to recruit the epigenetic repressor complex and the mice exhibit a hematopoietic phenotype identical to that of the full Gfi1 knockout [45]. So, an intact SNAG domain is required for the function of Gfi1 as a transcriptional repressor in blood cells. It is plausible that the recruitment of this epigenetic repressor complex might be a mechanism by which Gfi1 causes the repression of neuronal differentiation genes in the inner ear (***Figure 1.3***).

The function of the intermediary region of the protein, which is the part that separates the SNAG domain from the zinc finger is entirely unknown and is also the least conserved part among the vertebrate Gfi1 molecules. Gfi1 and the related transcription factor Gfi1b, also essential in hematopoiesis, share almost no sequence similarity in this region, but their other domains are nearly identical. *In vivo*, Gfi1b knock-in mice in the Gfi1 locus showed that Gfi1b can rescue the hematopoietic defect in Gfi1 null mice, but cannot rescue the defect in cochlear HCs [46]. So, it appears that in the context of HC differentiation program the Gfi1-specific intermediary region is important for function. It is possible that this middle part

of the Gfi1 serves as a specific platform for the interaction with co-factors. This would suggest that although both Gfi1 and Gfi1b can bind to the same DNA target sequence, and repress transcription, each one of them might act in a different molecular context depending on the specific recruitment of partners [37]. For example, it is possible that the intermediary region may recruit a partner that is required for repression of neuronal genes and/or activation of HC genes (***Figure 1.3***).

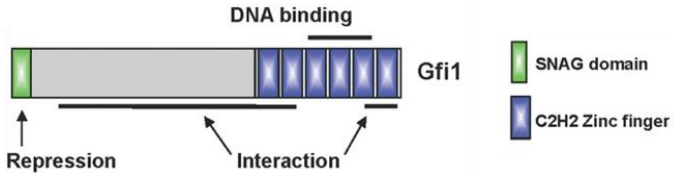

Figure 1.3 - Gfi1 structure: schematic structure of Gfi1 with its domains. Adapted from Möröy et al, 2015.

1.4. THE SNAG DOMAIN: THE IMPORTANCE OF THE RECRUITMENT OF THE LSD1/COREST/HDACS1-2 COMPLEX

Both Gfi1 and Gfi1b have been shown to epigenetically repress critical regulatory genes transcription in the hematopoietic system by recruiting the CoRest complex, mediated by SNAG domain, an essential region of Gfi1 proteins. The epigenetic complex includes the histone demethylase LSD1 and the histone deacetylases HDAC1 and HDAC2. When recruited to target sites, HDACs and LSD1 remove the activating acetylation and methylation marks from histones [44] (***Figure 1.4***). These epigenetic changes are implicate in a diversity of biological functions, such as transformation, differentiation, cell survival and cell death [47, 48, 49, 50]. The LSD1/CoRest/HDACs1-2 core is functionally and structurally conserved across phyla, highlighting the importance of this complex in regulating differentiation throughout evolution [51, 52]. Initiation of HCs development requires a switch in the differentiation program and the recruitment of this complex might be the mechanism behind it.

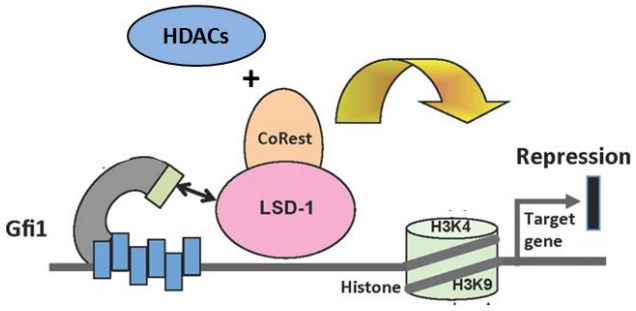

Figure 1.4 - Function of LSD1/CoRest/HDACs1-2 complex: schematic representation of the interaction between Gfi1 and the epigenetic repressor complex when recruited at Gfi1 target genes. Adapted from Möröy et al, 2015.

LSD1 is a histone demethylase that acts in a context-depending manner. It acts as a transcriptional inhibitor if it demethylates lysine 4 residues on histone 3 (H3-K4) or a facilitator of the transcription if it demethylates on lysine 9 (H3-K9) [53, 54]. CoRest is also required for demethylation by LSD1[55], serving as a partner in silencing neuronal genes in non-neuronal tissues and during neuronal differentiation [56]. In addition, histone deacetylase activity is also required, together with CoRest, for LSD1 demethylation both *in vivo* and *in vitro* [57, 55].

HDACs remove acetyl groups promoting chromatin condensation and reduced transcription [58]. Class I HDACs , including HDAC1 and HDAC2, are nuclear proteins expressed in most tissues and cell types, and function as transcriptional repressors [59]. Commonly used HDAC inhibitors, such as trichostatin A, efficiently block all class I HDACs [60].

Studies *in vivo* have demonstrated that downregulation of LSD1 or CoRest perturbs hematopoietic differentiation and LSD1 depletion also activates Gfi1b target genes, accompanied by an increase of H3-K4 methylation at the corresponding promoters. On the other hand, the interactions between Gfi1 and Gfi1b with HDAC were independent of the SNAG domain [55]. Chemical inhibition of LSD1 also reactivates gene transcription [61]. It can attenuate the binding to CoRest increasing H3-K4 methylation [62]. Furthermore, LSD1 inhibitor treatment can inhibit cell proliferation and decrease HC differentiation in zebrafish during development [49, 50]. In the *in vitro* system developed by Costa A., 2014 [41], a form of Gfi1 in which the LSD1-interaction domain was masked abolished the pro-HC activity (unpublished).

Treatment with HDAC inhibitors on cultured cells can lead to a variety of effects, including decreased proliferation and differentiation [63]. Besides, HDACs inhibition results in increased H3-K4 methylation levels whereas LSD1 inhibition does not stop histone deacetylation [61]. Studies in avian HCs *in vitro* and *in vivo* suggest that HDACs have an important role in cell cycle regulation of supporting cells and, thereby, in the regeneration of HCs. However, it does not seem to directly affect HC differentiation [64].

Based on these investigations, we hypothesize that deacetylation by HDACs is likely to be the first step [55] of the transcriptional repression and then LSD1, mediated by CoRest, demethylases on H3-K4, reversibly silencing the locus.

Interfering with any of these events can result in the loss of the repression and ectopic reactivation of neuronal genes [65].

1.5. AIMS OF THIS THESIS

Given the evidence about Gfi1 in HC development, in order to understand the mechanisms behind it, this project aims to identify the main mechanism by which Gfi1 modulates Atoh1 and Pou4f3 activity to orchestrate a HC differentiation program. To accomplish that, we will study the ability of HC differentiation by Gfi1. For that matter we will examine the expression of HC and neuronal markers, using immunocytochemistry and real-time quantitative polymerase chain reaction, in two assays:

1. Characterization of three Gfi1 knock-in cell lines that:
   1.1. Lack the Gfi1 intermediary region by Gfi1b knock-in:
   This cell line will specifically answer if Gfi1 acts through interactions between the intermediary region and co-factors to enable the activation of the HC fate.
   1.2. Lack a functional DNA binding domain:
   This Gfi1 form will answer if DNA binding directly regulates HC genes.
   1.3. Lack a functional SNAG domain:
   The mutation proline to alanine will test if the recruitment of the LSD1/CoRest/HDACs1-2 repressor complex is the mechanism by which Gfi1 alters the differentiation program to HCs.

2. Inhibition of LSD1/CoRest/HDACs1-2 repressor complex's function by chemical inhibition of HDACs1-2 or LSD1 domains:
   Assuming that the recruitment of this complex by SNAG domain is essential for HCs differentiation program, we aim to identify the mechanism by which the repressor complex works in the context of this thesis.

2. MATERIALS AND METHODS

2.1. GFI1 LINES

Given the insufficiency and difficult access to hair cells in the inner ear it is advantageous to use induced HCs in an *in vitro* system. Since it has been shown that the transcriptome is highly similar to that of endogenous HCs (70%) [2], it is possible to produce large numbers of HC-like cells with high reproducibility using simple culture conditions according to the programming strategy employed by Costa A., 2014 [41].

In order to further investigate the acquisition of HCs fate we used several cell lines to show the involvement of Gfi1 on the process of differentiation of HCs. Each inducible cell line contains a combination of the three transcription factors of interest: Gfi1, Pou4f3 and Atoh1; which can directly convert ES-derived progenitors toward HC fate. The four inducible Gfi1 lines were previously generated in S. Lowell's laboratory according to the inducible cassette exchange recombination system generated in *Iacovino et al.,* 2011[66] and 2014[67]. The inducible cassette exchange locus encodes a doxycycline-inducible floxed Cre, which replaces itself with the incoming gene of interest. The derivative cell lines thus bear doxycycline-inducible transgenes (***Table 2.1***).

Table 2.1 – Gfi1 knock-in lines: Doxycycline-inducible cell lines used in this study and respective modifications and clones used. Abbreviations: G – Gfi1; P – Pou4f3; A – Atoh1.

Knock-in line	Gfi1 variant	Clone used
GPA	Intact Gfi1 (wt)	3 and 4
Gfi1DZF6-PA	Zinc fingers removed	5
Gfi1b-PA	Insertion of the Gfi1b coding region at Gfi1 locus	2
Gfi1P2A-PA	A proline to alanine mutation at the amino acid 2 in the SNAG domain	4 and 7

2.2. CELL CULTURE TECHNIQUES

2.2.1. Expansion, inactivation and freezing procedures of mouse embryonic fibroblasts (MEFs)

All ES cell lines used were cultured requiring the presence of a MEFs feeder layer during the growth process. Therefore, expansion and inactivation of previously isolated MEFs by Costa A., was needed. MEFs, already frozen at -80ºC were thawed in pre-heated Glasgow Minimum Essential Medium (GMEM, Sigma), supplemented with 10% fetal calf serum (FCS) (Life Technologies), 2mM Glutamine/Pyruvate (Gl/Pyr) and 1% Penicillin/Streptomycin (P/S) (Invitrogen), and centrifuged for 3.5min at 378g (1300rpm). The supernatant was removed and resuspended in fresh GMEM, plated in a 150mm (diameter) culture dish (treated, Corning) and incubated at 37ºC in 5% CO_2. Their morphology and confluence were inspected every day by direct visualization in a bright field microscope (Motic AE2000 microscope). The culture medium was changed every two days. When MEFs reached approximately 90% of confluency the cells were passaged in a ratio of 1:3. The MEFs were washed with sterile Phosphate Buffered Saline (PBS, Sigma) and incubated with 4mL of 0.05% trypsin-EDTA (Life Technologies) (diluted in PBS) for 5min at 37ºC. Trypsin was inactivated by the addition of 14mL of

supplemented GMEM. The MEFs (of each culture dish) were equally distributed in new three 150mm culture dishes and incubated at 37ºC in 5% CO_2.

For inactivation of MEFs, after trypsinization, cells were centrifuged for 3.5min at 378g, supernatant removed, resuspended in fresh GMEM and inactivated for 42min and 51s by gamma irradiation (35Gy). Finally, the inactivated MEFs (iMEFs) cells were centrifuged for 3.5min at 378g, supernatant removed and resuspended in fresh GMEM. To prepare iMEFs stocks in freezing conditions, the cells were collected in a final volume of 1mL with GMEM and 10% dimethyl sulphoxide (DMSO, VWR Chemicals) into cryopreservation cryovials (ThermoFisher Scientific) and transferred to -80ºC.

2.2.2. Mouse embryonic stem (ES) cells cultures

All steps involved in the manipulation of ES cells were performed in a sterile laminar flow hood class II biosafety cabinet.

The growth of ES cell lines requires the presence of iMEFs feeder layer in 100mm culture dishes (treated, Corning). iMEFs were cultured in GMEM supplemented with 10% FCS, 2mM Gl/Pyr and 1% P/S and maintained at 37ºC in 5% CO_2 incubator.

For ES cells medium, Dulbecco's Modified Eagles Medium 1x (DMEM, Gibco) is supplemented with 10% of heat-inactivated fetal bovine serum (FBS, ES-qualified, Gibco), 2mM Gl/Pyr, 1% MEM non-essential amino acids 100x (Gibco), 7µM 2-Mercaptoethanol (Gibco) and 1% P/S. 2ng/mL of Leukemia Inhibitor Factor (LIF) were always added whenever DMEM medium is used for ES cell expansion but not differentiation.

2.2.3. Expansion and freezing procedures ES cells

ES cells were thawed in pre-heated supplemented DMEM medium and centrifuged for 3.5min at 378g. The supernatant was removed and the cells resuspended in fresh DMEM plus LIF and plated on culture dishes. Then ES cells were grown at 37ºC in 5% CO_2 incubator. The morphology and health of cells were assessed daily by direct visualization on a bright field microscope (Motic AE2000 microscope). Cells were passaged every other day, at a constant plating density of $2.7x10^4$ cells/cm^2. For each passage, cells were washed with sterile PBS and dissociated with 2mL of 0.05% trypsin-EDTA for 2min at 37ºC. The effect of trypsin was inactivated with 8mL of DMEM and cells were centrifuged for 3.5min at 378g. The supernatant was removed and cells were resuspended vigorously in 1mL of fresh DMEM in order to separate them into single cells for counting. Cells were counted using 1:2 concentrated trypan blue solution (diluted in PBS) which stains dead cells and helps to provide a measure of the number of viable ES cells with the sample. Trypan blue-stained cells suspension (20µL) is placed onto a hemocytometer and numbers of viable cells were counted under a bright field microscope at 10x magnification. The required amount of cells was then plated in supplemented DMEM plus LIF.

To prepare ES cells stocks for long storage in freezing conditions, after counting, $4x10^6$ cells were collected in a final volume of 1mL with DMEM and 10% DMSO into cryopreservation cryovials and transferred to -80ºC or to liquid nitrogen.

2.2.4. ES cell differentiation

ES cell differentiation was achieved using a non-adherent culture system (in suspension) throughout the formation of three-dimensional aggregates known as embryoid bodies (EBs). EB formation was considered as day 0 of differentiation.

ES cells were washed with PBS and dissociated using 0.05% trypsin-EDTA for 2min at 37ºC. Trypsin was neutralized by adding 8mL of DMEM and cells were plated in culture dishes (treated, Corning) and incubated for 1h at 37ºC to separate the ES cells from the iMEFs. Then cells were centrifuged for 3.5min at 378g, supernatant removed and pellet resuspended in 1mL into single cells for counting. ES cells were plated at a low density of $1.8x10^4$ cells/cm^2 with supplemented DMEM plus P/S in culture dishes (untreated, ThermoFisher Scientific). Medium was replaced every two days. The EBs' morphology was assessed everyday as with ES cells.

Supplementations with 2µg/mL doxycycline (Dox, Sigma), diluted in sterile PBS and filtered through a 0.45µm filter unit, was initiated at day 4 and maintained until the required time points for analysis (day 6, day 8 or day 12).

When HDACs or LSD1 inhibitors added (HDACi and LSD1i), additionally to Dox, at day 4 each inhibitor was added at 0.1µM or 1µM concentrations and maintained until the required time points for analysis (***Table 2.2***).

Table 2.2 – HDACs and LSD1 inhibition treatment: chemicals added to inhibit HDACs and LSD1 components and respective source and solutions prepared.

Treatment	Inhibitor	Source	Handling
HDACi	Trichostatin A (TSA)	1mg, BioVision	10mM solution diluted in DMSO, frozen at -20ºC (prepared by Costa A.)
LSD1i	SP2509	1mg, Cayman Chemical Company	

Since DMSO is toxic for cells this agent was also added to the Dox-treated control samples in a final concentration of 0.01%.

At each time point (day 6, day 8 or day 12) EBs were fixed with 1% paraformaldehyde (PFA, Sigma-Aldrich) for immunocytochemistry (ICC), or dissociated into single cells for flow cytometry analysis or RNA was extracted for real-time quantitative polymerase chain reaction (qPCR). We also selected an additional control at day 0, before the EBs formation, where RNA was extracted from ES cells for qPCR.

2.3. FLOW CYTOMETRY ANALYSIS

This technique was used to assess the GFP expression to check the induced overexpression of the transcription factors. The EBs to be analyzed were washed in PBS and dissociated into single cells with 500µL of trypsin-EDTA (0.05% for 1min at day 6, 0.25% for 1min at day 8 or 0.25% for 2min at day 12) and mechanically. Trypsin was neutralized with 2mL of DMEM. Cells were centrifuged for 3,5min at 378g, supernatant removed and cells were resuspended in PBS. 100µL of cells were resuspended in 500µL of FACS buffer (composed of 4% of FBS in PBS) and collected into 5mL tubes with cell-strainer cap (Falcon). TRO-PO-3 iodide (1µg/mL) was added to the FACS buffer just before analysis to exclude

dead cells and debris. Fluorescence analysis was performed in BD FACS Calibur cell analyser cytometer using the BD *CellQuest* software where gates were set appropriately in order to identify the GFP positive (GFP+) cells within the live ones. The data obtained was subsequently analyzed using the *FlowJo* software.

2.4. EXTRACTION AND ISOLATION OF TOTAL RNA

The RNA was then extracted, isolated and quantified using the *Absolutely RNA Microprep Kit* (Agilent Technologies).

The remaining single cells obtained were centrifuged for 3.5min at 378g, supernatant removed and cells washed in PBS. A total of $1 – 5x10^6$ cells were collected and lysed with a solution of 350µL of lysis buffer plus 2.5µL of β-Mercaptoethanol and stored at -80ºC.

The steps to isolate the total RNA are described in the protocol ***6.1*** in Supplementary Data.

The total RNA was then quantified (ng/µL) in a nanometer and stored at -80ºC.

2.5. cDNA SYNTHESIS

For cDNA synthesis, 200ng of the total RNA was used as a template for the reverse transcription performed with the *SuperScript IV First-Strand Synthesis System* (Invitrogen) in a final volume of 20µL in a PCR reaction tube. Reactions were performed at a T100 Thermal Cycler (Bio Rad). The steps used are as described in the protocol ***6.2*** in Supplementary Data.

The cDNA obtained was used to perform qPCR. If not immediately used for amplification it was stored at -80ºC.

2.6. qPCR

The primers used during this study for qPCR were synthetized by Sigma or Integrated DNA Technologies (*Table **2.3***).

Table 2.3 – Primers used for qPCRs, described in this section

Primer	Sequence 5'-3'
Sdha F	CAGTTCCACCCCACAGGTA
Sdha R	TCTCCACGACACCCTTCTGT
vGFP F	GAAGCGCGATCACATGGT
vGFP R	CCATGCCGAGAGTGATC
Myo7a F	TGGGGAGTACAGGTGTGAGA
Myo7aR	CCACAAAGTACTGCTGAGAAGC
Myo6 F	GAGAGGCGGATGAAACTTGAGA
Myo6 R	CTTCGGAGTGCCATGTCACC
Otof F	CCCAGATCACGGACAGGA
Otof R	GCCACCAGCTCTTGATATAGATG
Lhx3 F	GCAGTTCCAAGTCCGACAA
Lhx3 R	TAGCAGGCCCCATGTCAG
Cdh23 F	AACAGCACAGGCGTGGTGA
Cdh23 R	TGGCTGTGACTTGAAGGACTG
Espn F	AGCAGAAGATGCAGGAGGAA
Espn R	TTCCGAAGAATGTCTCGTCTC
Tuj1 F	AAGGTAGCCGTGTGTGACATC
Tuj1 R	ACCAGGTCATTCATGTTGCTC
Dcx F	GACTCAGGTAACGACCAAGACG
Dcx R	TTCCAGGGCTTGTGGGTGTAG

The PCR reaction was performed on 384-well plated covered with optical adhesive covers. The instruments used were Light Cycler System Real-Time PCR (Roche Life Science). The cDNA was used as template for each pair of primer in a triplicate PCR reaction. Sdha (housekeeping gene) was used as a calibrator. The qPCR was carried out using *Light Cycler 480 SyBR Green I Master* mix (Roche Life Science). 2µL of the retrotranscription cDNA template was diluted in 5µL of SyBR Green, 0.5µL of 5µM of each primer (forward (F) and reverse (R)) (except for double-courting (Dcx) primer that was added 0.2µL). High-pure water was added up to 8µL.

Reaction conditions are as follows:

- One step of 50ºC for 2min;
- One step of 95ºC for 10min;
- 40 cycles of 95ºC for 15s denaturation;
- One step of 60ºC for 1min annealing and extension.

The quantitative values obtained from the amplification, expressed as Ct values, were used to calculate the relative expression of the primers, using an adaption of the method delta-delta Ct by Livak. K and Schmittgen. T, 2001 [68]. Relative expression levels in the various Dox/inhibitor-treated samples are referred to the levels of expression in the negative control (without Dox/inhibitor) at day 6 (first time point) which are arbitrarily set to 1.

The calculations steps were:

1. $\Delta Ct = Ct_{target\ gene} - Ct_{housekeeping\ gene}$
2. Average of ΔCt of the controls at day 6
3. $\Delta\Delta Ct = \Delta Ct_{treated} - \Delta Ct_{control}$
4. $2^{-(\Delta\Delta Ct)}$
5. Average of $2^{-(\Delta\Delta Ct)}$ of the control at day 6
6. $2^{-(\Delta\Delta Ct)}_{treated} / 2^{-(\Delta\Delta Ct)}_{control}$

2.7. EBS FIXATION, EMBEDDING AND CRYOSTAT SECTIONING

The EBs were allowed to sediment and then the supernatant was removed, washed in PBS and incubated in 1% PFA in PBS for 2min at RT. Then EBs were washed twice in PBS and stored at 4ºC. After fixation, EBs were passed through a solution of 15% sucrose (Fisher Scientific) in PBBS for cryoprotection and left overnight. The EBs were then embedded in a solution containing 7.5% gelatin (Sigma) and 15% sucrose in PBS and left for 30min in water bath at 37ºC. The gelatin containing the EBs was let to cool at 4ºC and then frozen in cold isopenthane (provided by A. P. Jarman's lab) at -75ºC. Frozen embedded EBs were stored at -80ºC until sectioned on a cryostat (ThermoFisher Scientific) where 10µm sections were collected on Superfrost slides (ThermoFisher Scientific).

2.8. IMMUNOCYTOCHEMISTRY (ICC)

Sections were de-gelatinized (in PBS at 37ºC) and incubated twice in PBS for 5min, in 0.1% Triton (Sigma) in PBS for 10min and two times in PBS for 5min (by immersing the slides). The sections were blocked with 10 % fetal donkey serum (FDS) in TBST (20mM Tris-HCl pH 8.0, 150mM NaCl, 0.05% Tween-20, in MILLI-Q water). Primary antibodies were diluted in blocking solution and incubated at 4ºC overnight. After primary antibodies binding, sections were washed in TBST for 15min three times. Appropriate secondary antibodies were diluted in blocking solution and incubated for 1h at RT (***Table 2.4***). From this step on, the slides were protected from light, since we are working with fluorochromes. The incubation with secondary antibodies was followed by three washes in TBST for 5min. All sections were counterstained with 0.15% DAPI (Biotium), washed in TBST three times for 5min and mounted with Prolong Gold mounting medium (ThermoFisher Scientific).

Table 2.4 – Primary and secondary antibodies used and respective manufacturer's information and dilutions.

Antibody	Source	Host	Dilution (µL)
Myo7a	Proteus Biosciences	Rabbit	1:400
Myo6	Proteus Biosciences	Rabbit	1:50
Lhx3	Abcam	Rabbit	1:200
Tuj1	Abcam	Mouse	1:500
Dcx	EMD Millipore	Guinea Pig	1:1000
vGFP	Abcam	Chicken	1:400
Casp3	A. Williams (Gift)	Rabbit	1:200
Goat anti-Chicken, secondary antibody, Alexa Fluor 488	Invitrogen	Goat	1:400
Donkey anti-Rabbit, secondary antibody, Alexa Fluor 555	Invitrogen	Donkey	1:400
Donkey anti-Mouse, secondary antibody, Alexa Fluor 568	Invitrogen	Donkey	1:400
Goat anti-Guinea Pig, secondary antibody, Alexa Fluor 568	A. Williams (Gift)	Goat	1:400

2.9. MICROSCOPY AND IMAGE ANALYSIS

Brightfield images of the fixed sections were acquired using an inverted microscope (widefield Zeiss observer), a 20x/0.8 objective and a Hamamatsu Orca-Flash 4.0 camera. Using the *Zeiss Zen* software, the acquisition parameters were optimized for proper laser penetration and exposition. All the image analysis was done with the open source software *Fiji/ImageJ*, where contrast/brightness and lookup table were adjusted.

2.10. STATISTICS

All data were expressed as means ± standard error of mean and statistical significance was assessed using a two-way ANOVA. Data and graphs were tabulated and prepared using Microsoft Excel and *GraphPad Prims* software. $P<0.05$ was considered statistically significant.

3. RESULTS

3.1. VALIDATION OF METHOD

In order to understand how Gfi1 is involved in the mechanism of the differentiation of HCs, we first need to determine what domain(s) are essential for this function. We used three Dox-inducible Gfi1 lines, generated by A. Costa: Gfi1b-PA; Gfi1DZF6-PA; Gfi1P2A-PA. Each cell line contains a combination of the three transcription factors Gfi1, Pou4f3 and Atoh1, which can directly convert ES-derived progenitors towards HC fate. The knock-in lines under study had its Gfi1 altered in order to analyze the mechanism by which Gfi1 modulates Atoh1 and Pou4f3 activity: Gfi1b-PA was generated by a Gfi1b knock-in at Gfi1's locus (Gfi1b differ from Gfi1 on its intermediary region); Gfi1DZF6-PA has all its zinc fingers (DNA binding site) removed; Gfi1P2A-PA has its SNAG domain function (recruitment of a repressor complex) abolished.

We then focused on the repression of neuronal differentiation function of the LSD1/CoRest/HDACs1-2 complex recruited by Gfi1's SNAG domain. HDACs and LSD1 execute epigenetic changes on target genes. Abrogation of HDACs and LSD1 activity cause HC differentiation impairments and therefore they might specifically modulate the Gfi1 target genes. To address this question we used the wt cell line GPA (Gfi1-Pou4f3-Atoh; intact Gfi1). To note that this line is being examined in the laboratory to identify the genes that are specifically being upregulated and downregulated.

We propose that the promotion of HC differentiation passes through a repression of neuronal differentiation. Saying this, we assessed the expression levels (HC/neuronal markers) of the Dox-inducible cells overexpressing the transcription factors combination. We performed immunocytochemistry and qPCR on EBs at days 6, 8 and 12 of differentiation followed by brightfield imaging and analysis. For immunocytochemistry, vGFP antibody was used in combination with HC (Myo7a, Myo6, Lhx3) and neuronal (Tuj1, Dcx) antibodies for the identification of the overexpressing cells. The co-localization (positive expression of the marker) of vGFP with the markers, obtained with the wt line treated with Dox (positive control), was used as reference to characterize the differentiation happening in the other samples. For qPCR, the housekeeping gene Sdha was used as a calibrator to measure the expression levels of the HC (*Myo7a*, *Myo6*, *Lhx3*, *Otof*, *Cdh23*, *Espn*) and neuronal (*Tuj1*, *Dcx*) genes referred to control at day 6. Similarly, *vGFP* gene was used to identify the quantity of overexpressing transcripts, in order to corroborate the immunocytochemistry observations. In addition, at each time point we tested the viability of the Dox treatment by flow cytometry analysis of the GFP+ cells (***Figure 3.1***).

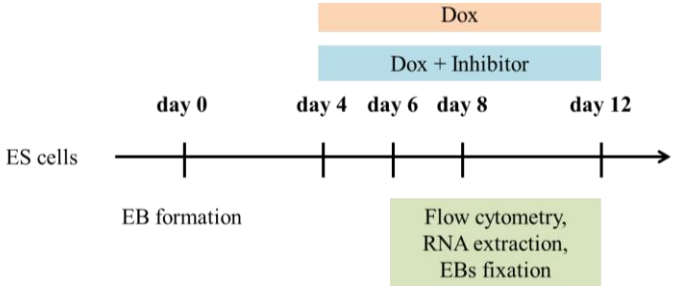

Figure 3.1 - Schematic representation of the ES cells differentiation (through EB formation and subjected to Dox/Dox+inhibitor treatment) and sampling protocols.

For each line under study we examine the expression of GFP (GFP+ cells/vGFP expression) (transgenes expressed) followed by the analysis of the HC and neuronal markers. For each line and differentiation day, the best representative control (if control does not add information it is not represented) and treated samples are presented in the figures below with graphics of the relative gene expression levels.

At the end of each descriptive section, the results are summarized in a written summary focusing on the most prominent features to the question asked, providing a general overview.

3.2. CHARACTERIZATION OF THE KNOCK-IN LINES

The wt cell line GPA Dox-treated (wt Dox) was used as a positive control for HC differentiation. It is known that this cell line expresses HC markers but fail to express neuronal markers. For each cell line used, an untreated sample was used as a negative control (wt control, Gfi1b-PA control, Gfi1DZF6-PA control, Gfi1P2A-PA control). The negative controls did not exhibit differences between them.

Additionally to the analysis described in the previous section, we performed a qPCR control on ES cells at day 0 (prior EB formation) in an attempt to establish the background expression of all genes prior to differentiation. It is visible that ES cells and EBs that did not undergo the Dox treatment do not overexpress *vGFP*, which translates the transgenes expressed by the induction of the transcription factors. Accordingly, the relative gene expression levels of interest of ES cells do not differ from the negative control (untreated EBs) (***Figure 3.2***).

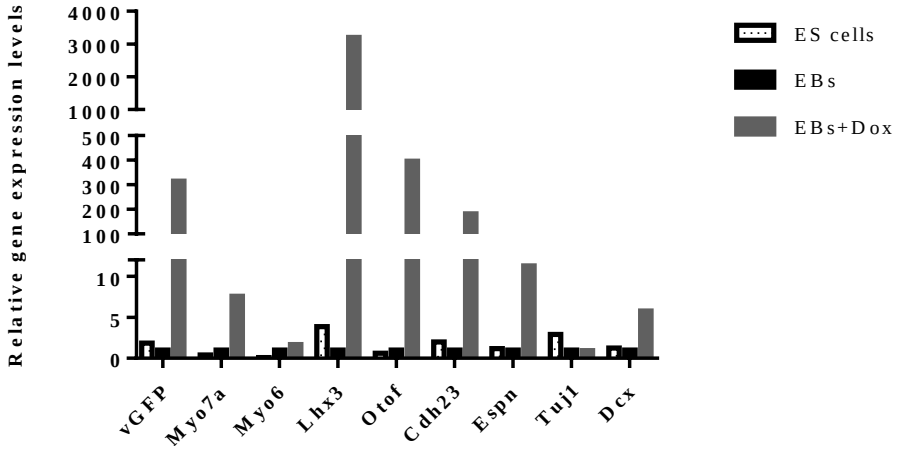

Figure 3.2 - Gene quantification of ES cell vs EBs: Bar diagram showing the relative RNA levels of *vGFP*, HC (*Myo7a*, *Myo6*, *Lhx3*, *Otof*, *Cdh23* and *Espn*) and neuronal (*Tuj1* and *Dcx*) markers in ES cells (prior EB formation), EBs without Dox and EBs with 48h after Dox Treatment. Relative expression of each marker normalized to the mean of untreated EBs at day 6 (set to 1).

3.2.1. Gfi1b-PA

This Gfi1 cell line has the Gfi1 replaced by its paralogue Gfi1b, which *in vivo* has been described that it cannot rescue the defect in HCs. The two transcription factors share nearly identical zinc finger and SNAG domain but share practically no sequence in the intermediary region and therefore, the Gfi1b knock-in aims to investigate the hypothesis that Gfi1's intermediary region plays a role in HC differentiation fate as a platform for protein-protein interactions.

Primarily, to analyze the Dox-inducible gene expression, through flow cytometry, the analysis show a low percentage of GFP+ cells, compared to wt cells. It is also visible the low number of cells expressing vGFP through immunostaining analysis (see ***Figure 6.1*** in Supplementary data), confirmed by qPCR analysis (see ***Figure 6.2*** in Supplementary data).

The dot plots obtained on the percentage of live cells, by flow cytometry, do not explain the differences between Gfi1b Dox and wt Dox samples. We also verified if the low percentage of GFP+ cells seen in Gfi1b line is due cell death through immunocytochemistry with the apoptosis' marker caspase 3 (Casp3). A co-localization of the apoptotic marker with the overexpressing cells (vGFP positives) is not observed (see ***Figure 6.3*** in Supplementary data).

To evaluate the capacity of Gfi1b-PA to determine HC program, we then examined the expression of HC versus neuronal markers. Given the fact that this line presents a notable lower number of vGFP positive cells, an additional normalization of the qPCR values obtained for HC and neuronal markers was necessary, to be able to relate this cell line with the wt line. The values were normalized to the percentage of GFP+ cells at day 6.

The immunostaining experiments demonstrated that vGFP is co-localized with Myo7a (***Figure 3.3***). At day 8, there are more co-localizing cells, and Myo7a forms a clear pattern with vGFP (comparing to day 6) (***Figure 3.3.D***), which appears to be maintained at day 12 (***Figure 3.3.F***). The qPCR reveals *Myo7a* expression from day 6. The increment observed follows the expression pattern of the wt line (***Figure 3.4***).

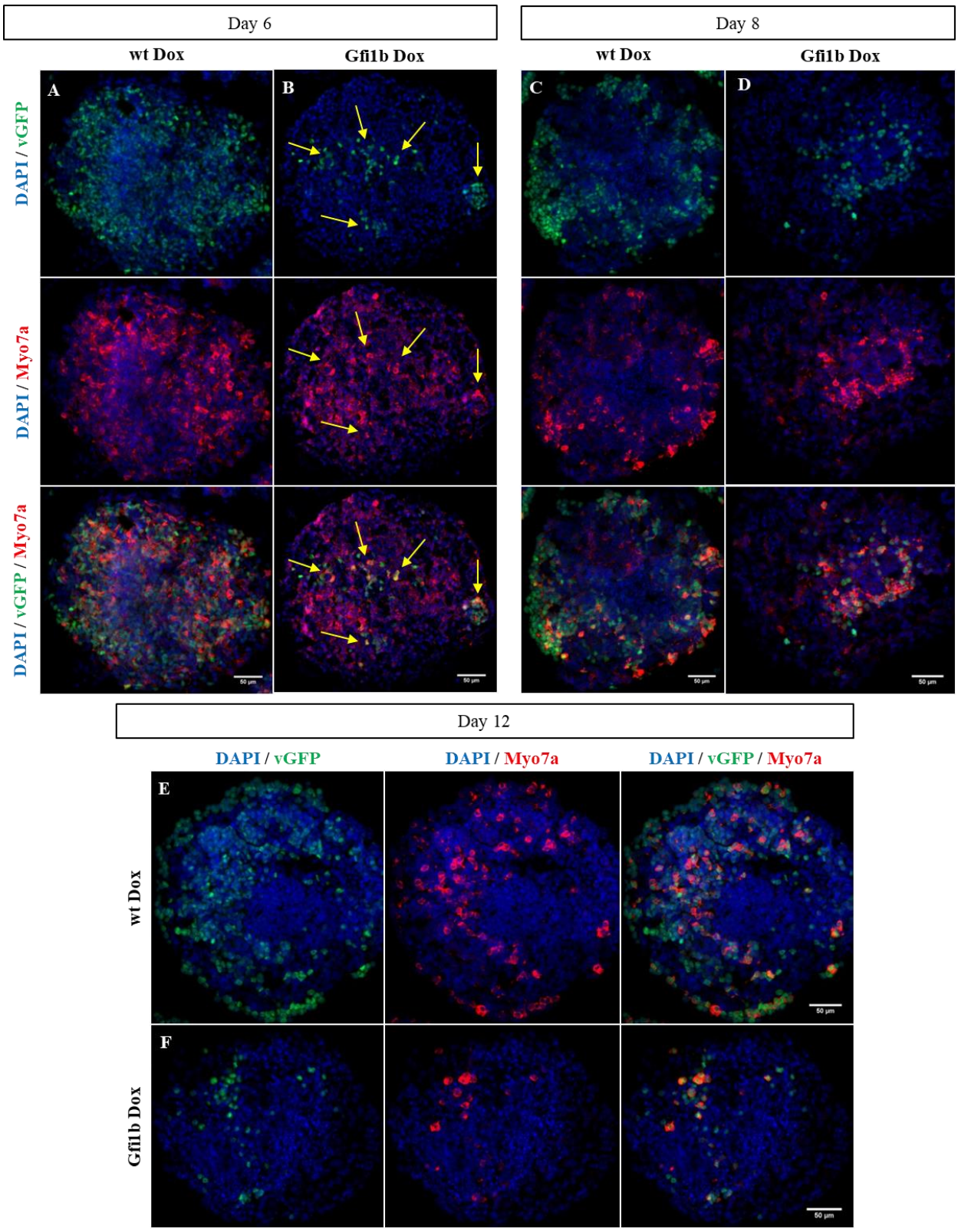

Figure 3.3 - Induction of Myo7a expression in Gfi1b-PA: Representative images obtained from ICC for Myo7a (red) from EBs treated for 2 (A, B), 4 (C, D) and 8 (E, F) days with Dox in (A, C, E) wt Dox and (B, D, F) Gfi1b Dox. Overexpressing cells were identified with vGFP (green) and nuclei with DAPI (blue). Scale bar set to 50µm. Arrows point out co-localization.

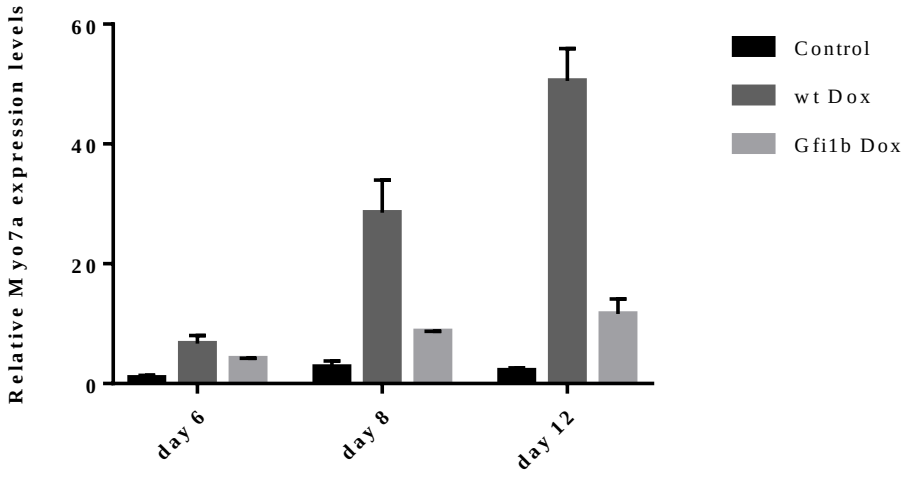

Figure 3.4 - *Myo7a* quantification present in Gfi1b-PA: Bar diagram showing the relative RNA levels of *Myo7a* in untreated EBs and EBs treated for 2, 4 and 8 days with Dox. Relative expression of the marker normalized to the mean of untreated EBs and to the percentage of GFP+ cells at day 6 (set to 1) ± SEM (n=2).

In general, Myo6 marker is expressed at day 6 at a low extent (***Figure 3.5.B***), but several EBs did not label for Myo6. At days 8 and 12, Gfib Dox exhibits more co-localization between Myo6 and vGFP (***Figure 3.5.D*** and ***F***). By qPCR analysis, it is visible that this line presents low levels of *Myo6* at day 8, which increases at day 12. At day 6, there is no difference between the control and Gfib Dox samples (***Figure 3.6***), contrarily to the generality of the immunostaining analysis.

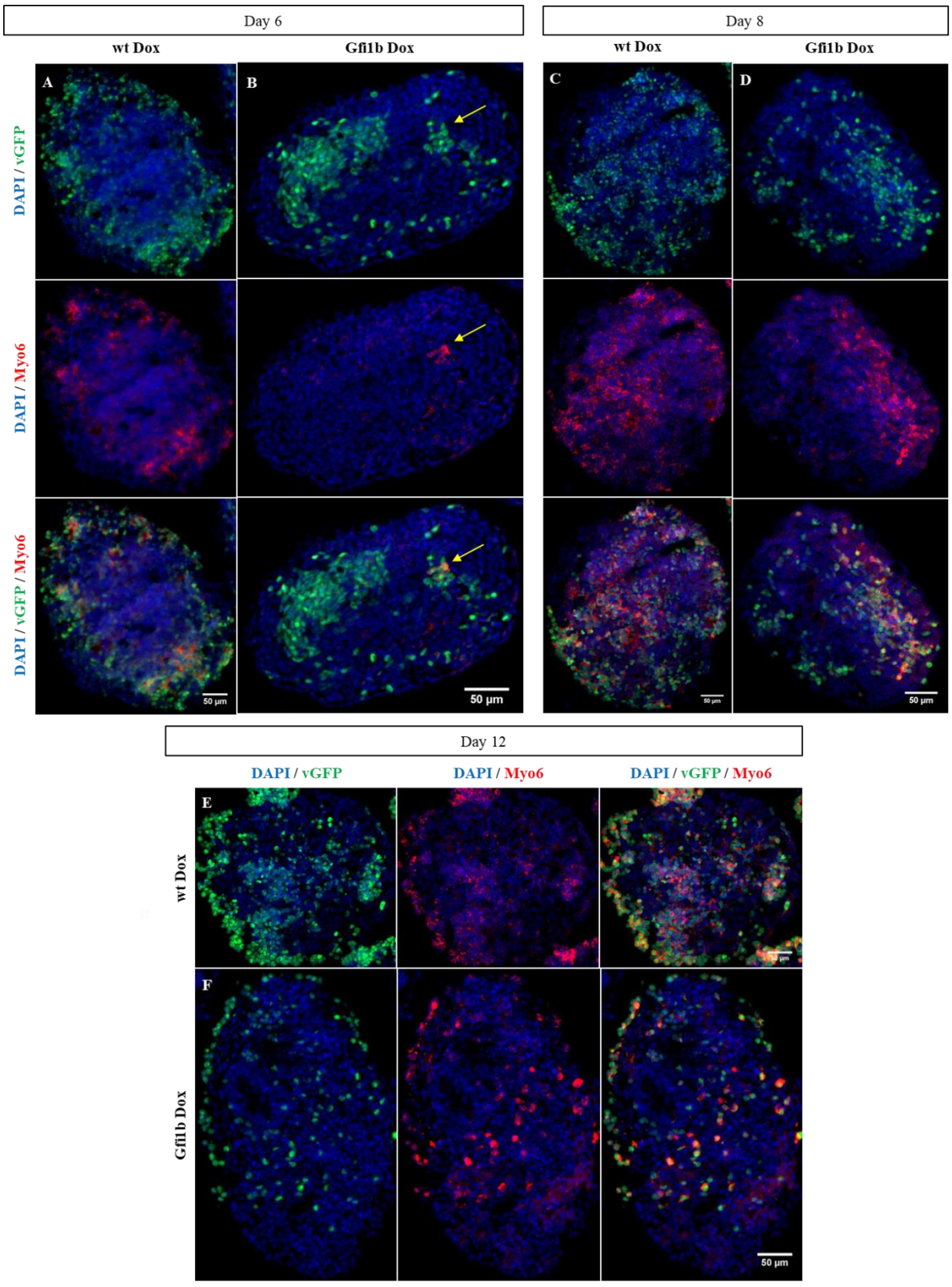

Figure 3.5 - Induction of Myo6 expression in Gfi1b-PA: Representative images obtained from ICC for Myo6 (red) from EBs treated for 2 (A, B), 4 (C, D) and 8 (E, F) days with Dox in (A, C, E) wt Dox and (B, D, F) Gfi1b Dox. Overexpressing cells were identified with vGFP (green) and nuclei with DAPI (blue). Scale bar set to 50µm. Arrows point out co-localization.

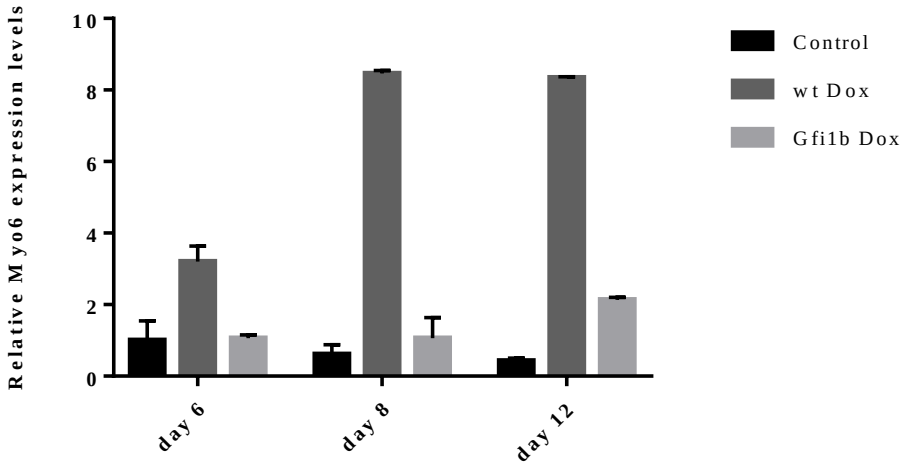

Figure 3.6 - *Myo6* quantification present in Gfi1b-PA: Bar diagram showing the relative RNA levels of *Myo6* in untreated EBs and EBs treated for 2, 4 and 8 days with Dox. Relative expression of the marker normalized to the mean of untreated EBs and to the percentage of GFP+ cells at day 6 (set to 1) ± SEM (n=2).

There is co-localization of Lhx3 with vGFP. Lhx3 expression is visible at day 6 (***Figure 3.7.B***) and it increases progressively at day 8 (***Figure 3.7.D***) and 12 (***Figure 3.7.F***). By qPCR analysis, at day 6, the expression levels obtained do not present a great difference from wt Dox. Then, however, Gfi1b Dox does not follow wt Dox pattern (***Figure 3.8).***

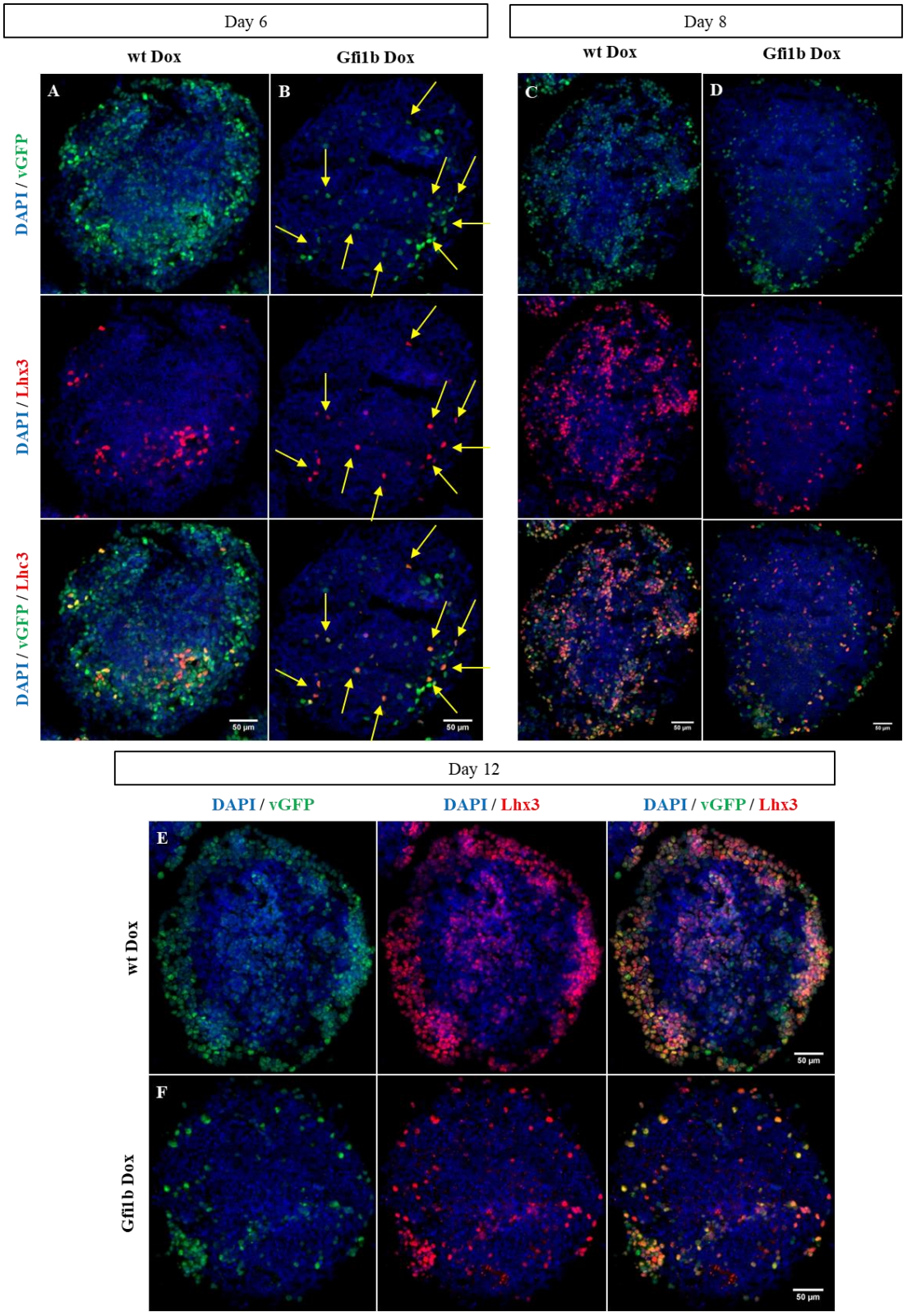

Figure 3.7 - Induction of Lhx3 expression in Gfi1b-PA: Representative images obtained from ICC for Lhx3 (red) from EBs treated for 2 (A, B), 4 (C, D) and 8 (E, F) days with Dox in (A, C, E) wt Dox and (B, D, F) Gfi1b Dox. Overexpressing cells were identified with vGFP (green) and nuclei with DAPI (blue). Scale bar set to 50µm. Arrows point out co-localization.

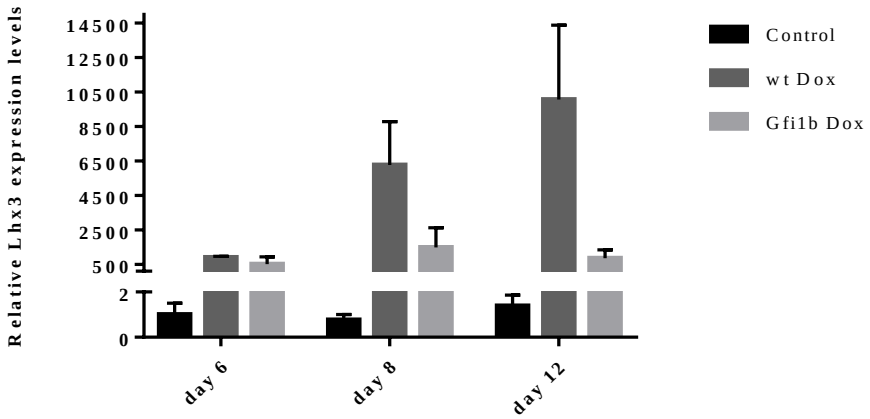

Figure 3.8 - *Lhx3* quantification present in Gfi1b-PA: Bar diagram showing the relative RNA levels of *Lhx3* in untreated EBs and EBs treated for 2, 4 and 8 days with Dox. Relative expression of the marker normalized to the mean of untreated EBs and to the percentage of GFP+ cells at day 6 (set to 1) ± SEM (n=2).

Otof expression matches the levels of wt Dox at day 6. There is a slight increase in the expression levels throughout the days of analysis, which follows the pattern obtained with wt Dox samples (***Figure 3.9***).

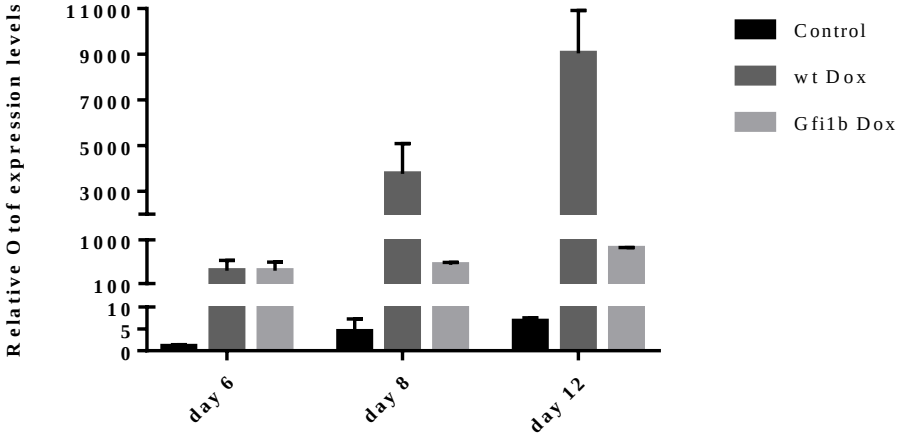

Figure 3.9 - *Otof* quantification present in Gfi1b-PA: Bar diagram showing the relative RNA levels of *Otof* in untreated EBs and EBs treated for 2, 4 and 8 days with Dox. Relative expression of the marker normalized to the mean of untreated EBs and to the percentage of GFP+ cells at day 6 (set to 1) ± SEM (n=2).

Both hair bundle-specific markers *Cdh23* and *Espn* present expression levels at every time point but their expression patterns do not coincide with the patterns obtained with wt Dox samples (***Figure 3.10***).

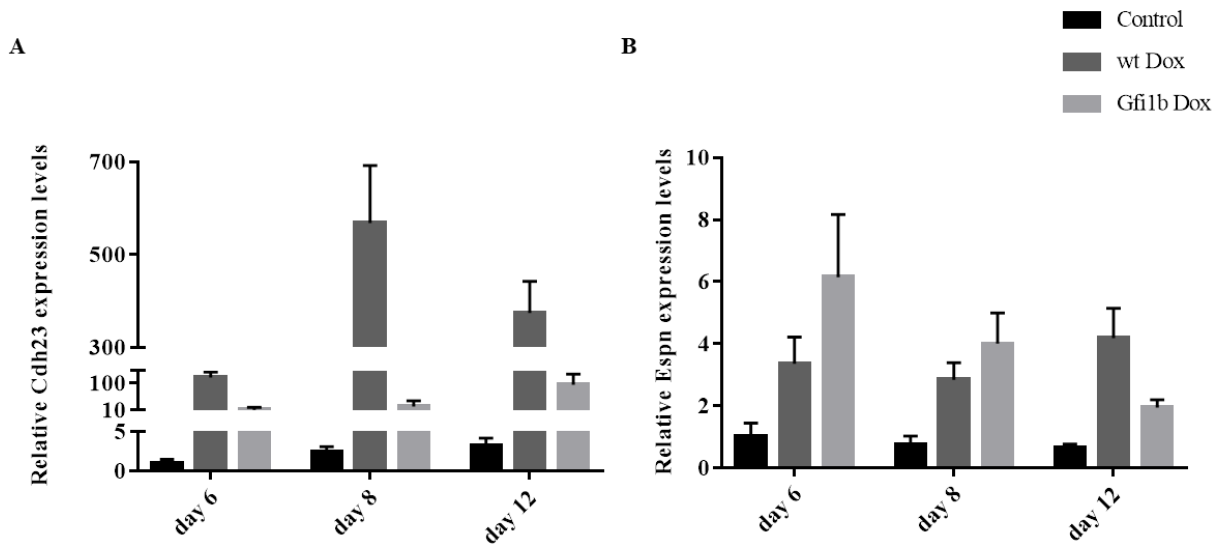

Figure 3.10 - Hair bundle-specific markers quantification present in Gfi1b-PA: (A, B) Bar diagrams showing the relative RNA levels of (A) *Cdh23* and (B) *Espn* in untreated EBs and EBs treated for 2, 4 and 8 days with Dox. Relative expression of the marker normalized to the mean of untreated EBs and to the percentage of GFP+ cells at day 6 (set to 1) ± SEM (n=2).

The samples do not stain for neuronal markers, therefore there is no expression of Tuj1 (***Figure 3.11.A***, ***B***) and Dcx (***Figure 3.11.C***, ***D***) (see days 6 and 12 in Supplementary data: ***Figure 6.4*** for Tuj1 and ***Figure 6.5*** for Dcx). By qPCR analysis, very low levels of *Tuj1* expression are observed at days 6 and 12 (***Figure 3.11.E***). Low levels of *Dcx* are detected at days 6 and 8 (***Figure 3.11.F***). To note that the expression levels detected in wt Dox for neuronal markers are not visible by immunostaining analysis (in accordance with previous observations in the lab).

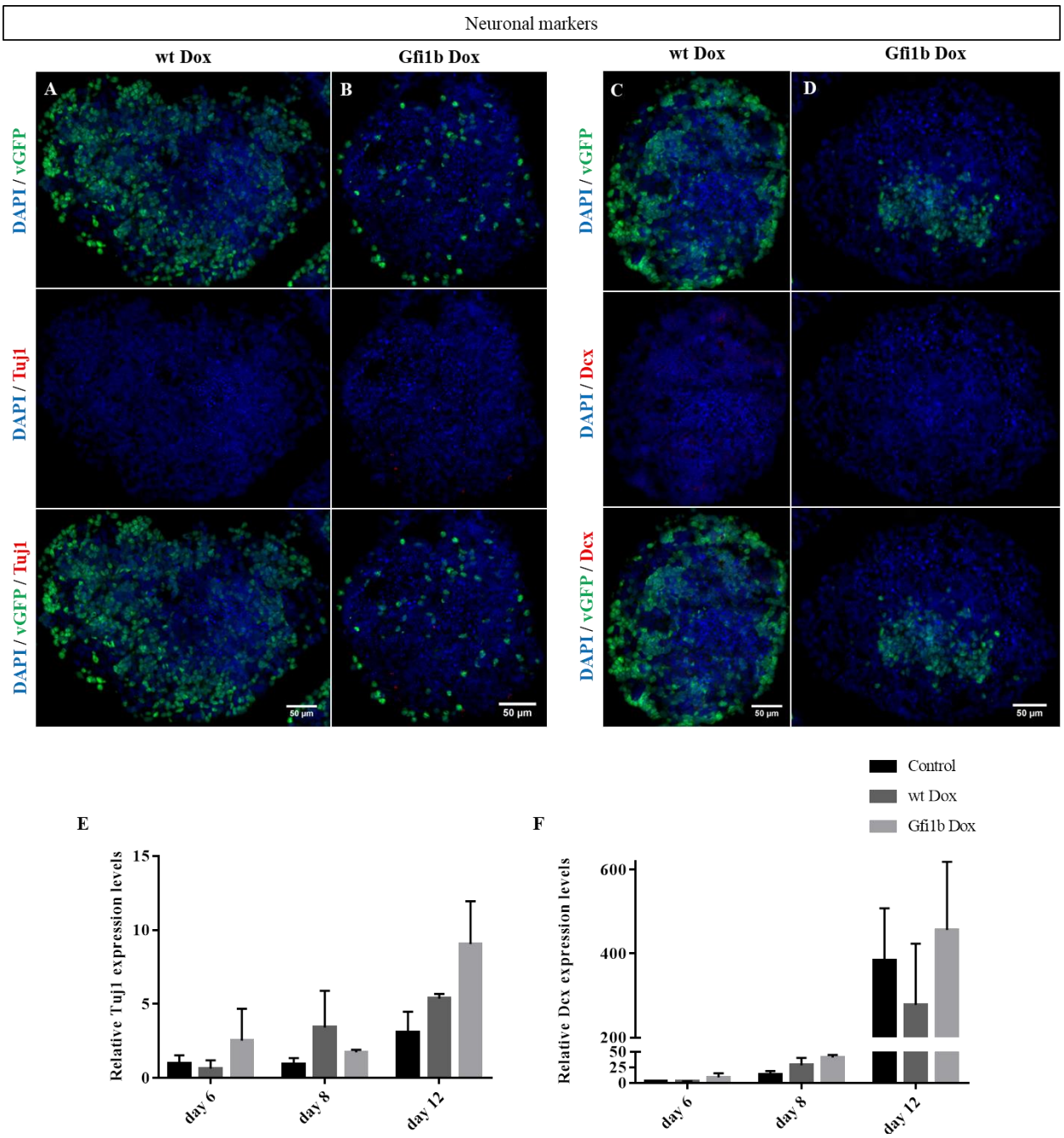

Figure 3.11 - Induction of neuronal-specific markers in Gfi1b-PA: (A, B, C, D) Representative images of day 8 of development, obtained from ICC for (A, B) Tuj1 (red) and (C, D) Dcx (red). EBs were treated for 2, 4 and 8 days with Dox in (A, C) wt Dox and (B, D) Gfi1b Dox. Overexpressing cells were identified with vGFP (green) and nuclei with DAPI (blue). Scale bar set to 50µm. (E, F) Bar diagrams showing the relative RNA levels of (E) *Tuj1* and (F) *Dcx* in untreated EBs and EBs treated for 2, 4 and 8 days with Dox. Relative expression of the marker normalized to the mean of untreated EBs and to the percentage of GFP+ cells at day 6 (set to 1) ± SEM (n=2).

3.2.2. Gfi1b-PA: expression overview

In general, the amount of HC transcripts present in Gfi1b-PA cell line are much lower than the ones obtained in the Gfi1-PA line (wt).

Gfi1b-PA line expresses some HC markers like the wt cell line, namely Myo7a, Myo6, Lhx3 and Otof, but fails to express the hair bundle markers Cdh23 and Espn, based on the pattern exhibited by the wt line.

Although, Tuj1 and Dcx are not observed by immunostaining, these neuronal markers are detected by qPCR, the same way as the wt. Previous observations in the lab have shown that the Gfi1-PA line does not express neuronal markers.

The results show that Gfi1b is able to activate HC associated genes, regardless of the fact that Gfi1b and Gfi1 share almost no sequence in the intermediary region, which contradicts the observations *in vivo* where Gfi1b failed to rescue HC defects.

3.2.3 Gfi1DZF6-PA

The zinc finger domain of Gfi1 is the region by which it binds to the DNA but it can also be a platform for protein-protein interactions, since only three of the six zinc fingers seem to be required for DNA binding. Therefore this cell line has all its six fingers removed to address if the direct regulation of HC genes occur by interactions with the zinc finger domain by binding DNA and/or by recruiting co-factors.

Regarding to Dox-inducible gene expression, Gfi1DZF6 Dox samples exhibit similar capacity of inducing the transgenes as the wt cell line, as percentages of GFP+ cells show (see ***Figure 6.6*** in Supplementary data). However, the relative *vGFP* expression shows a reduction of this induction at each time point, contrarily to wt Dox (see ***Figure 6.7*** in Supplementary data)

The influence of the zinc finger domain on programming HC differentiation was then assessed by characterization of the HC and neuronal markers.

Both immunostaining and qPCR analysis indicate no expression of the HC markers Myo7a (***Figure 3.12.B and E***) or Myo6 (***Figure 3.12.D and F***) by the Gfi1DZF6 line, at any time point of analysis (see days 6 and 12 in Supplementary data: ***Figure 6.8*** for Myo7a and ***Figure 6.9*** for Myo6).

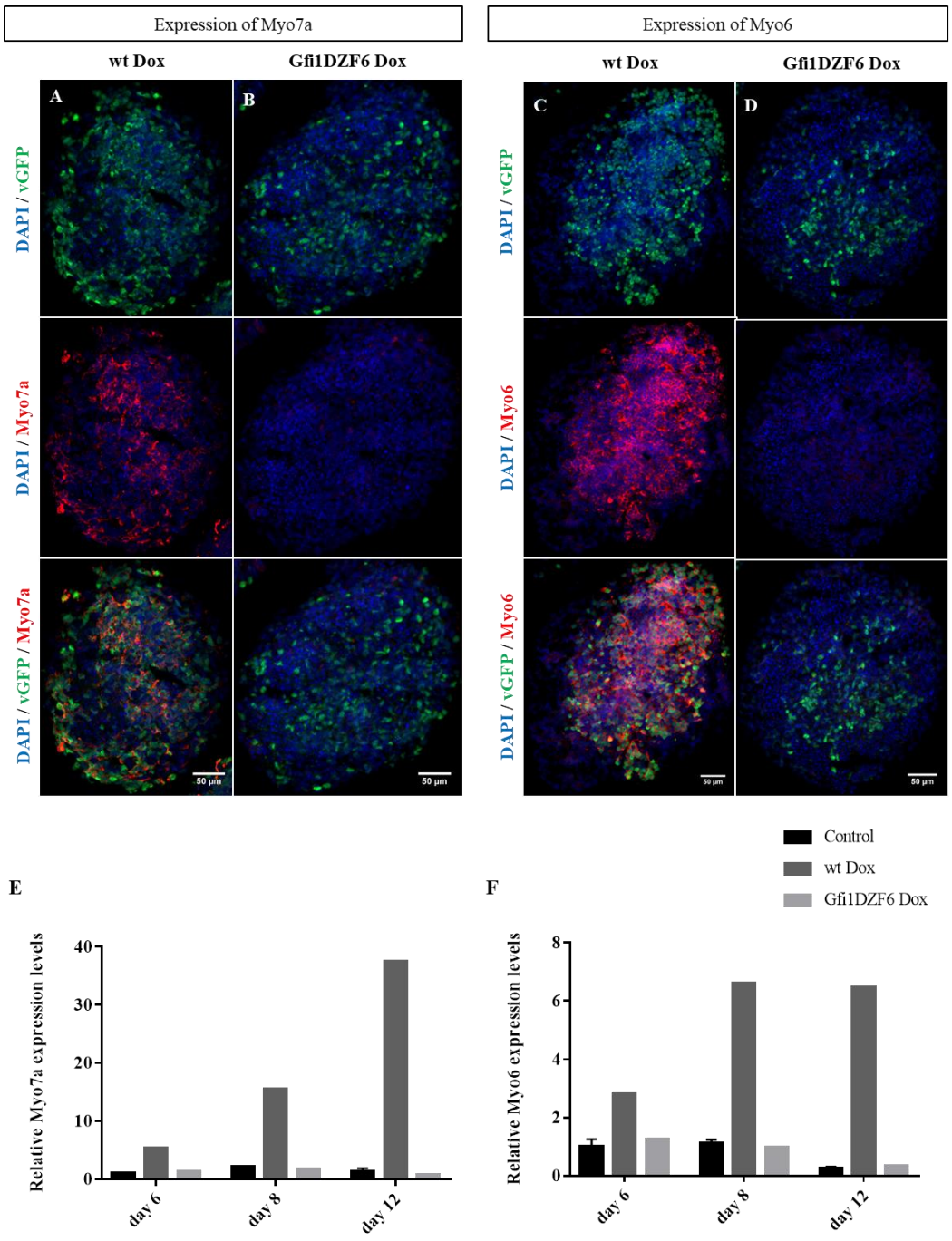

Figure 3.12 - Induction of the HC markers Myo7a and Myo6 in Gfi1DZF6-PA: (A, B, C, D) Representative images of day 8 of development, obtained from ICC for (A, B) Myo7a (red) and (C, D) Myo6 (red). EBs were treated for 2, 4 and 8 days with Dox in (A, C) wt Dox and (B, D) Gfi1DZF6 Dox. Overexpressing cells were identified with vGFP (green) and nuclei with DAPI (blue). Scale bar set to 50µm. (E, F) Bar diagrams showing the relative RNA levels of (E) *Myo7a* and (F) *Myo6* in untreated EBs and EBs treated for 2, 4 and 8 days with Dox. Relative expression of the marker normalized to the mean of untreated EBs at day 6 (set to 1) (n=1).

Co-localization is observed with Lhx3 at a low extent, only at day 8 (***Figure 3.13.D***). The quantification by qPCR shows very low levels of expression of *Lhx3* and its pattern is different than that observed with wt Dox samples (***Figure 3.14***).

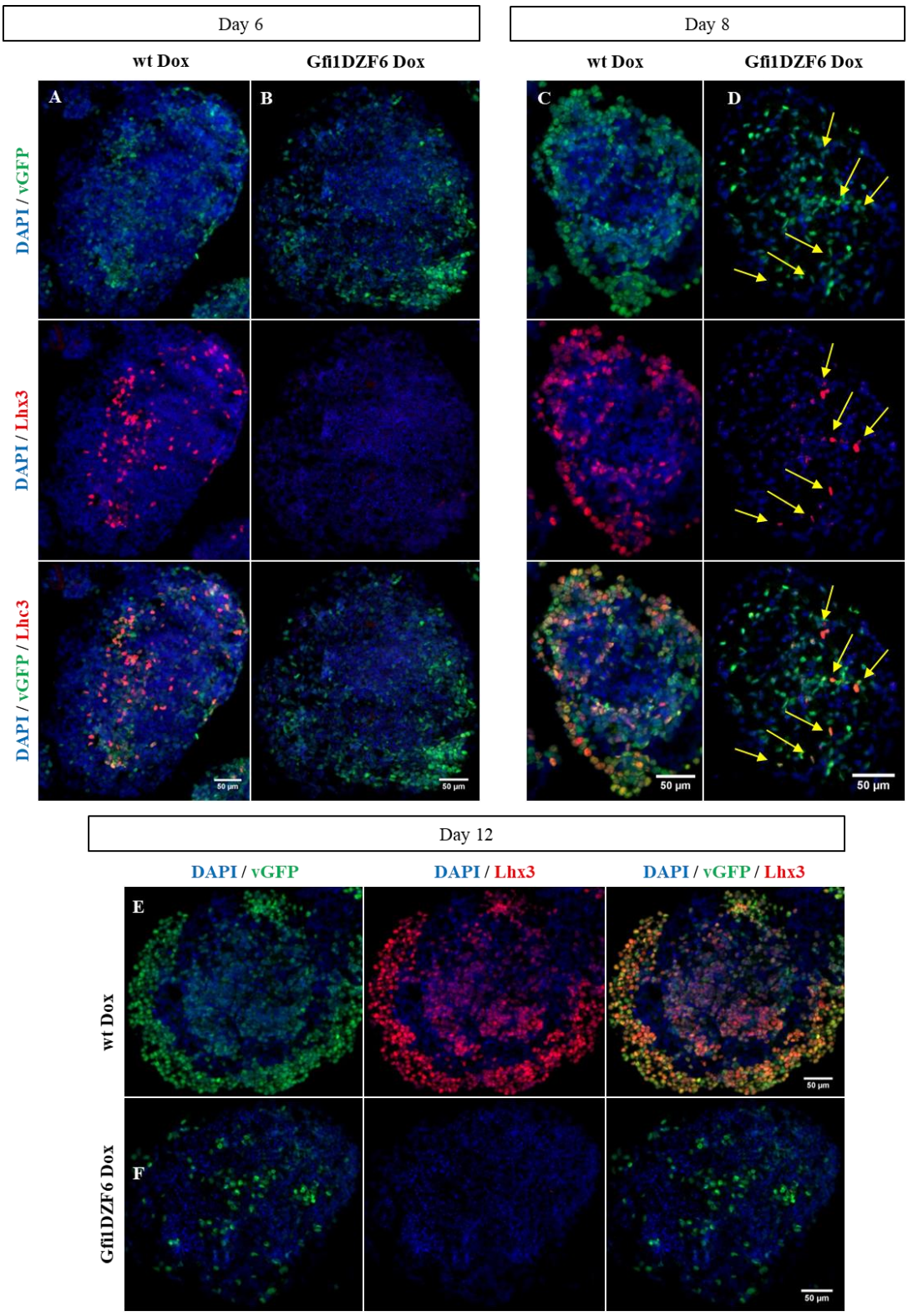

Figure 3.13 - Induction of Lhx3 expression in Gfi1DZF6-PA: Representative images obtained from ICC for Lhx3 (red) from EBs treated for 2 (A, B), 4 (C, D) and 8 (E, F) days after Dox exposure in (A, C, E) wt Dox and (B, D, F) Gfi1DZF6 Dox. Overexpressing cells were identified with vGFP (green) and nuclei with DAPI (blue). Scale bar set to 50µm. Arrows point out co-localization.

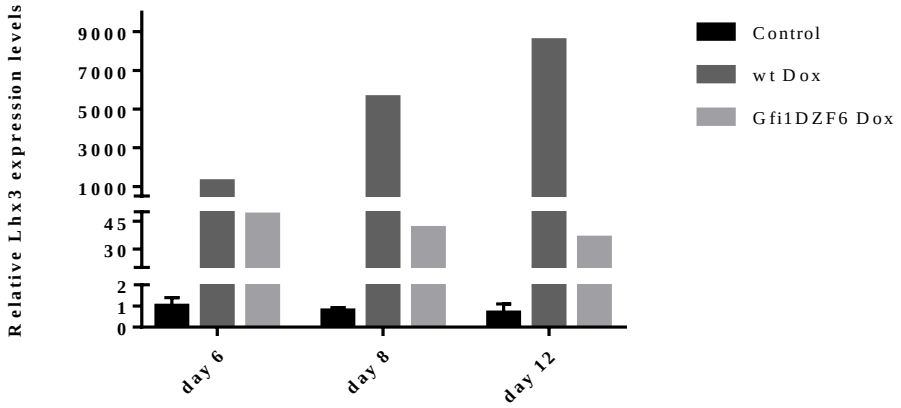

Figure 3.14 - *Lhx3* quantification present in Gfi1DZF6-PA: Bar diagram showing the relative RNA levels of *Lhx3* in untreated EBs and EBs treated for 2, 4 and 8 days with Dox. Relative expression of the marker normalized to the mean of untreated EBs at day 6 (set to 1) (n=1).

At days 8 and 12, low levels of *Otof* are detected. In relation to wt Dox, the values obtained in this cell line do not present the constant increment over time of wt Dox samples (***Figure 3.15***).

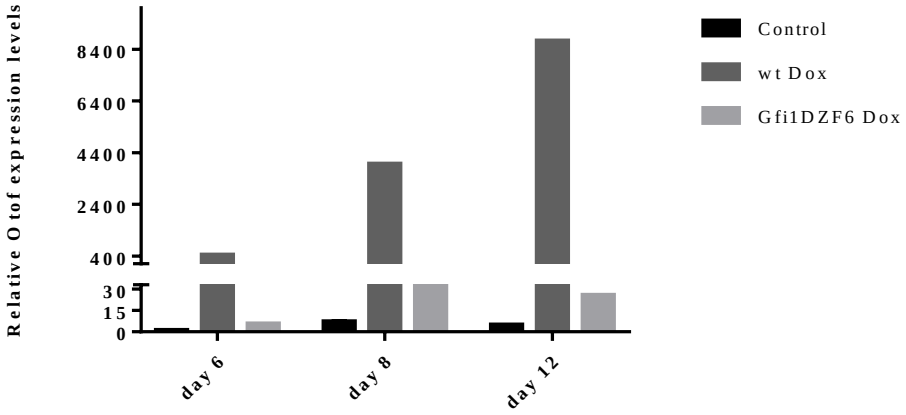

Figure 3.15 - *Otof* quantification present in Gfi1DZF6-PA: Bar diagram showing the relative RNA levels of *Otof* in untreated EBs and EBs treated for 2, 4 and 8 days with Dox. Relative expression of the marker normalized to the mean of untreated EBs at day 6 (set to 1) (n=1).

The expression pattern of *Cdh23* follows the pattern observed in the wt Dox. Additionally, the expression levels are notably lower than what is observed in the wt Dox (***Figure 3.16.A***).

Low levels of *Espn* are detected, only at day 8. To note that this is the time point where wt Dox presents the lowest levels of *Espn* relative expression (***Figure 3.16.B***).

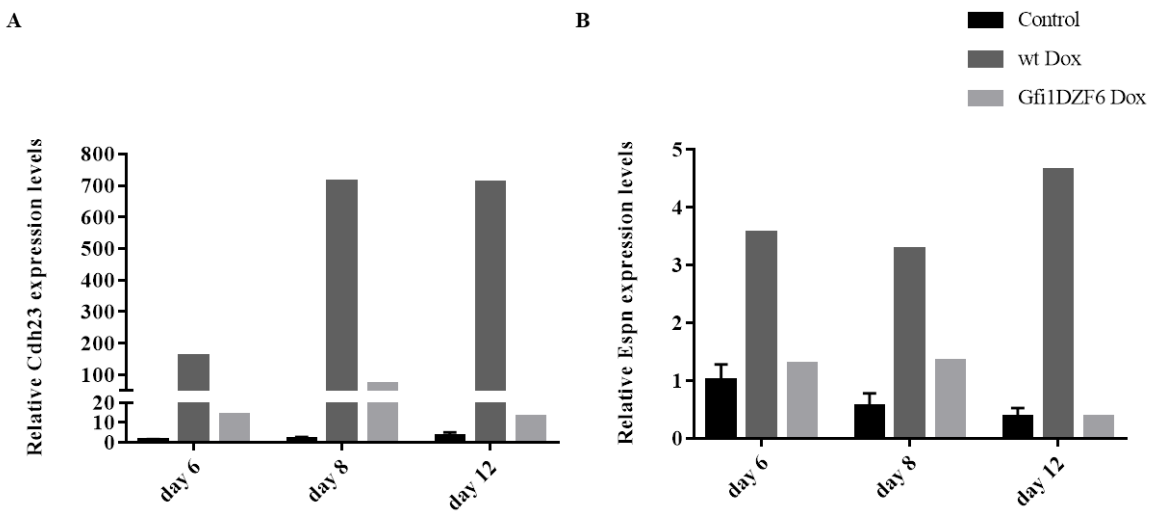

Figure 3.16 - Hair bundle-specific markers quantification present in Gfi1DZF6-PA: (A, B) Bar diagrams showing the relative RNA levels of (A) *Cdh23* and (B) *Espn* in untreated EBs and EBs treated for 2, 4 and 8 days with Dox. Relative expression of the marker normalized to the mean of untreated EBs at day 6 (set to 1) (n=1).

About the neuronal markers Tuj1 and Dcx, the Gfi1DZF6 Dox EBs exhibit co-localization with vGFP, from day 6. At days 6 and 8, Tuj1 expression is strong and widespread. At day 12, there is no co-localization between vGFP and Tuj1 (***Figure 3.17.B***, ***D*** and ***F***).

In turn, Dcx is co-localized with vGFP at every time point of development. It is expressed at a higher extent, at day 8, with a clear peripheral pattern (***Figure 3.18.B***, ***D*** and ***F***).

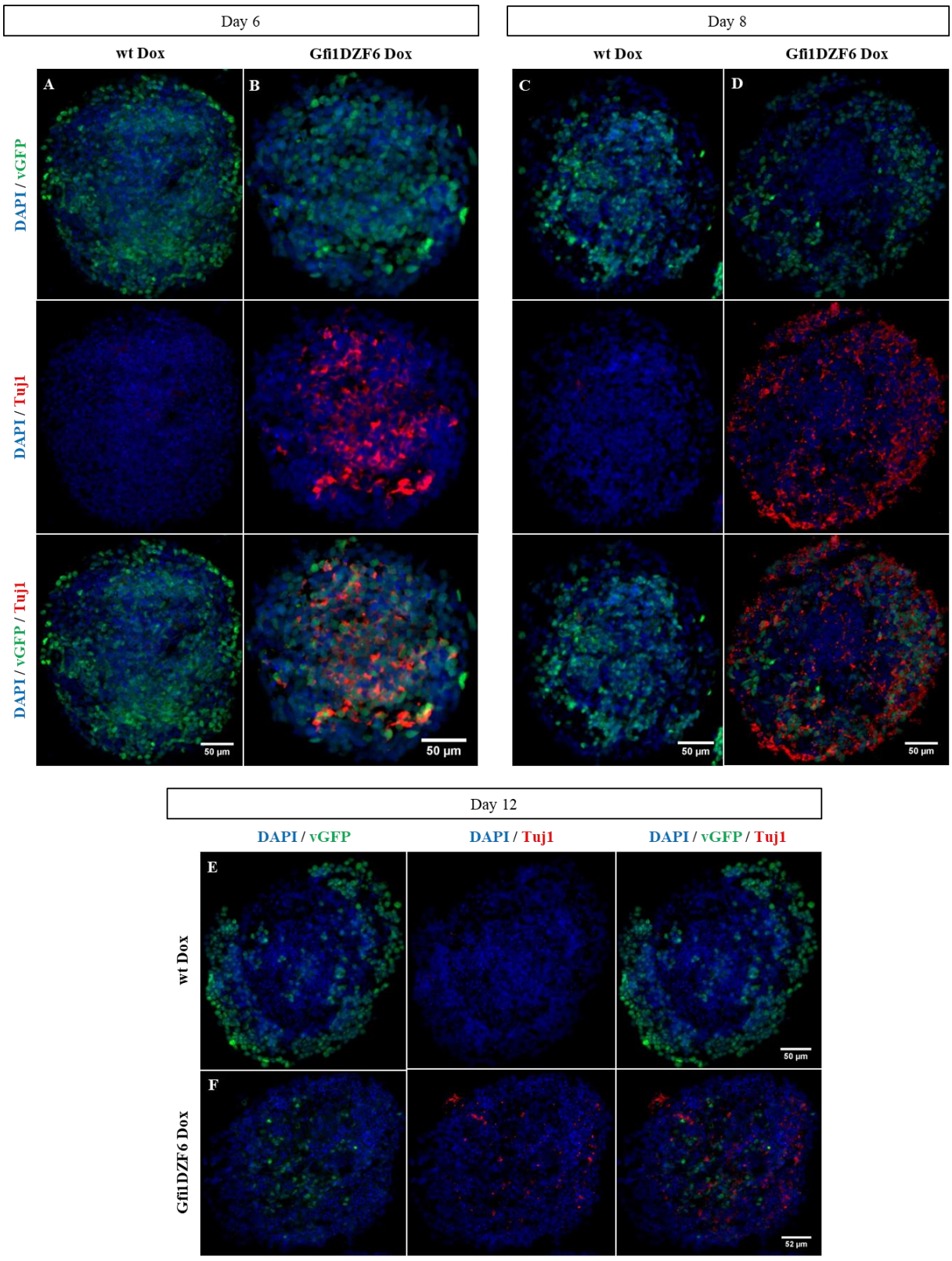

Figure 3.17 - Induction of Tuj1 expression in Gfi1DZF6-PA: Representative images obtained from ICC for Tuj1 (red) from EBs treated for 2 (A, B), 4 (C, D) and 8 (E, F) days after Dox exposure in (A, C, E) wt Dox and (B, D, F) Gfi1DZF6 Dox. Overexpressing cells were identified with vGFP (green) and nuclei with DAPI (blue). Scale bar set to 50µm.

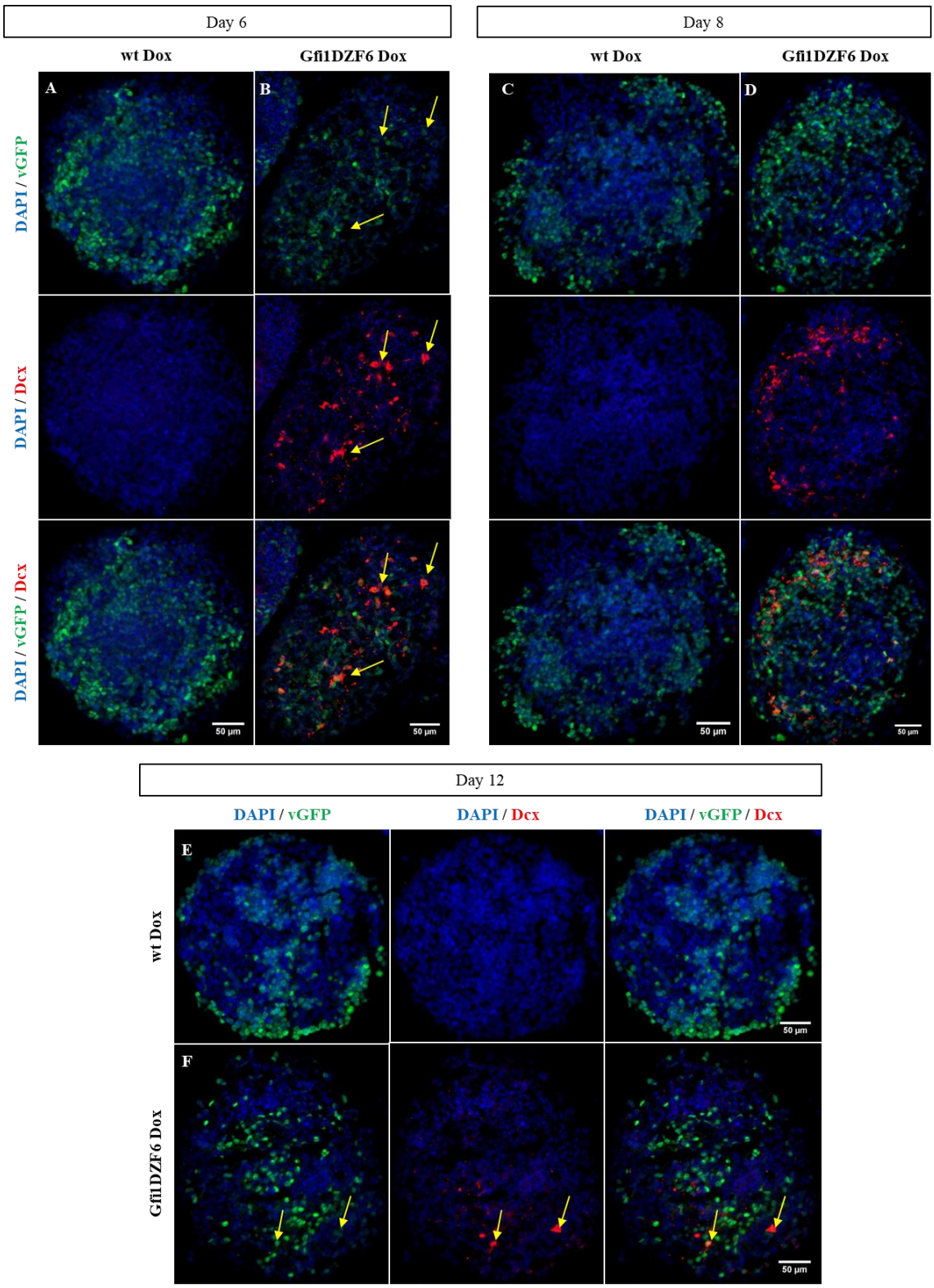

Figure 3.18 - Induction of Dcx expression in Gfi1DZF6-PA: Representative images obtained from ICC for Dcx (red) from EBs treated for 2 (A, B), 4 (C, D) and 8 (E, F) days after Dox exposure in (A, C, E) wt Dox and (B, D, F) Gfi1DZF6 Dox. Overexpressing cells were identified with vGFP (green) and nuclei with DAPI (blue). Scale bar set to 50µm. Arrows point out co-localization.

The qPCR data shows that this cell line exhibits high levels of *Tuj1* expression. At day 12, *Tuj1* expression levels decrease drastically according to the immunostaining analysis (***Figure 3.19.A***).

qPCR analysis with *Dcx* agrees with the immunostaining analysis (***Figure 3.19.B***).

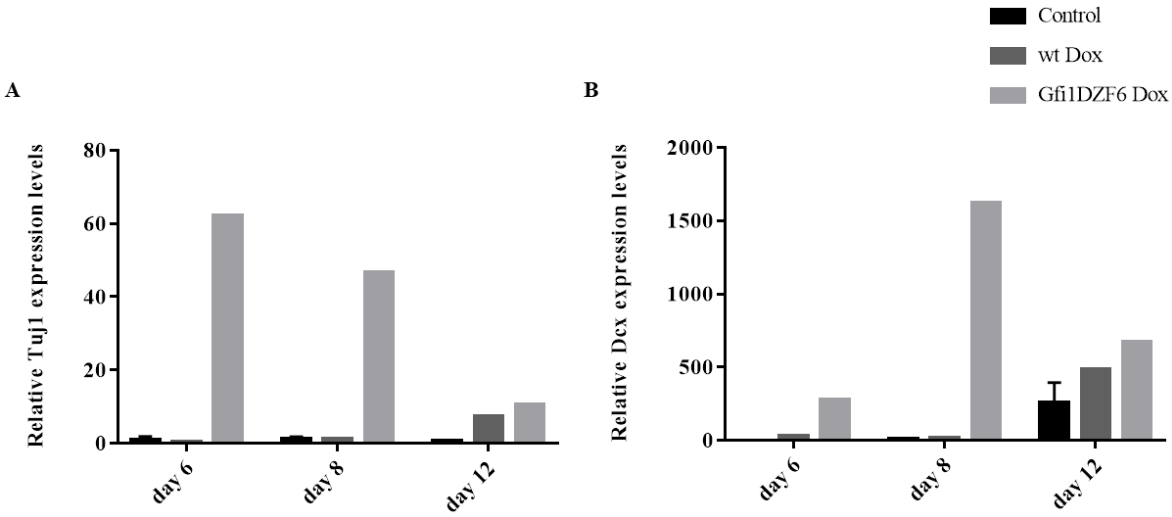

Figure 3.19 - Neuronal-specific markers quantification present in Gfi1DZF6-PA: (A, B) Bar diagrams showing the relative RNA levels of (A) *Tuj1* and (B) *Dcx* in untreated EBs and EBs treated for 2, 4 and 8 days with Dox. Relative expression of the marker normalized to the mean of untreated EBs at day 6 (set to 1) (n=1).

3.2.4. Gfi1DZF6-PA: expression overview

In summary, there is no repression of the neuronal markers (Tuj1 and Dcx) in Gfi1DZF6-PA cell line and, in general, HC markers are not expressed, showing the requirement of the zinc finger domain for HC fate specification.

Lhx3 is co-localized with vGFP, at day 8, however quantitative analysis by qPCR does not register such levels.

Although its values are considerably lower, the hair bundle-specific marker *Cdh23* is expressed in the same pattern as observed in Gfi1-wt.

Further analyses are needed to investigate whether the expression of neuronal markers and failure of HC markers is due DNA binding or protein-protein interactions.

3.2.5 Gfi1P2A-PA

Gfi1 recruits a chromatin-regulating complex (LSD1/CoRest/HDACs1-2) through its SNAG domain, functioning as a transcription repressor (hematopoietic system). This cell line contains the mutation proline to alanine at amino acid 2 of Gfi1, previously studied *in vivo*. This mutation caused the failure of epigenetic repressor recruitment and a phenotype identical to full Gfi1 knockout mice. Gfi1P2A-PA line aims to reflect the results obtained *in vivo.*

The analysis regarding to the capability of Dox-inducible transgenes show that Gfi1P2A-PA cannot maintain the induction along the days of development studied. After day 6, Gfi1P2A Dox

overexpressing cells decline considerably (see *Figure* ***6.10*** in Supplementary data), which is visible by qPCR analysis of the relative *vGFP* expression levels (see ***Figure 6.11*** in Supplementary data).

The dot plots obtained do not show differences in the number of live cells between Gfi1P2A-PA and the wt line (see ***Figure 6.12*** in Supplementary data) and do not explain the reduction of GFP+/vGFP cells from day 8.

In relation to Gfi1's SNAG domain function in determining HC fate, we explored the expression of HC and neuronal markers in Gfi1P2A-PA line.

Co-localization of HC markers, Myo7a (***Figure 3.20.B***), Myo6 (***Figure 3.20.D***) and Lhx3 (***Figure 3.21.B***) with vGFP is not detected, at any time point (see days 6 and 12 in Supplementary data: ***Figure 6.13*** for Myo7a; ***Figure 6.14*** for Myo6; ***Figure 6.15*** for Lhx3).

The quantification of relative RNA expression levels confirms the immunostaining analysis regarding *Myo7a* (***Figure 3.20.E***) and *Myo6* (***Figure 3.20.F***). There is no expression of either HC marker. Regarding *Lhx3* the analysis reveals low levels of expression, but the pattern is different to that observed in the wt Dox (***Figure 3.21.C***).

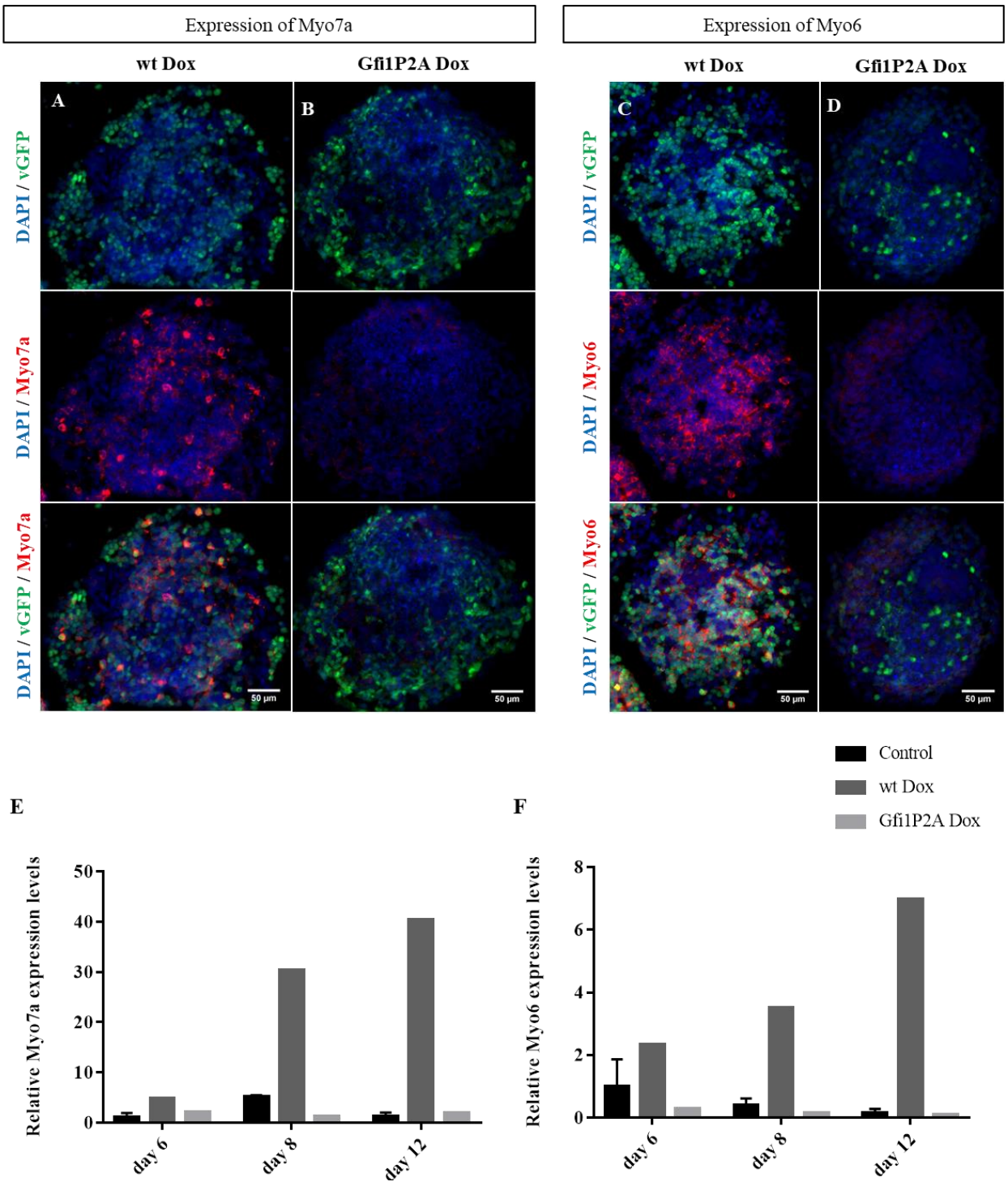

Figure 3.20 - Induction of the HC markers Myo7a and Myo6 in Gfi1P2A-PA: (A, B, C, D) Representative images of day 8 of development, obtained from ICC for (A, B) Myo7a (red) and (C, D) Myo6 (red). EBs were treated for 2, 4 and 8 days with Dox in (A, C) wt Dox and (B, D) Gfi1P2A Dox. Overexpressing cells were identified with vGFP (green) and nuclei with DAPI (blue). Scale bar set to 50µm. (E, F) Bar diagrams showing the relative RNA levels of (E) *Myo7a* and (F) *Myo6* in untreated EBs and EBs treated for 2, 4 and 8 days with Dox. Relative expression of the marker normalized to the mean of untreated EBs at day 6 (set to 1) (n=1).

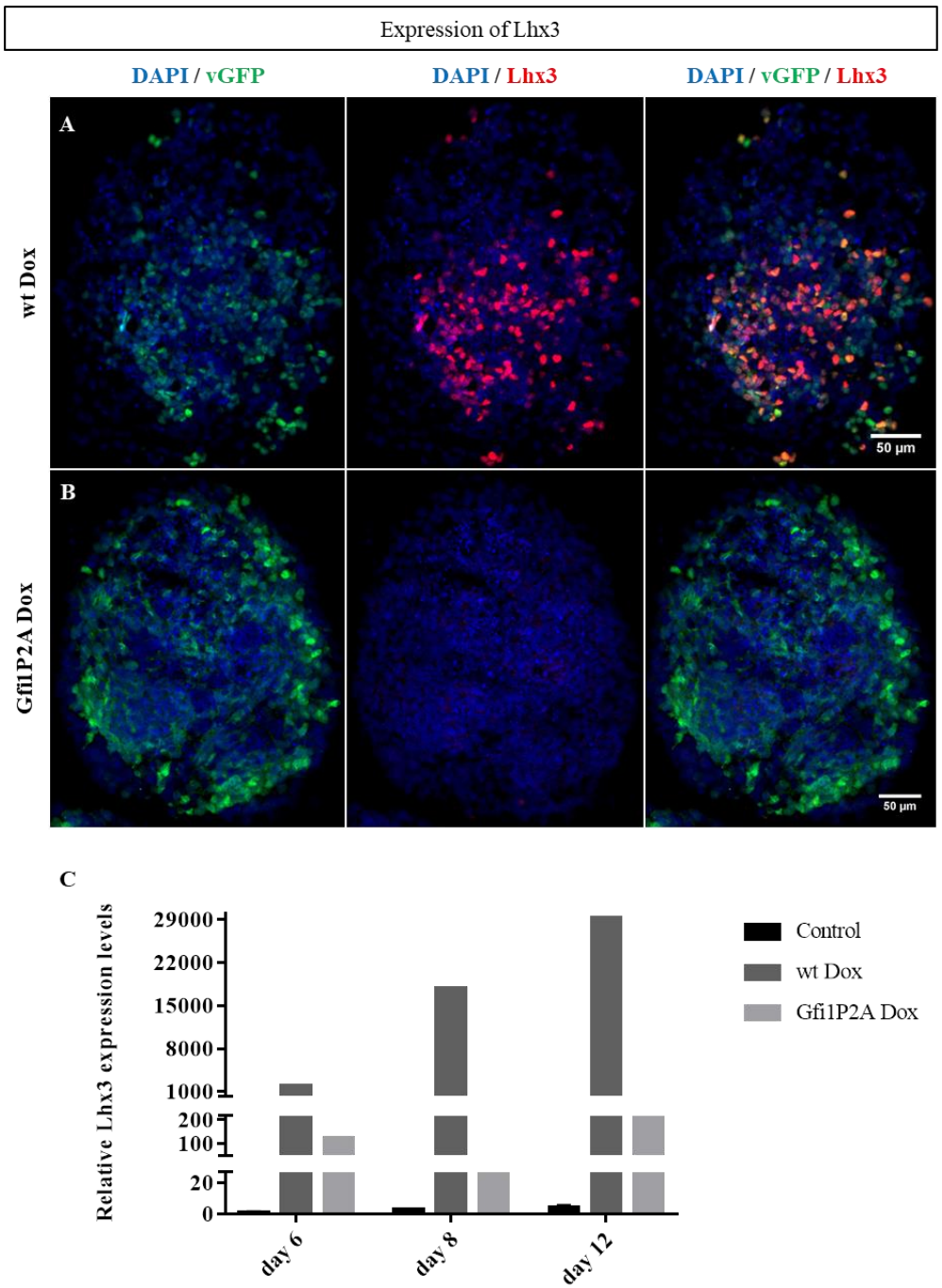

Figure 3.21 - Induction of Lhx3 in Gfi1P2A-PA: (A, B) Representative images of day 8 of development, obtained from ICC for Lhx3 (red). EBs were treated for 2, 4 and 8 days with Dox in (A) wt Dox and (B) Gfi1P2A Dox. Overexpressing cells were identified with vGFP (green) and nuclei with DAPI (blue). Scale bar set to 50µm. (C) Bar diagram showing the relative RNA levels of *Lhx3* in untreated EBs and EBs treated for 2, 4 and 8 days with Dox. Relative expression of the marker normalized to the mean of untreated EBs at day 6 (set to 1) (n=1).

This cell line shows very low levels of *Otof* expression, which increase slightly from day 6 to day 8 (***Figure 3.22***).

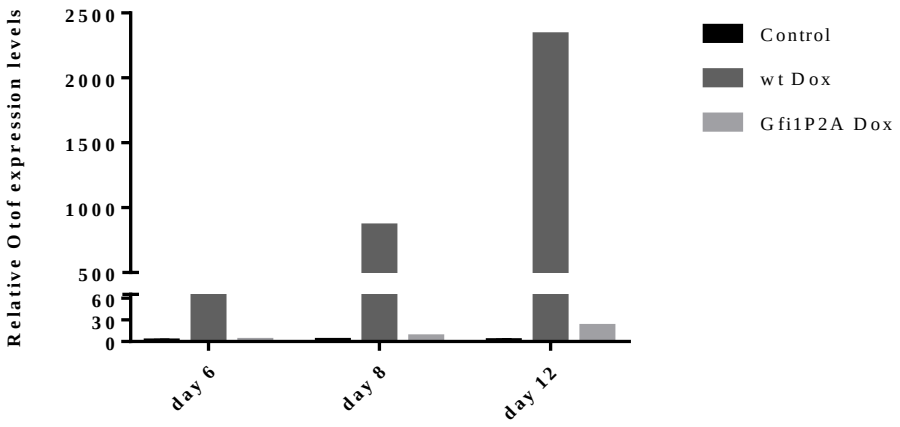

Figure 3.22 - *Otof* quantification present in Gfi1P2A-PA: Bar diagram showing the relative RNA levels of *Otof* in untreated EBs and EBs treated for 2, 4 and 8 days with Dox. Relative expression of the marker normalized to the mean of untreated EBs at day 6 (set to 1) (n=1).

Both *Cdh23* and *Espn* are detected only at day 6. The *Cdh23* marker presents very low levels of expression (***Figure 3.23.A***), whereas *Espn* is expressed at higher levels (***Figure 3.23.B***).

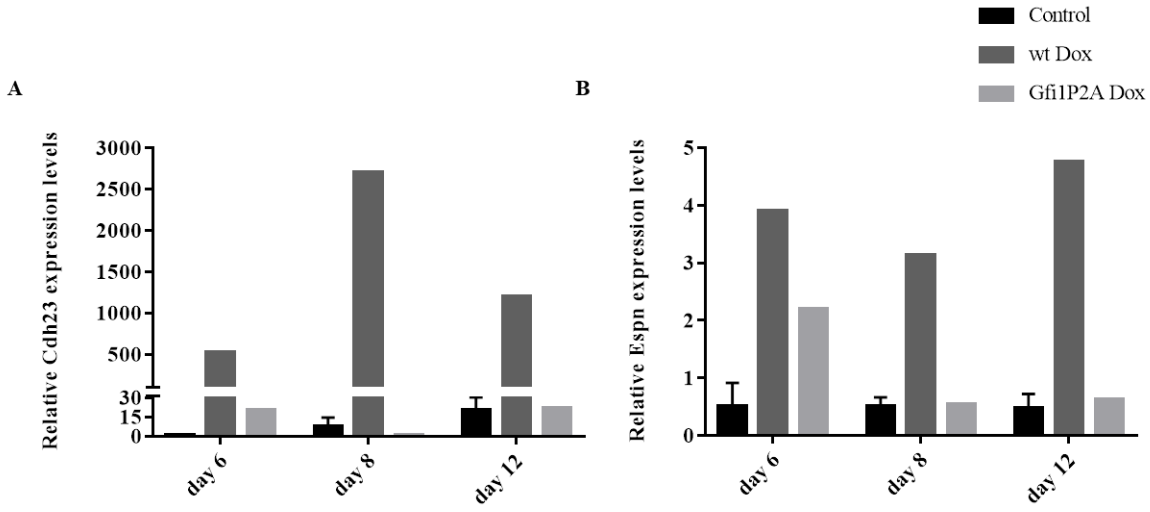

Figure 3.23 - Hair bundle-specific markers quantification present in Gfi1P2A-PA: (A, B) Bar diagrams showing the relative RNA levels of (A) *Cdh23* and (B) *Espn* in untreated EBs and EBs treated for 2, 4 and 8 days with Dox. Relative expression of the marker normalized to the mean of untreated EBs at day 6 (set to 1) (n=1).

About the neuronal marker Tuj1, at day 6, some co-localization with vGFP is observed (***Figure 3.24.B***). At day 8 (***Figure 3.24.D***), there is a higher number of cells expressing Tuj1 and this is maintained at day 12 (***Figure 3.24.F***). The relative expression levels of *Tuj1* obtained in this line are much lower than the ones of the Gfi1DZF6-PA line. In addition, here, there is an increase in expression levels over the time. At day 8, the difference in *Tuj1* expression between the wt Dox and Gfi1P2A Dox is small (***Figure 3.25***), which is not seen in the immunostaining analysis (***Figure 3.24.D***).

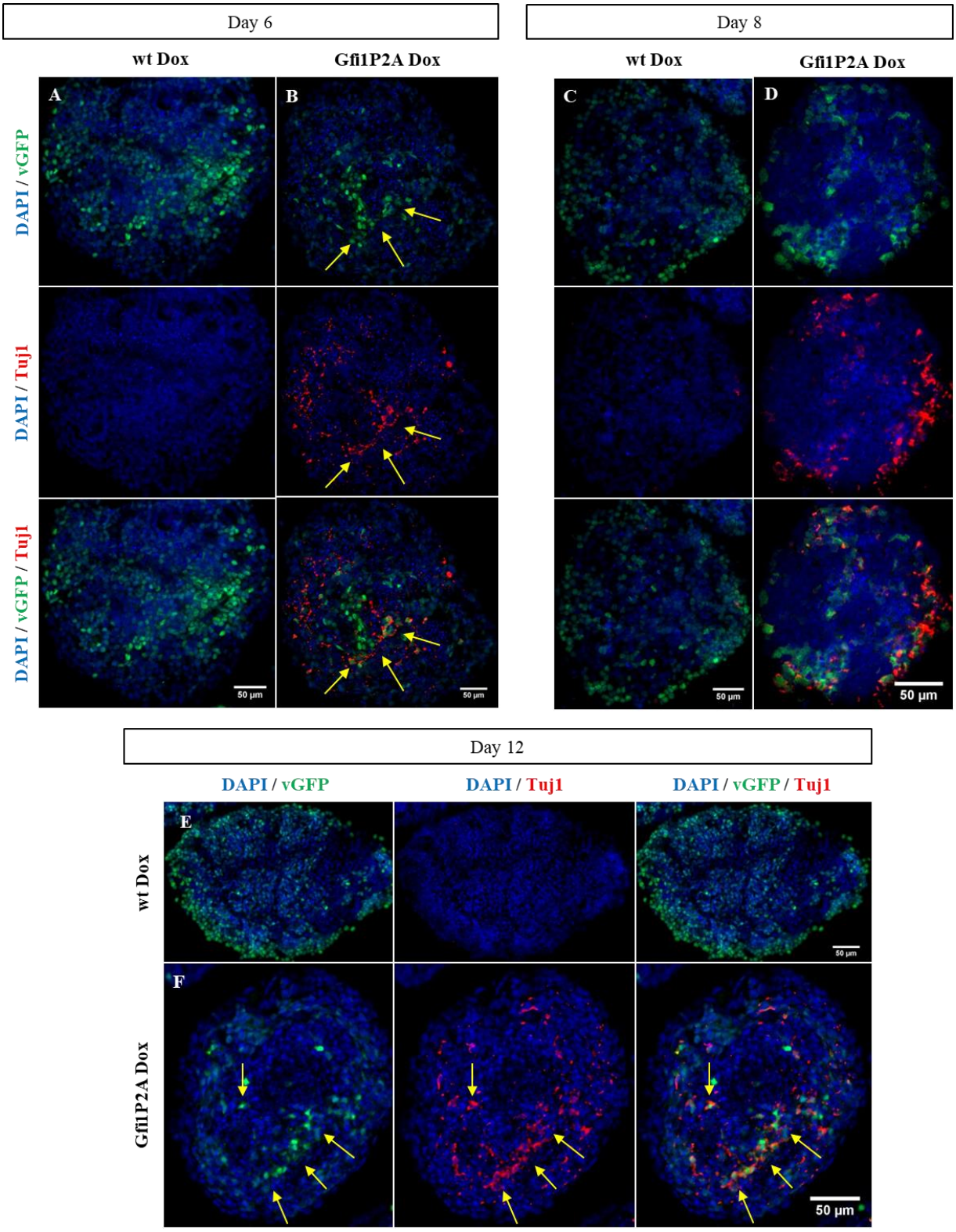

Figure 3.24 - Induction of Tuj1 expression in Gfi1P2A-PA: Representative images obtained from ICC for Tuj1 (red) from EBs treated for 2 (A, B), 4 (C, D) and 8 (E, F) days after Dox exposure in (A, C, E) wt Dox and (B, D, F) Gfi1P2ADox. Overexpressing cells were identified with vGFP (green) and nuclei with DAPI (blue). Scale bar set to 50µm. Arrows point out to co-localization.

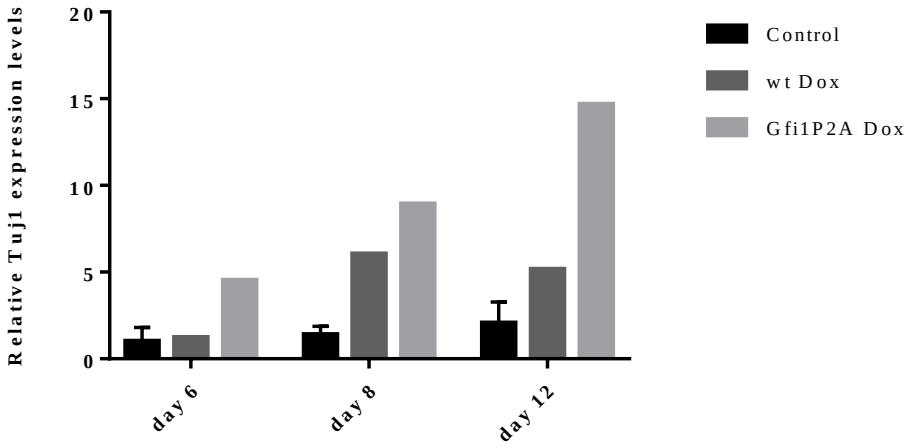

Figure 3.25 - *Tuj1* quantification present in Gfi1P2A-PA: Bar diagram showing the relative RNA levels of *Tuj1* in untreated EBs and EBs treated for 2, 4 and 8 days with Dox. Relative expression of the marker normalized to the mean of untreated EBs at day 6 (set to 1) (n=1).

At day 6, there is also some co-localization of Dcx with vGFP (***Figure 3.26.B***). At the following time points of analysis, there are more co-localizing cells (***Figure 3.26.D*** and ***F***). However, at day 12, a considerable number of non-inducible cells are positive for Dcx (***Figure 3.26.F***). By qPCR analysis, the *Dcx* expression pattern is opposite from the one obtained in the Gfi1DZF6 line (***Figure 3.27***), where the pick of expression happens at day 8 of differentiation.

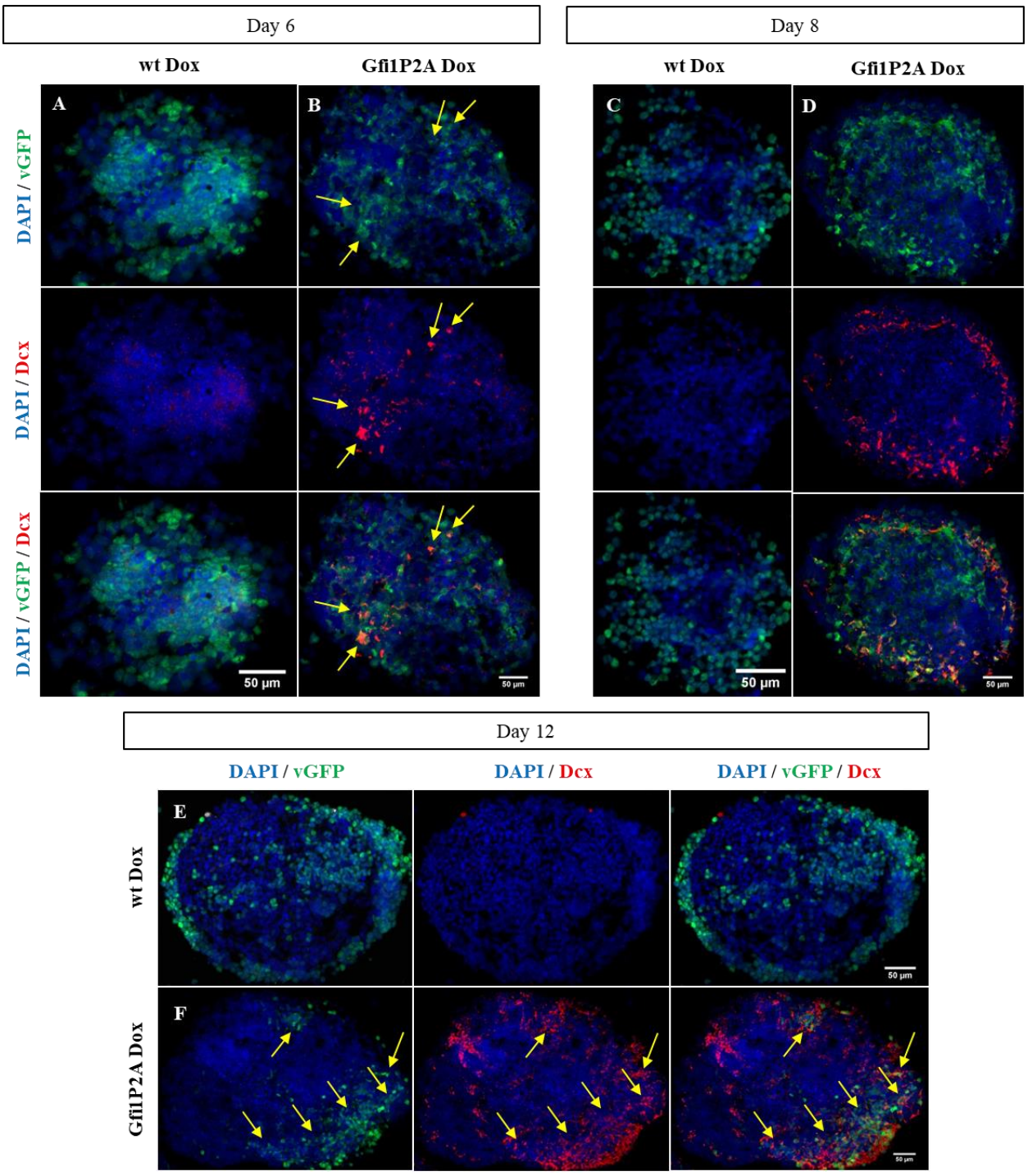

Figure 3.26 - Induction of Dcx expression in Gfi1P2A-PA: Representative images obtained from ICC for Dcx (red) from EBs treated for 2 (A, B), 4 (C, D) and 8 (E, F) days after Dox exposure in (A, C, E) wt Dox and (B, D, F) Gfi1P2A Dox. Overexpressing cells were identified with vGFP (green) and nuclei with DAPI (blue). Scale bar set to 50µm. Arrows point out to co-localization.

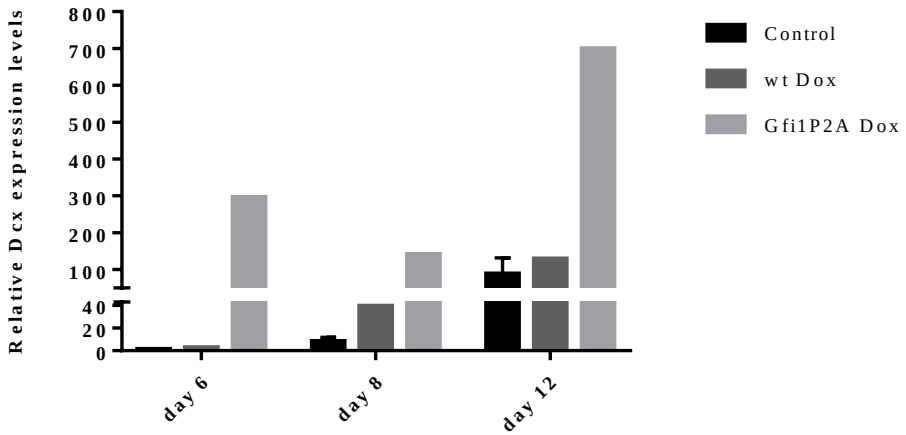

Figure 3.27 - *Dcx* quantification present in Gfi1P2A-PA: Bar diagram showing the relative RNA levels of *Dcx* in untreated EBs Dox and EBs treated for 2, 4 and 8 days with Dox. Relative expression of the marker normalized to the mean of untreated EBs at day 6 (set to 1) (n=1).

3.2.6. Gfi1P2A-PA: expression overview

Gfi1P2A-PA line exhibits neuronal marker expression (Tuj1 and Dcx), although the qPCR and immunostaining analysis do not give the same result regarding the Dcx marker.

Contrarily to immunostaining analysis, low levels of Lhx3 are detected by qPCR, with a different pattern from wt Dox. Also the HC marker Otof is detected by qPCR, however these levels are considerably lower than that observed for the positive control (wt Dox).

In relation to hair bundle-specific markers (Cdh23 and Espn), after day 6 repression appears to take place.

Our data shows that the SNAG domain, and consequently the recruitment of the epigenetic complex, is required for the repression of neuronal differentiation and a full activation of HC program. Additional experiments are needed to examine how the recruitment of the epigenetic complex influences the HC fate.

3.3. RECRUITMENT OF THE LSD1/COREST/HDACS1-2 COMPLEX

In order to scrutinize the mechanistic role of the epigenetic complex in question, we looked into deacetylation and demethylation processes individually by chemically inhibiting the HDACs and LDS1 function, respectively. The inhibitors used are known to cause HC differentiation impairments, suggesting that both processes are important for proper hearing function. Here we propose that deacetylation and demethylation processes play key roles in the repression of neuronal genes.

For this assay the treatment (Dox+inhibitor diluted in DMSO) was applied in the Gfi1-PA (wt) cell line, since it has its SNAG domain intact. The negative control consisted of untreated Gfi1-PA and the positive control of Gfi1-PA treated with Dox and 0.01% of DMSO. We chose a low and a high concentration of the inhibitors to certify that the effect observed by the analysis were due the inhibitors.

In this case, we focused on the qPCR analysis that provides a broader image of what is being expressed. Immunostaining analysis was used in case of doubts in the qPCR analysis. The markers used were Myo7a and Lhx3 (HC markers) and Tuj1 and Dcx (neuronal markers).

In the course of EBs development it was visible with naked eye the lower number of EBs after 48h of the treatment addition with the chemical inhibitors at different concentrations. Higher concentrations showed to be toxic and the cells either died or stopped proliferating. The treatment with the HDAC's inhibitor originated a more drastic effect on the number of EBs than with the LSD1 inhibitor treatment (see ***Figure 6.16*** on Supplemetary data). It was not possible to perform the third time point (day 12) owing to insufficient EBs treated with Dox+inhibitor obtained after day 8. An immunostaining analysis with Casp3 was performed for both EBs treated with the HDACs or LSD1 inhibitor.

3.3.1. HDACs inhibition

To assess the consequence of the HDACs on neuronal repression in a HC fate context, we used chemicals to inhibit HDACs recruitment. The histone deacetylases HDAC1 and HDAC2 remove active acetylation marks from histones within their proximity. TSA is a chemical inhibitor commonly used to block class I HDACs such as HDAC 1 and HDAC2. The concentrations used were 0.1µM and 1µM. Initially a concentration of 5µM of TSA was tested but the EBs, developing in this condition, were insufficient in number to take samples for analysis (cell death/inhibition of proliferation).

Despite the fact that, at day 8, there is a significant difference (P=0.032) on the percentage of live cells between the positive control (Dox) and the EBs treated with 1µM HDACi, the percentage of live cells detected by flow analysis does not justify the differences in the number of EBs observed during cell culture (see ***Figure 6.17.A*** in Supplementary data). Moreover, Casp3 (apoptosis marker) immunostaining analysis does not indicate a co-localization with vGFP (inducible cells) (see ***Figure 6.17.C***, ***D*** and ***E*** in Supplementary data). It was observed by microcopy analysis that the EBs treated with 1µM were smaller than the rest of the EBs and, in general, produced a predominantly peripheral vGFP pattern.

All treated conditions (Dox, 0.1µM HDACi, 1µM HDACi) show similar capability of transgenes induction, according to the percentage of GFP+ cells, presenting a clearly significant difference (P<0.001) from the control (see ***Figure 6.18*** in Supplementary data). According to qPCR, the EBs treated 1µM HDACi reveal unusually high *vGFP* expression levels, at day 6, originating significant differences from every other condition (P<0.001). At day 8 it normalizes (see ***Figure 6.19*** in Supplementary data).

Inhibition of deacetylation of target genes was then assessed by evaluating expression of HC and neuronal markers.

The quantification of relative RNA for *Myo7a* indicates that the samples treated with 0.1µM HDACi express this HC marker at day 8, which is significantly different from the control (P=0.009). Yet, the levels of expression are low and significant differences are found between these samples and Dox samples (P<0.001). Expression of *Myo7a* in 1µM HDACi samples is not detected (no significant differences with the control and significant differences at day 6 (P=0.042) and at day 8 (P<0.001) with Dox samples) (***Figure 3.28.A***). The immunostaining corroborates the qPCR analysis (see ***Figure 6.20*** for day 6 in Supplementary data; see ***Figure 3.28.B, C*** and ***D*** for day 8).

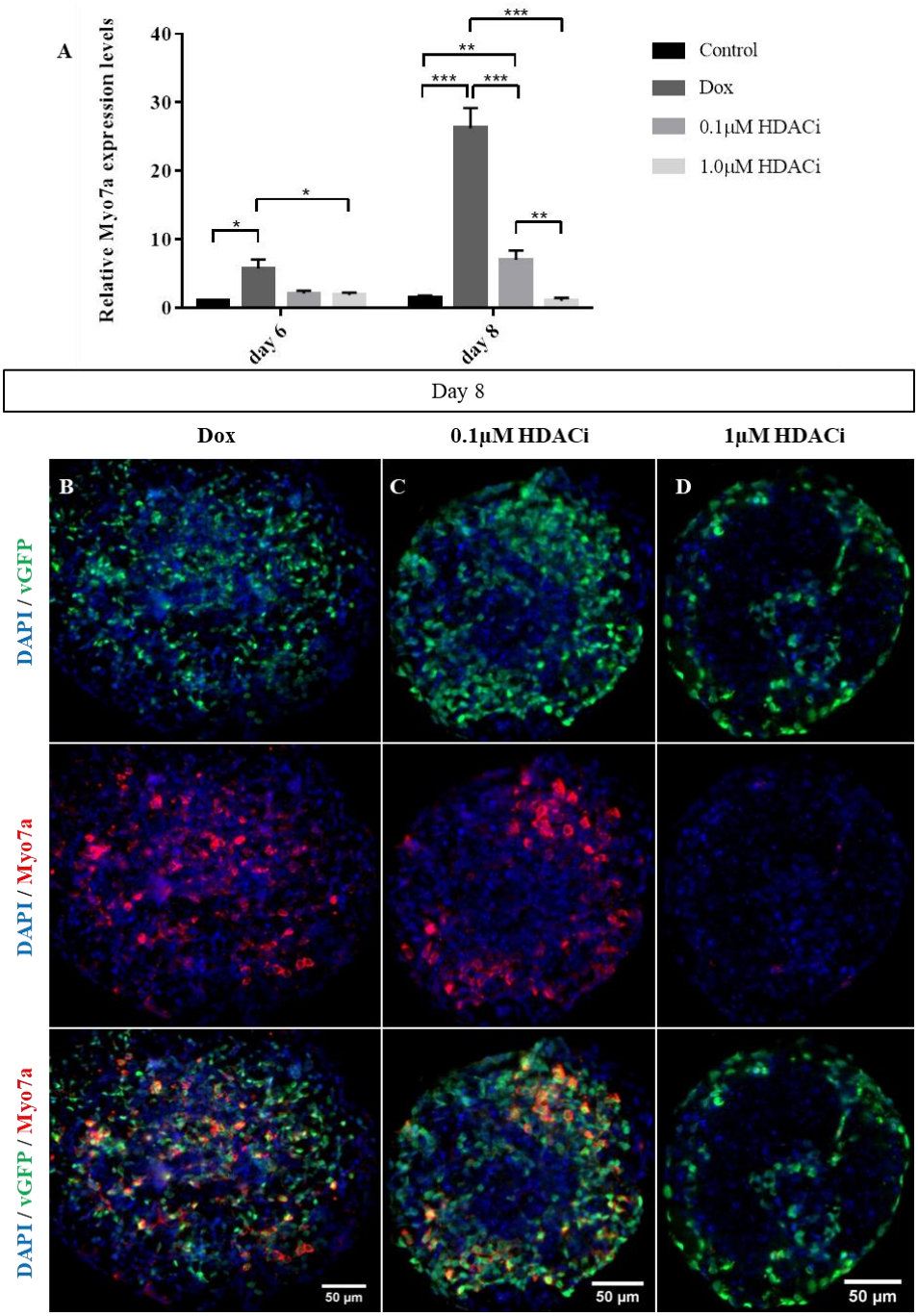

Figure 3.28 - Induction of Myo7a on Gfi1's HDACs inhibition: (A) Bar diagram showing the relative RNA levels of *Myo7a* in untreated EBs and EBs treated for 2 and 4 days with Dox, Dox+0.1µM HDACi or Dox+1µM HDACi (diluted in DMSO). Relative expression normalized to the mean of untreated EBs at day 6 (set to 1) ±SEM (n=4). Two-way ANOVA was used for statistical analysis (*0.01≤P<0.05; **0.001≤P<0.01; ***P<0.001). (B, C, D) Representative images of day 8 of development, obtained from ICC for Myo7a (red). EBs were treated for 2 and 4 days with Dox in (B) wt Dox, (C) Dox+0.1µM HDACi and (D) Dox+1µM HDACi. Overexpressing cells were identified with vGFP (green) and nuclei with DAPI (blue). Scale bar set to 50µm.

At day 6, low levels of *Myo6* expression are detected in 1µM HDACi, however no significant differences are found between *Myo6* expression in these cells and control cells. At day 8, *Myo6* is expressed in samples treated with 0.1µM HDACi. Nevertheless, *Myo6* levels are low and significant

differences are found with Dox samples (P<0.001). The 1µM HDACi samples maintain the expression levels observed at day 6 and significant differences are found with Dox (P<0.001) and 0.1µM HDACi cells (P=0.019), but no significant differences are found with control cells (***Figure 3.29***).

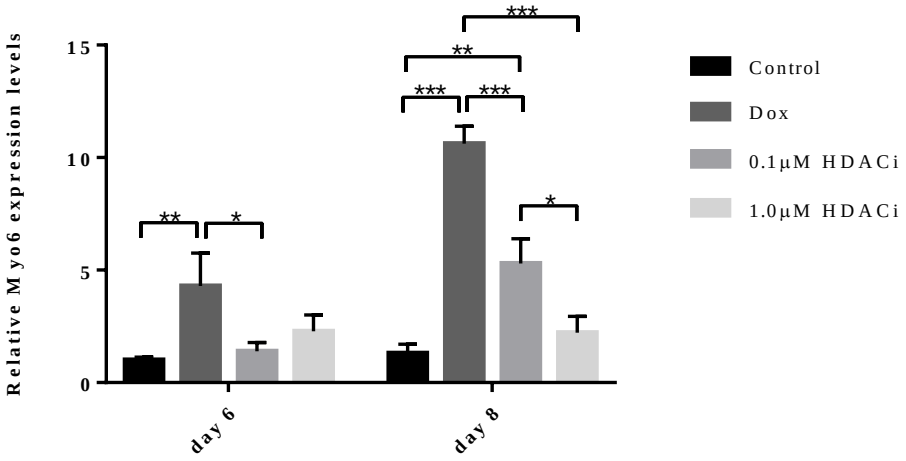

Figure 3.29 - *Myo6* quantification on Gfi1's HDACs inhibition: Bar diagram showing the relative RNA levels of *Myo6* in untreated EBs and EBs treated for 2 and 4 days with Dox, Dox+0.1µM HDACi or Dox+1µM HDACi (diluted in DMSO). Relative expression normalized to the mean of untreated EBs at day 6 (set to 1) ±SEM (n=4). Two-way ANOVA was used for statistical analysis (*0.01≤P<0.05; **0.001≤P<0.01; ***P<0.001).

Expression of *Lhx3* is found in samples treated with both concentrations of the inhibitor. However, at day 6, no significant differences are found compared with the control. At day 8, whereas 1µM HDACi samples maintain the *Lhx3* levels, the expression levels in 0.1µM HDACi samples follow the increase observed in Dox samples, and significant differences are found in relation to the control (P<0.001) (***Figure 3.30.A***). The immunostaining analysis shows that in fact EBs treated with 0.1µM HDACi express Lhx3. But there is no positive signal for this HC marker in the EBs treated with 1µM HDACi, which is in agreement with the non-significant differences found with the control (see ***Figure 6.21*** for day 6 in Supplementary data; see ***Figure 3.30.B, C*** and ***D*** for day 8).

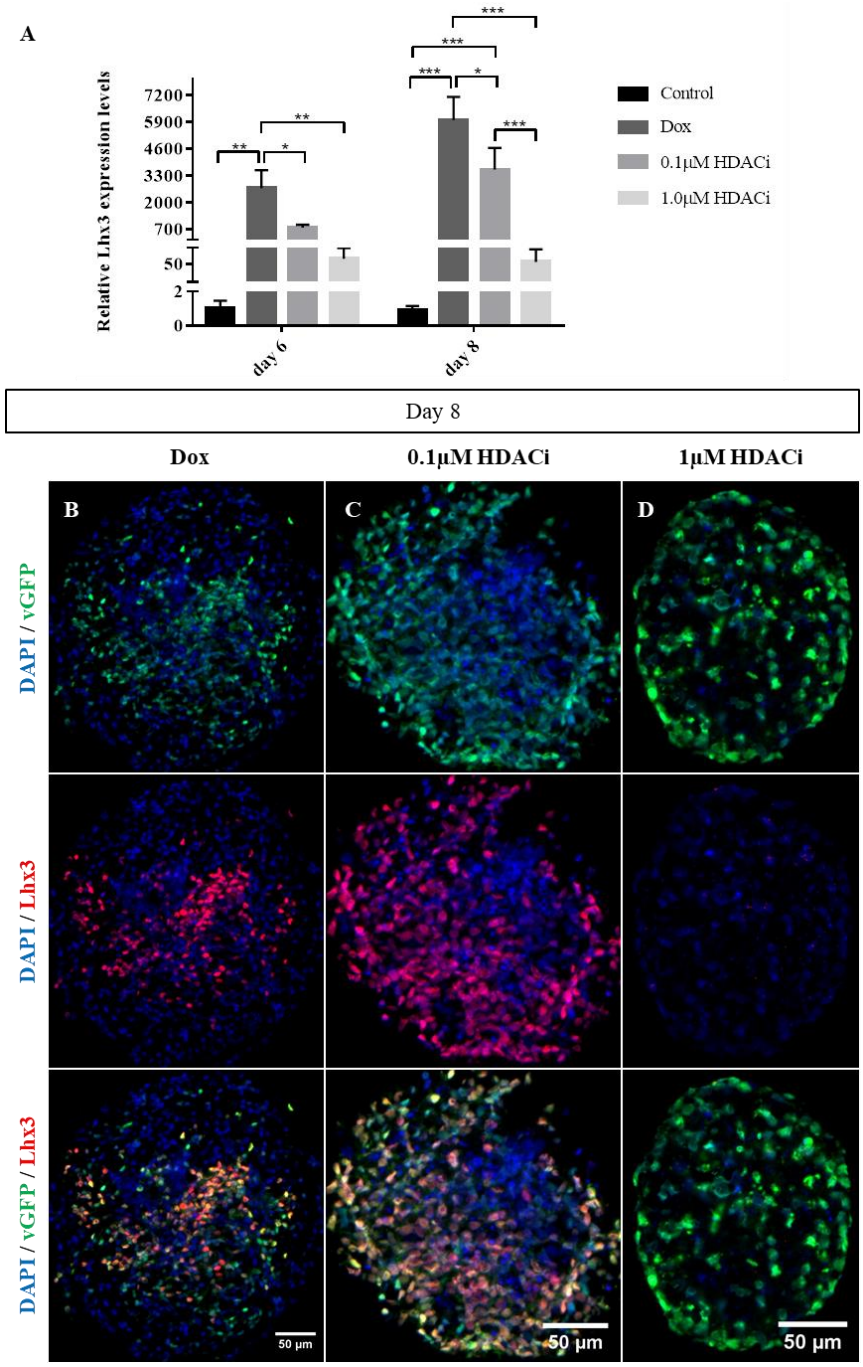

Figure 3.30 - Induction of Lhx3 on Gfi1's HDACs inhibition: (A) Bar diagram showing the relative RNA levels of *Lhx3* in untreated EBs and EBs treated for 2 and 4 days with Dox, Dox+0.1µM HDACi or Dox+1µM HDACi (diluted in DMSO). Relative expression normalized to the mean of untreated EBs at day 6 (set to 1) ±SEM (n=4). Two-way ANOVA was used for statistical analysis (*0.01≤P<0.05; **0.001≤P<0.01; ***P<0.001). (B, C, D) Representative images of day 8 of development, obtained from ICC for Lhx3 (red). EBs were treated for 2 and 4 days with Dox in (A) wt Dox, (B) Dox+0.1µM HDACi and (C) Dox+1µM HDACi. Overexpressing cells were identified with vGFP (green) and nuclei with DAPI (blue). Scale bar set to 50µm.

Regarding the relative expression levels of *Otof*, 0.1µM HDACi samples present low levels of this HC marker, at day 6. However no significant differences are found between these cells and control cells.

At day 8, there is a significant increase in the *Otof* expression levels in relation to control samples (P<0.001). No significant differences are found between 1µM HDACi and control cells (***Figure 3.31***).

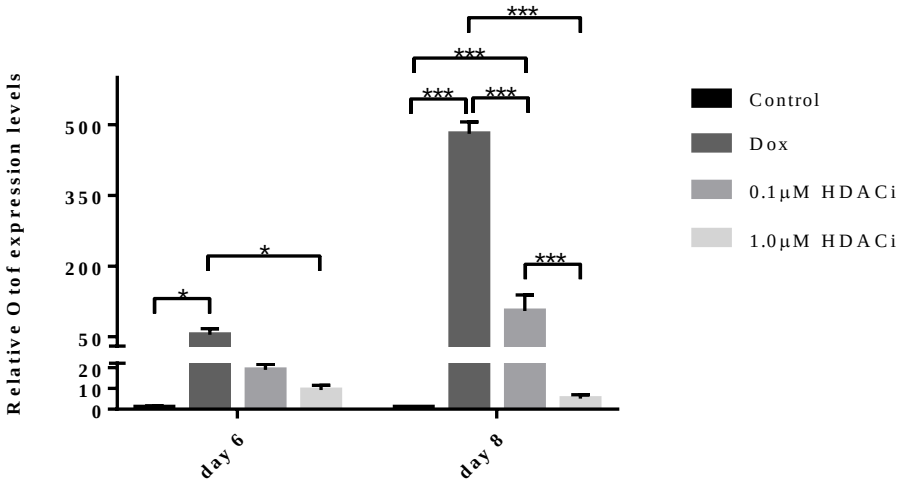

Figure 3.31 - *Otof* quantification on Gfi1's HDACs inhibition: Bar diagram showing the relative RNA levels of *Otof* in untreated EBs and EBs treated for 2 and 4 days with Dox, Dox+0.1µM HDACi or Dox+1µM HDACi (diluted in DMSO). Relative expression normalized to the mean of untreated EBs at day 6 (set to 1) ±SEM (n=4). Two-way ANOVA was used for statistical analysis (*0.01≤P<0.05; ***P<0.001).

Regarding to hair bundle-specific markers, at day 6, *Cdh23* is detected in samples treated with HDACi, with similar levels of Dox samples. However, no significant differences are found with the control cells. At day 8, in 0.1µM HDACi samples there is a significant increase of *Cdh23* expression levels, compared to control samples (P=0.007) (***Figure 3.32.A***).

About *Espn*, at day 6, all treated conditions (Dox, 0.1µM HDACi and 1µM HDACi) present significant differences with the control (P<0.001) and there is no significant differences between the three treated conditions. At day 8, 0.1µM HDACi samples maintain the Dox's levels of *Espn* expression, while there is a significant decrease in expression of *Espn* in 1µM HDACi samples in relation to the control samples (P=0.034) (***Figure 3.32.B)***

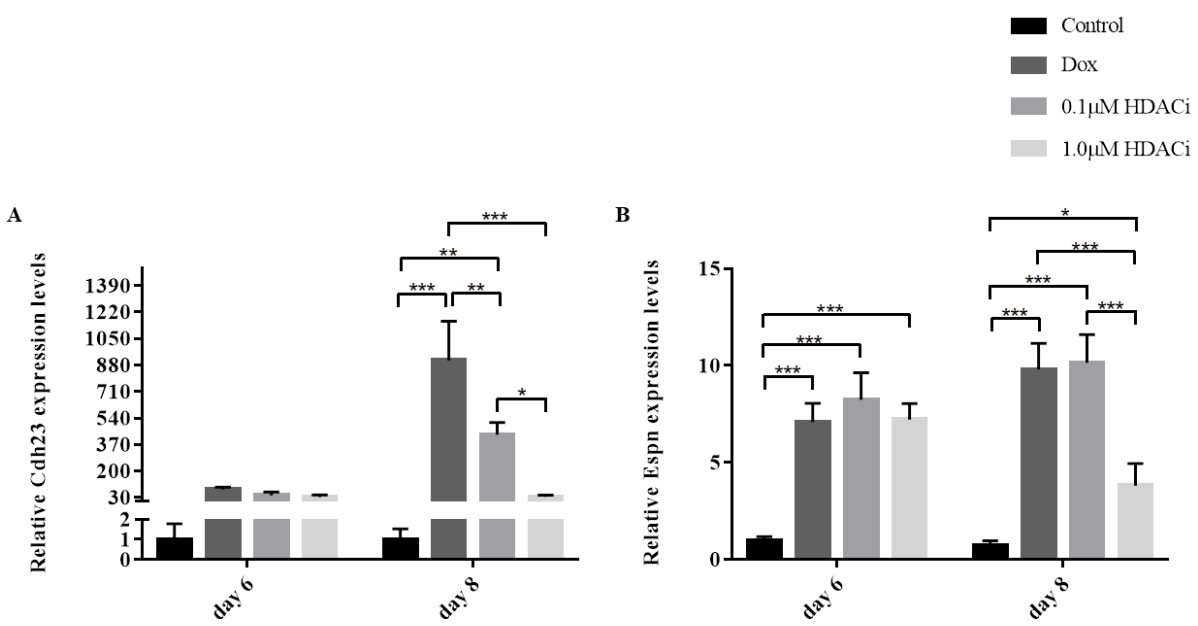

Figure 3.32 - Hair bundle-specific markers quantification on Gfi1's HDACs inhibition: (A, B) Bar diagrams showing the relative RNA levels of (A) *Cdh23* and (B) *Espn* in untreated EBs and EBs treated for 2 and 4 days with Dox, Dox+0.1µM HDACi or Dox+1µM HDACi (diluted in DMSO). Relative expression normalized to the mean of untreated EBs at day 6 (set to 1) ±SEM (n=4). Two-way ANOVA was used for statistical analysis (*0.01≤P<0.05; **0.001≤P<0.01; ***P<0.001).

Concerning the neuronal markers, at day 6, it is observed low levels of *Tuj1* in 1µM HDACi samples, and significant differences are found between these cells and the other conditions. However, at day 8, no *Tuj1* expression is detected (*Figure **3.33.A***). By immunostaining analysis most EBs treated with 1µM HDACi do not express Tuj1, and the co-localization (with vGFP) is rare (see *Figure **3.33.B, C*** and ***D*** for day 6; see ***Figure 6.22*** for day 8 in Supplementary data).

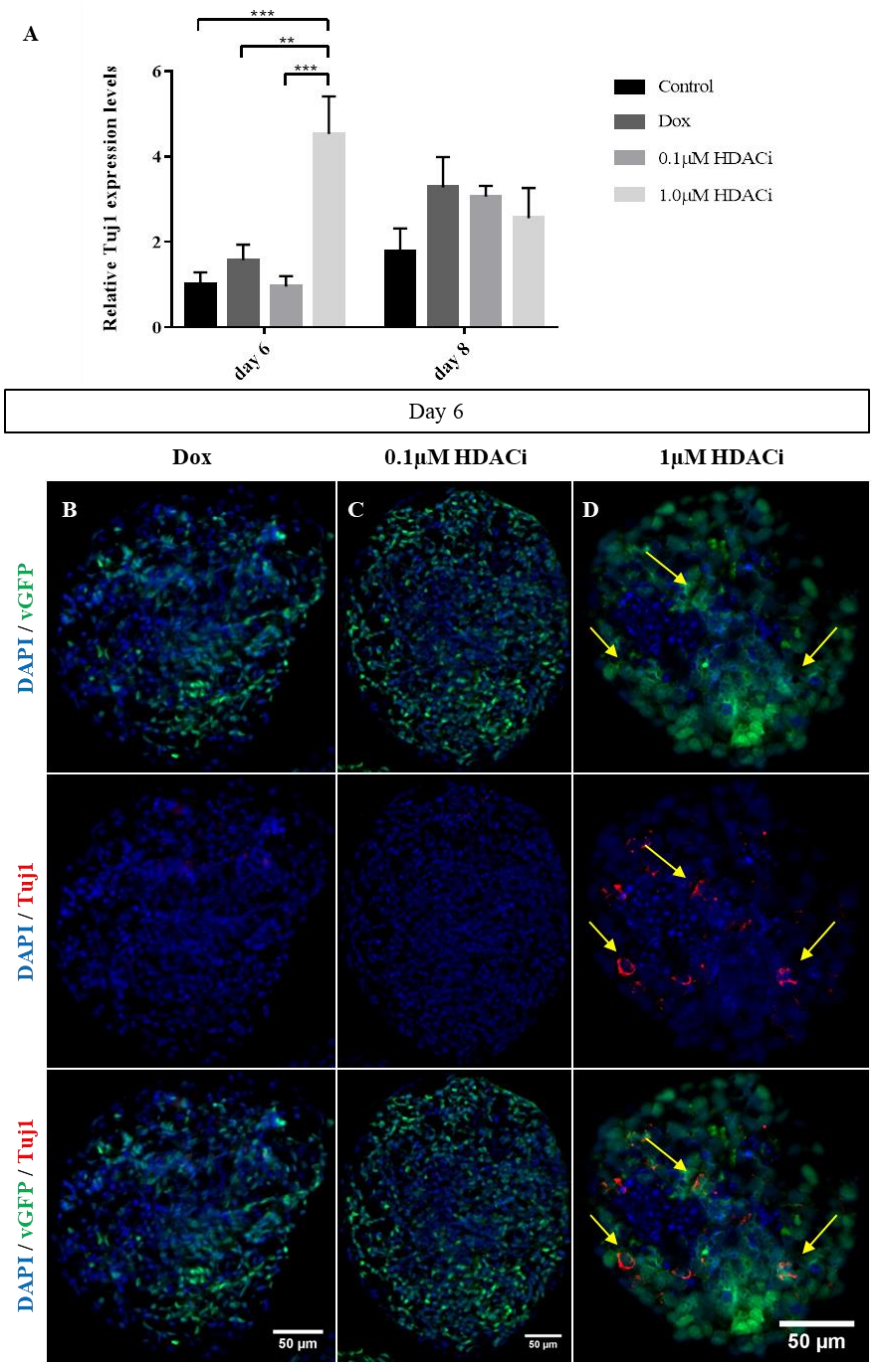

Figure 3.33 - Induction of Tuj1 on Gfi1's HDACs inhibition: (A) Bar diagram showing the relative RNA levels of *Tuj1* in untreated EBs and EBs treated for 2 and 4 days with Dox, Dox+0.1µM HDACi or Dox+1µM HDACi (diluted in DMSO). Relative expression normalized to the mean of untreated EBs at day 6 (set to 1) ±SEM (n=4). Two-way ANOVA was used for statistical analysis (**0.001≤P<0.01; ***P<0.001). (B, C, D) Representative images of day 6 of development, obtained from ICC for Tuj1 (red). EBs were treated for 2 and 4 days with Dox in (B) wt Dox, (C) Dox+0.1µM HDACi and (D) Dox+1µM HDACi. Overexpressing cells were identified with vGFP (green) and nuclei with DAPI (blue). Scale bar set to 50µm. Arrows point out to co-localization.

Despite the fact that, for *Dcx* expression, Dox samples are significant different from the control (***Figure 3.34.A***), these different levels of expression are not observed by immunostaining (as previously

seen during Characterization of the Knock-in Lines section). No significant differences are found between HDACi samples and the control (***Figure 3.34.A***), as the immunostaining analysis demonstrate (see ***Figure 3.34.B, C*** and ***D*** for day 8; see ***Figure 6.23*** for day 6 in Supplementary data).

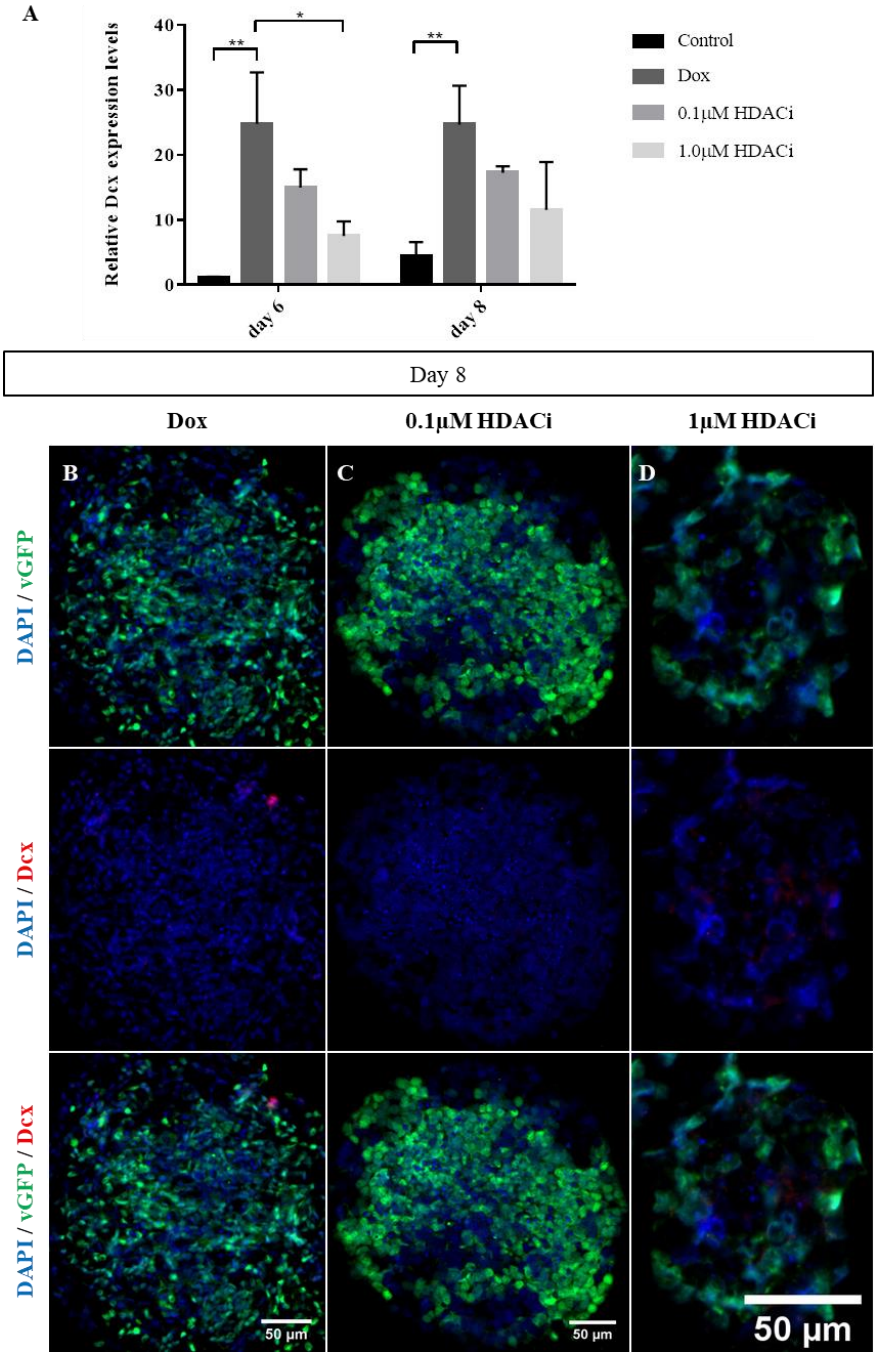

Figure 3.34 - Induction of Dcx on Gfi1's HDACs inhibition: (A) Bar diagram showing the relative RNA levels of *Dcx* in untreated EBs and EBs treated for 2 and 4 days with Dox, Dox+0.1µM HDACi or Dox+1µM HDACi (diluted in DMSO). Relative expression normalized to the mean of untreated EBs at day 6 (set to 1) ±SEM (n=4). Two-way ANOVA was used for statistical analysis (*0.01≤P<0.05; **0.001≤P<0.01). (B, C, D) Representative images of day 8 of development, obtained from

ICC for Dcx (red). EBs were treated for 2 and 4 days with Dox in (B) wt Dox, (C) Dox+0.1µM HDACi and (D) Dox+1µM HDACi. Overexpressing cells were identified with vGFP (green) and nuclei with DAPI (blue). Scale bar set to 50µm.

3.3.2. HDACs inhibition: expression overview

The inhibition of HDACs provoke a reduction of proliferation/increase of cell death, but whether this effect is specifically happening for cells undergoing HC differentiation or if it is a side effect is not clear.

Except for Espn, a gradient of HDACs inhibition on HC markers expression it is detectable, where the increase of the inhibitor drives to the decrease of HC marker expression.

Contrarily to the expected, the inhibition of HDACs did not fail to repress neuronal expression, except in some EBs that expressed Tuj1, mainly at day 6. Additional steps in the mechanism to repress neuronal genes might be required.

3.3.3. LSD1 inhibition

Besides the histones deacetylases the complex LSD1-CoRest-HDACs1-2 also includes the histone demethylase LSD1 that acts as a transcriptional inhibitor or facilitator depending on the context. SP2509 is an LDS1 inhibitor that attenuates its binding to CoRest, causing an increase of methylation. Therefore failure of repression of neuronal genes by the epigenetic complex and consequently failure of HC differentiation is possible. This inhibitor was used in concentrations of 0.1µM and 1µM.

The difference in the number of EBs, easily seen with the naked eye during development of the cultures, is not explained by cell death, since we observe by flow cytometry analysis, that all conditions (control, Dox, 0.1µM LSD1 and 1µM LSD1) present high percentages of life cells (see ***Figure 6.24.A*** in Supplementary data). In addition, the immunostaining with Casp3 (apoptosis marker) does not show a co-localization with vGFP (see ***Figure 6.24.C***, ***D*** and ***E*** in Supplementary data).

The flow cytometry analysis also shows that the treatments (Dox, 0.1µM LDS1i, 1µM LSD1i) have high capacity of transgene induction, indicated by the high percentage of GFP+ cells (see ***Figure 6.25*** in Supplementary data) and by the *vGFP* quantitative analysis (see ***Figure 6.26*** in Supplementary data).

The role of LSD1 as a neuronal repressor in HC differentiation context, through its inhibition, was then examined over HC and neuronal markers expression.

Myo7a expression is detected in the samples treated with LDS1i and the expression levels decrease with a higher concentration. At day 6, besides the fact that treated cells (Dox, 0.1µM LSD1i and 1µM LSD1i) do not present significant differences amongst them, 1µM LSD1i samples are not significantly different from the control samples (***Figure 3.35.A***). Moreover, with the immunostaining performed, a clear difference between Dox and LSD1i samples was not observed (see ***Figure 3.35.B, C*** and ***D*** for day 8; see ***Figure 6.27*** for day 6 in Supplementary data).

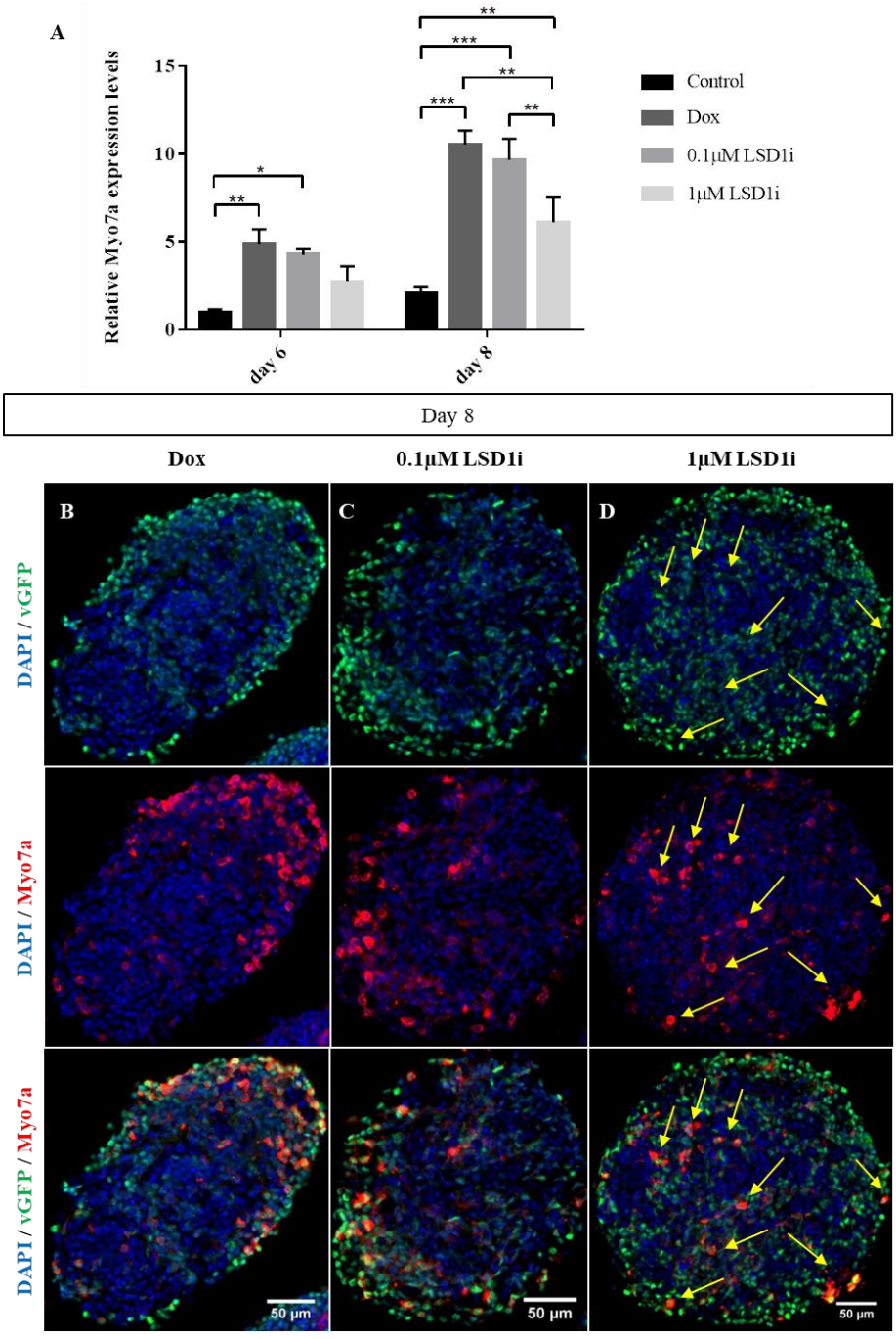

Figure 3.35 - Induction of Myo7a on Gfi1's LSD1 inhibition: (A) Bar diagram showing the relative RNA levels of *Myo7a* in untreated EBs and EBs treated for 2 and 4 days with Dox, Dox+0.1µM LSD1i or Dox+1µM LSD1i (diluted in DMSO). Relative expression normalized to the mean of untreated EBs at day 6 (set to 1) ±SEM (n=4). Two-way ANOVA was used for statistical analysis (*0.01≤P<0.05; **0.001≤P<0.01). (B, C, D) Representative images of day 8 of development, obtained from ICC for Myo7a (red). EBs were treated for 2 and 4 days with Dox in (B) wt Dox, (C) Dox+0.1µM LSD1i and (D) Dox+1µM LSD1i. Overexpressing cells were identified with vGFP (green) and nuclei with DAPI (blue). Scale bar set to 50µm. Arrows point out to co-localization.

The qPCR analysis indicates low levels of *Myo6* in LSD1i samples, however, these cells do not present significant differences from the control cells (***Figure 3.36***).

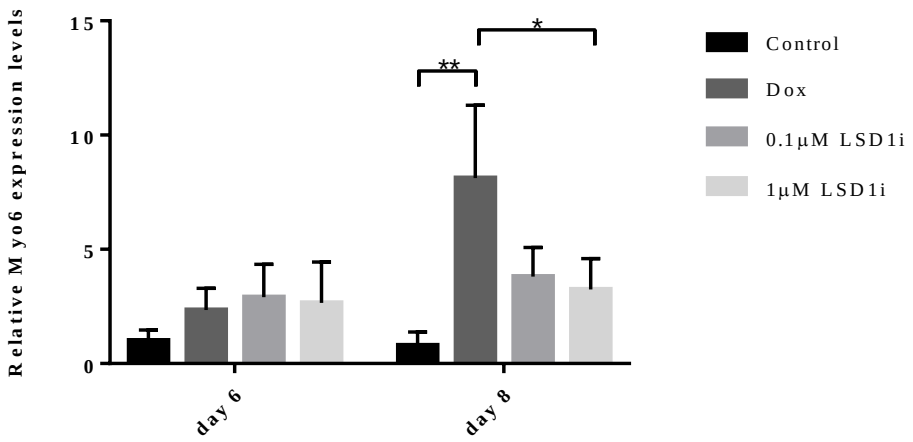

Figure 3.36 - *Myo6* quantification on Gfi1's LSD1 inhibition: Bar diagram showing the relative RNA levels of *Myo6* in untreated EBs and EBs treated for 2 and 4 days with Dox, Dox+0.1µM LSD1i or Dox+1µM LSD1i (diluted in DMSO). Relative expression normalized to the mean of untreated EBs at day 6 (set to 1) ±SEM (n=4). Two-way ANOVA was used for statistical analysis (*$0.01 \leq P < 0.05$; **$0.001 \leq P < 0.01$).

At day 6, *Lhx3* expression levels in treated samples are not significantly different from the control, but it is visible that expression of this marker is detected in LSD1i samples as in Dox samples. At day 8, *Lhx3* expression levels in LSD1i samples are significantly increased in relation to control samples ($P<0.001$). To note that, 1µM LSD1i cells present higher *Lhx3* levels than 0.1µM LSD1i cells (***Figure 3.37.A***). By immunostaining analysis it can be observed that there is more cells co-localizing Lhx3 with vGFP at day 8 (see ***Figure 3.37.B, C*** and ***D*** for day 8; see ***Figure 6.28*** for day 6 in Supplementary data).

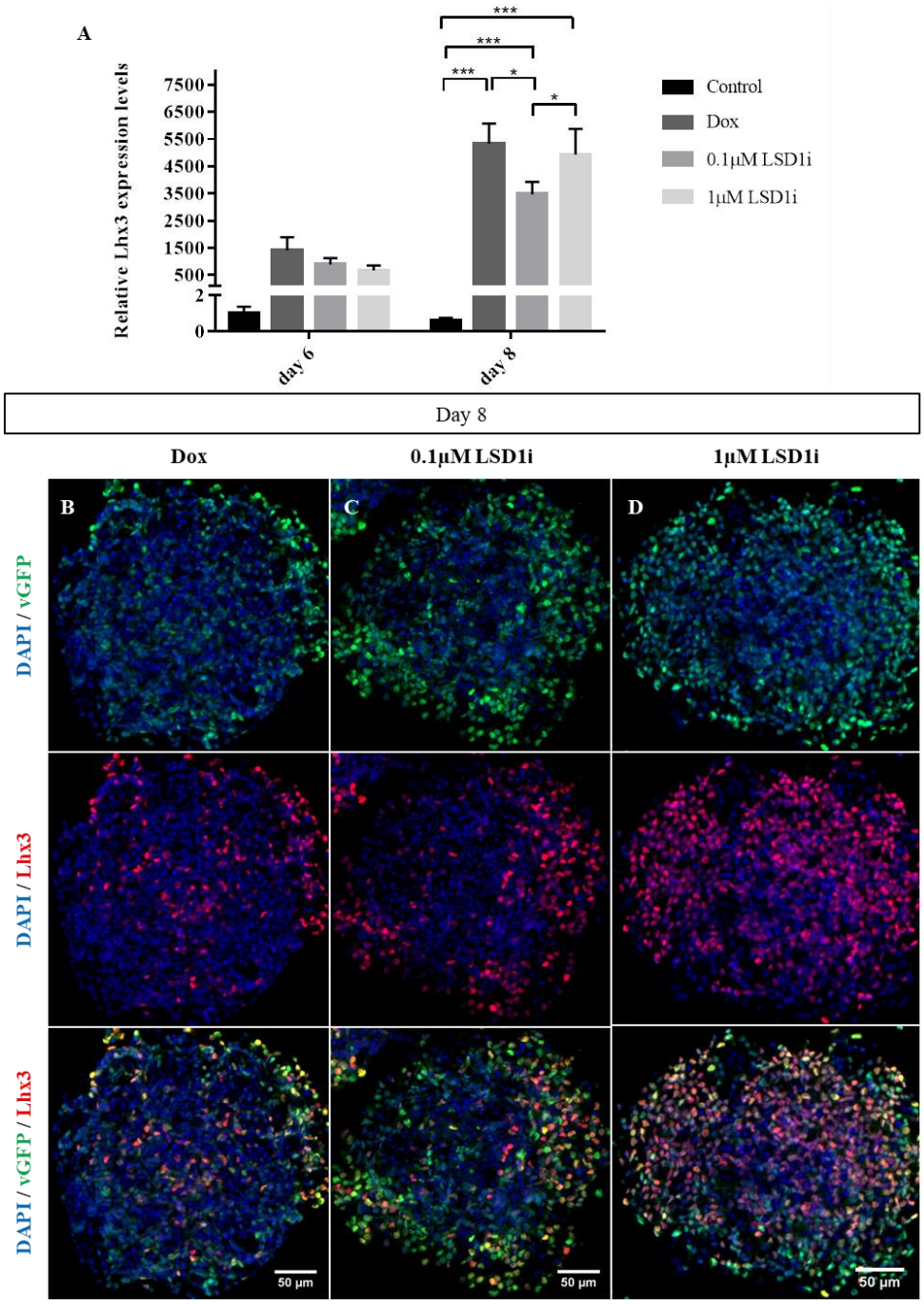

Figure 3.37 - Induction of Lhx3 on Gfi1's LSD1 inhibition: (A) Bar diagram showing the relative RNA levels of *Lhx3* in untreated EBs and EBs treated for 2 and 4 days with Dox, Dox+0.1µM LSD1i or Dox+1µM LSD1i (diluted in DMSO). Relative expression normalized to the mean of untreated EBs at day 6 (set to 1) ±SEM (n=4). Two-way ANOVA was used for statistical analysis (*$0.01 \leq P < 0.05$; **$0.001 \leq P < 0.01$). (B, C, D) Representative images of day 8 of development, obtained from ICC for Lhx3 (red). EBs were treated for 2 and 4 days with Dox in (B) wt Dox, (C) Dox+0.1µM LSD1i and (D) Dox+1µM LSD1i. Overexpressing cells were identified with vGFP (green) and nuclei with DAPI (blue). Scale bar set to 50µm.

Low levels of *Otof* expression appear at day 6, although no significant differences are found with the control. At day 8, there is a significant increase in *Otof* expression levels in LSD1i cells, relative to control cells. The expression decreases with the increase in concentration of the inhibitor (***Figure 3.38***).

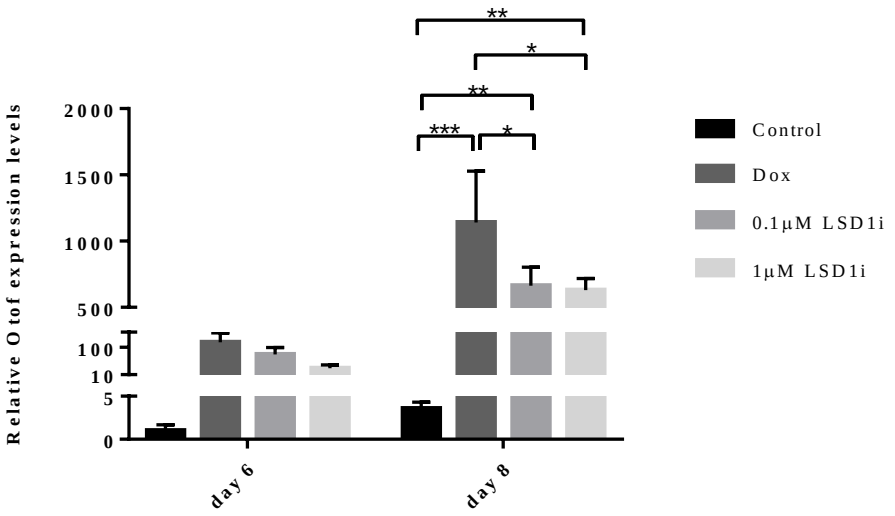

Figure 3.38 - *Otof* quantification on Gfi1's LSD1 inhibition: Bar diagram showing the relative RNA levels of *Otof* in untreated EBs and EBs treated for 2 and 4 days with Dox, Dox+0.1µM LSD1i or Dox+1µM LSD1i (diluted in DMSORelative expression normalized to the mean of untreated EBs at day 6 (set to 1) ±SEM (n=4). Two-way ANOVA was used for statistical analysis (*0.01≤P<0.05; **0.001≤P<0.01; ***P<0.001).

Regarding *Cdh23* expression, low expression levels are observed at day 6, however no significant differences are found between treated (Dox, 0.1µM LSD1i and 1µM LSD1i) and untreated cells (control). At day 8, 1µM LSD1i samples expression levels increase significantly, regarding control cells (P=0.007) (***Figure 3.39.A***).

About *Espn* expression, it is visible that LSD1i samples do not present significant differences in relation to Dox samples. In addition, 0.1µM LSD1i samples exhibit higher expression levels of *Espn* (***Figure 3.39.B***).

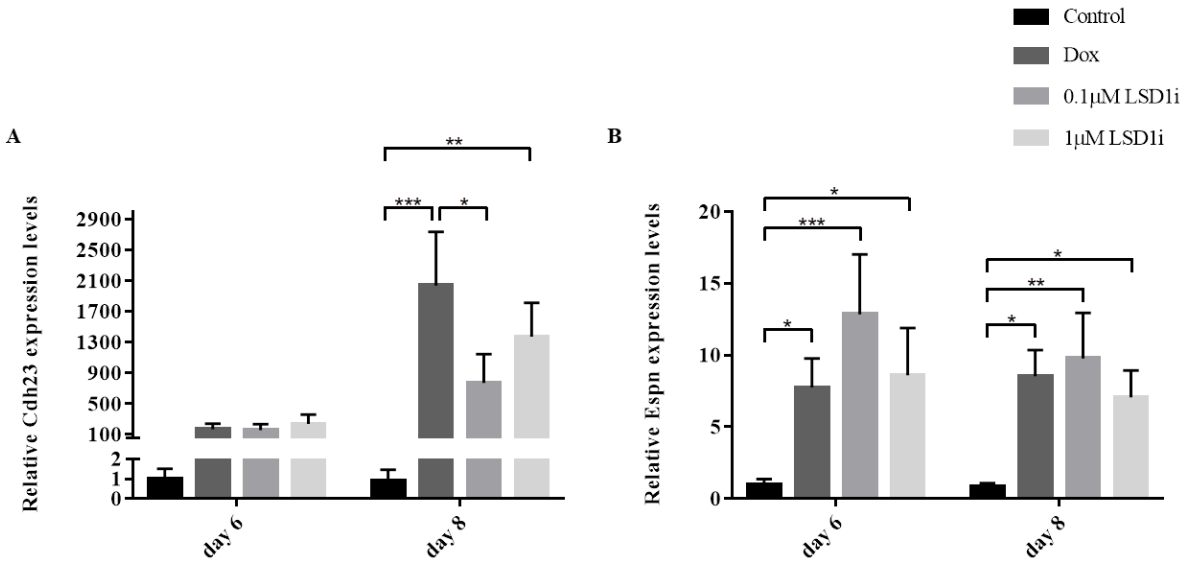

Figure 3.39 - Hair bundle-specific markers quantification on Gfi1's LSD1 inhibition: (A, B) Bar diagrams showing the relative RNA levels of (A) *Cdh23* and (B) *Espn* in untreated EBs and EBs treated for 2 and 4 days with Dox, Dox+0.1µM LSD1i or Dox+1µM LSD1i (diluted in DMSO). Relative expression normalized to the mean of untreated EBs at day 6 (set to 1) ±SEM (n=4). Two-way ANOVA was used for statistical analysis (*0.01≤P<0.05; **0.001≤P<0.01; ***P<0.001).

Concerning the neuronal marker *Tuj1*, no expression is detected by qPCR analysis (***Figure 3.40***). However, by immunostaining analysis co-localization between Tuj1 and vGFP in LSD1i samples is observed (see ***Figure 3.40.B, C*** and ***D*** for day 8; see ***Figure 6.29*** for day 6 in Supplementary data).

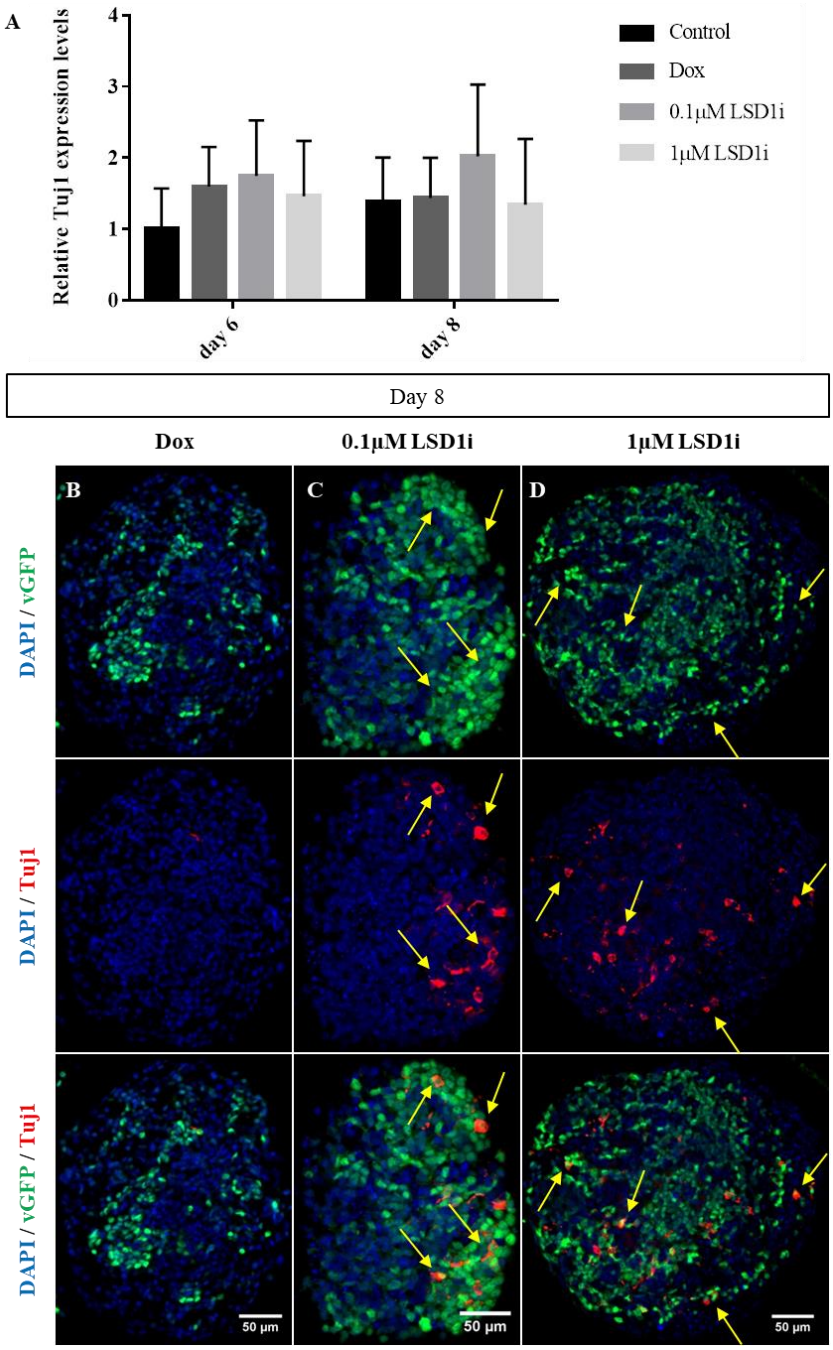

Figure 3.40 - Induction of Tuj1 on Gfi1's LSD1 inhibition: (A) Bar diagram showing the relative RNA levels of *Tuj1* in untreated EBs and EBs treated for 2 and 4 days with Dox, Dox+0.1µM LSD1i or Dox+1µM LSD1i (diluted in DMSO). Relative expression normalized to the mean of untreated EBs at day 6 (set to 1) ±SEM (n=4). Two-way ANOVA was used for statistical analysis (*0.01≤P<0.05; **0.001≤P<0.01). (B, C, D) Representative images of day 8 of development, obtained from ICC for Tuj1 (red). EBs were treated for 2 and 4 days with Dox in (B) wt Dox, (C) Dox+0.1µM LSD1i and (D) Dox+1µM LSD1i. Overexpressing cells were identified with vGFP (green) and nuclei with DAPI (blue). Scale bar set to 50µm. Arrows point out to co-localization.

Low *Dcx* expression levels are detected with qPCR (***Figure 3.41***) although no signal is observed with immunostaining analysis (see ***Figure 3.41.B, C*** and ***D*** for day 8; see ***Figure 6.30*** for day 6 in Supplementary data). Again, the levels observed in Dox cells do not correspond with previous findings in the lab.

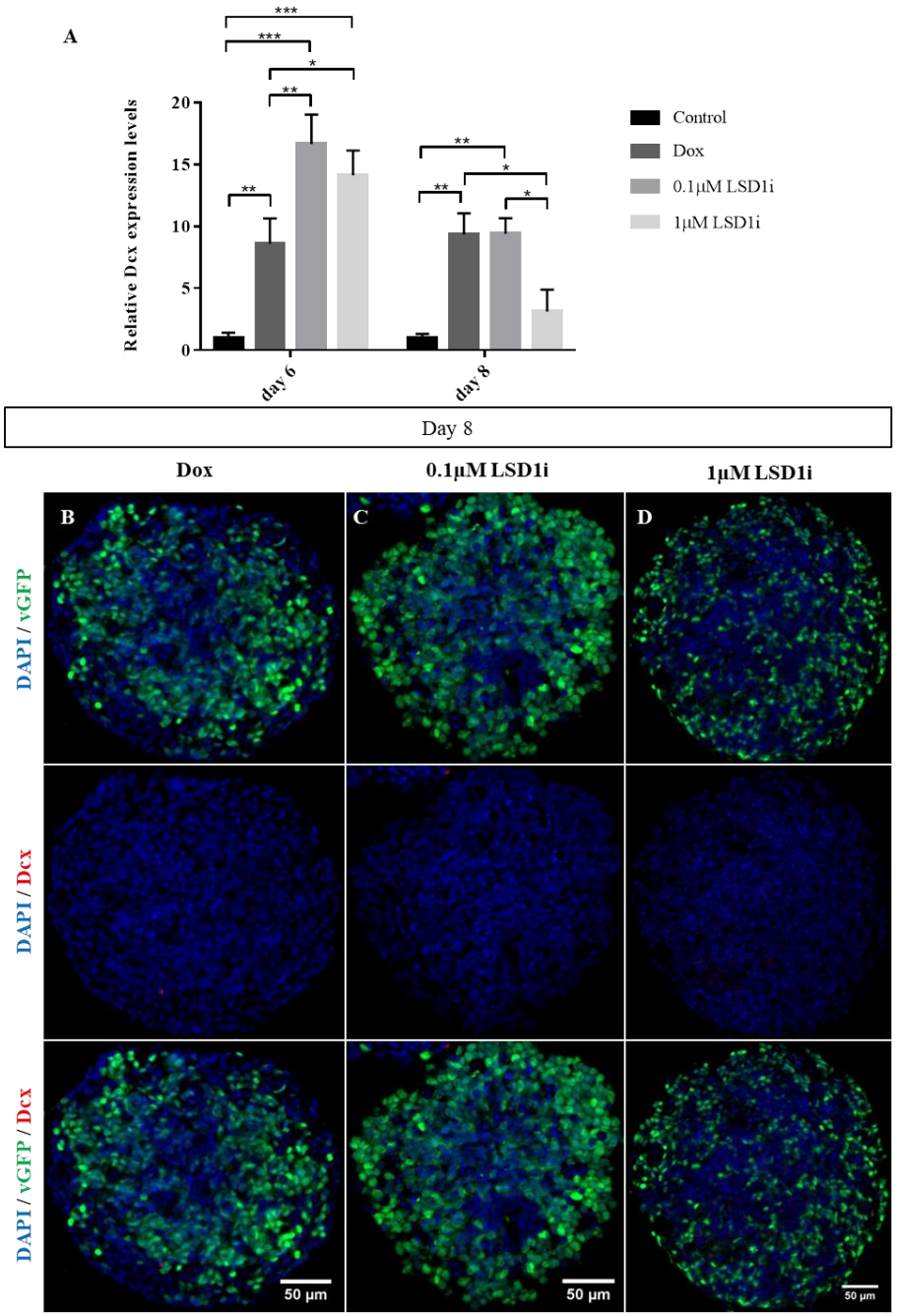

Figure 3.41 - Induction of Dcx on Gfi1's LSD1 inhibition: (A) Bar diagram showing the relative RNA levels of *Dcx* in untreated EBs and EBs treated for 2 and 4 days with Dox, Dox+0.1µM LSD1i or Dox+1µM LSD1i (diluted in DMSO). Relative expression normalized to the mean of untreated EBs at day 6 (set to 1) ±SEM (n=4). Two-way ANOVA was used for statistical analysis (*0.01≤P<0.05; **0.001≤P<0.01). (B, C, D) Representative images of day 8 of development, obtained from ICC for Dcx (red). EBs were treated for 2 and 4 days with Dox in (B) wt Dox, (C) Dox+0.1µM LSD1i and (D) Dox+1µM LSD1i. Overexpressing cells were identified with vGFP (green) and nuclei with DAPI (blue). Scale bar set to 50µm.

3.3.4. LSD1 inhibition: expression overview

As in the HDACs inhibition assay, according to our data, the low number of EBs produced is not explained by cell death.

In general, there is a gradient of HC marker expression that decreases with the increase of LSD1 inhibitor, except for Lhx3, Cdh23 and Espn.

Regarding neuronal marker expression, the results show that Tuj1 is expressed, although it is not detectable by qPCR analysis. In turn, Dcx is not detected by immunostaining analysis but significant differences are found with the negative control in the qPCR analysis. The fact that these differences are also found between the positive and negative control (that should behave the same regarding expression of neuronal markers) brings doubts to the analysis.

4. DISCUSSION

4.1. GFI1 KNOCK-IN LINES: CHARACTERIZATION

In this study, three Gfi1 cell lines, constituted by the combination of the transcription factors Gfi1-Pou4f3-Atoh1, known for, together, to be determinant for HC differentiation, were chosen by their Gfi1 variation and characterized in the first eight days of development (days 6, 8 and 12, after EB formation), after Dox-induction of the transgenes, through immunocytochemistry and qPCR. HC differentiation seems to happen by repression of the neuronal differentiation program, and Gfi1 was proven to have a key role in these processes. In the absence of Gfi1 Atoh1 and Pou4f3 neuronal differentiation is induced. Therefore, looking to Gfi1 structure is an essential step to understand the mechanism behind the regeneration of HCs.

The different forms of Gfi1 where chosen in order to focus at each region of this transcription factor: zinc finger domain (Gfi1DZF6 – zinc fingers removed), SNAG domain (Gfi1P2A – mutation proline to alanine at amino acid 2) and intermediary region (Gfi1b knock-in at Gfi1 locus). HC and neuronal expression was analyzed by comparison to an intact Gfi1 line (wt), on protein (Myo7a, Myo6, Lhx3, Tuj1 and Dcx) and gene (*Myo7a*, *Myo6*, *Lhx3*, *Otof*, *Cdh23*, *Espn*, *Tuj1* and *Dcx*) expression.

4.1.1. Problems and limitations to the interpretation

One limitation of the results to be taken into account is the lack of replicates. The outcome presented in this section (4.1.) did not show enough relevant data to pursue its consolidation during this particular thesis, besides the time constraints associated with it. Consequently, a qualitative interpretation is more adjusted than a quantitative interpretation of the data. However, even this interpretation has to be cautious and based on existent literature.

It is important to mention the variability between samples in GFP expression, which indicates the degree of induction of the transgenes. In general, throughout the days of development analyzed, the differences between wt Gfi1 and modified Gfi1 samples become evident. The GFP expression should not be affected. Consequently, it can affect the expression of HC/neuronal markers. With the production of replicates it would be clear if the GFP differences, in relation to the wt Gfi1, are constant or if there were technical errors handling the lines.

A special caution had to be taken with Gfi1b-PA line. During maintenance and growth of the cells, it generated a lower number of cells. However at any time point it affected the cells passage process (that requires a minimum number of cells), ES cells behave in the same manner and therefore no visible differences should be noticed. Furthermore it is the only cell line displaying such low amounts of GFP. One explanation is that the insertion of Gfi1b at the Gfi1 locus affected other enhancers/regulatory regions that may change their interactions with GFP. Another influencing factor could be that the GFP overexpressing cells were dying, which we tested by immunostaining with Casp3 (apoptosis marker) that confirmed the observations by flow cytometry analysis, where Dox-inducible cells did not show higher levels of cell death. We cannot rule out the hypothesis that other cell death mechanism may be taking part, not marked by Casp3, such as necrosis. In order to a better comparison between wt and Gfi1b samples, after different approaches, the normalization of the values (obtained by qPCR) for the percentage of GFP+ cells at day 6, showed to be more adjusted.

Specifically for quantification of Dcx by qPCR, high CT values (above 29 cycles) were obtained for samples expressing Dcx. Ct value is the cycle number where the fluorescence generated by the PCR produced is distinguishable from the background noise and it is inversely proportional to the amount of target sequence. Although it was verified that higher values are common to happen for this primer, Ct values above 29 bring uncertainties about the expression of this neuronal marker.

Another factor worth mentioning is that we are using an *in vitro* system and the expression of the markers observed here is not necessarily the same as observed *in vivo*, although this system has been developed to model what happens *in vivo*.

4.1.2. Gfi1b-PA

This cell line has inserted Gfi1b at Gfi1 locus in order to examine the role of the intermediary region of Gfi1 transcription factor on HC differentiation program. The intermediary region, as the name indicates, is located between the SNAG domain and the zinc finger domain. Both Gfi1 and Gfi1b play essential roles in hematopoiesis and curiously share deeply similar SNAG and zinc finger domains, but their intermediary region practically does not share any sequence. *In vivo*, Gfi1b knock-in mice fail to rescue the defect in cochlear HCs, although it rescued the hematopoietic defects in Gfi1 null mice [46] and therefore Gfi1 intermediary region might be important for hearing function. This line was expected to produce the behavior observed *in vivo*.

Contrarily to the previous observations *in vivo*, Gfi1b-PA showed expression of HC markers from early on in the development, namely Myo7a, Myo6, Lhx3 and Otof. However, Lhx3 does not seem to follow the expression pattern of the Gfi1-wt. Since Lhx3 is not directly associated with deafness, the mechanism behind its upregulation might differ from the one behind the upregulation of Myo7a, Myo6 and Otof.

The expression patterns for Cdh23 and Espn do not coincide with the Gfi1-wt. These are specific markers for the hair bundle, specifically its structure [8, 9]. A proper hair bundle structure is essential for function since it is where the mechanotransduction machinery is located [3, 5, 6]. Owing to its specificity it is probable that it requires a different mechanism that Gfi1b is not capable of rescuing.

About the neuronal markers Tuj1 and Dcx, our results showed a discrepancy between the immunostaining and qPCR analysis. Based on previous qPCR expression levels for these two markers, the levels obtained in our data are not high enough to indicate a true expression. However we cannot rule out handling errors or contaminations during steps of qPCR.

To note that given the discrepancies between Gfib-PA and Gfi1-PA in relation to GFP expression, the results have to be interpreted carefully having a more qualitative than quantitative value, in spite of the adjustments adopted. Again, this can be due to the way the line was constructed, i.e. the GFP expression can be driven by other regulatory regions.

The fact that our results do not replicate the failure of Gfi1b at rescuing HC differentiation, observed *in vivo,* can be due the fact that our *in vitro* system is only including the transcription factors Gfi1, Pou4f3 and Atoh1. Although these factors might be the essential mechanistic complex [34, 35, 25], the

environment *in vivo* is not a closed system and there are other components/phenomena that can possibly influence the HC differentiation program.

Altogether, these findings lead us to believe that Gfi1b is partially capable of rescuing the functions of Gfi1 in this *in vitro* system, since it leads to the expression of HC markers (Myo7a, Myo6, Lhx3 and Otof), but hair bundle-specific markers (Cdh23 and Espn) fail to be expressed, suggesting that the formation of the hair bundle might occur through a distinct mechanism. Nevertheless, our data does not reflect the *in vivo* evidence, where Gfi1b failed to substitute Gfi1 function in the inner ear. It can be a clue that the intermediary region in fact does not influence the HC differentiation program and it is the inner ear environment (that we do not see in our *in vitro* system) that plays a key role in the process. It is also important to refer that Gfi1b has its SNAG and zinc finger domains intact and despite of being nearly identical to Gfi1 domains [46], the present dissimilarities may be a reason why Gfi1b does not fully behave as Gfi1-wt.

4.1.3. Gfi1DZF6-PA

Gfi1 is characterized by the presence of a six zinc fingers domain and evidence show that this domain is essential for its function as a transcription factor, suggesting that it binds to DNA. However, only the third, fourth and fifth zinc fingers appear to bind to DNA [43]. In the Gfi1DZF6-PA cell line all its six zinc fingers were removed and thus it lacks a functional DNA binding domain. Therefore, it was expected for this Gfi1 cell line to not be functional and fail to repress the neuronal program.

Our results show expression of the neuronal markers, Tuj1 and Dcx, and the expression of HC markers, such as Myo7a and Myo6, is not activated, according to our predictions. However, Lhx3 and Cdh23 (HC markers) are also present.

Besides the fact that the relative expression of Lhx3 in the Gfi1DZF6-PA line does not follow Gfi1-wt expression, the immunostaining data show evidence that Gfi1DZF6-PA express Lhx3 at day 8. It can be explained by its involvement in differentiation of multiple cell types, including neuronal subpopulations [69]. On the other hand, Lhx3 is an *in vivo* target regulated by Pou4f3 [19], which lead us to suggest that it can be expressed by hair cell-like cells to a partial extend in the Gfi1DZF6 cell line. One approach to confirm this would be by performing a co-immunostaining against Lhx3 and neuronal/HC markers.

In relation to Cdh23, very low levels of expression are present compared to Gfi1-wt. However, Gfi1DZF6-PA reflects the wt expression pattern.

In addition, the HC markers Otof and Espn are detected, but the expression does not follow the wt expression.

In summary, even though there is presence of some HC markers their degree of expression is not representative when compared with that of neuronal markers. It suggests that in fact the zinc finger domain is required for Gfi1 function as a neuronal repressor. However, we cannot ignore the presence of the HC markers, which strengthens the hypothesis that the activation of the HC differentiation program is complex and depends on multiple factors [4].

4.1.4. Gfi1P2A-PA

In the Gfi1P2A-PA cell line, a mutation proline to alanine is inserted at amino acid 2 of the SNAG domain that, *in vivo*, proved to be required for hematopoietic function by the recruitment of the epigenetic repressor LSD1/CoRest/HDACs1-2 [44, 45]. It was expected that this cell line at least partly reflects the evidence from hematopoietic system, and fail to repress neuronal genes.

Like our results suggest, Gfi1P2A-PA cells fail to express HC markers, such as Myo7a, Myo6 and Lhx3, and in turn show neuronal expression of Tuj1 and Dcx, which coincides with the previous findings *in vivo.*

However, expression of Otof (HC marker) seems to follow the pattern observed in Gfi1-wt cell line. Additionally, both hair bundle markers, Cdh23 and Espn, appear to be expressed at day 6, followed by their deactivation. One explanation is that there is still activation of HC differentiation to some extent and subsequently the switch from neuronal to HC differentiation is not absolute.

The amount of Tuj1 expression in this cell line seems to be considerably lower from the ones present in Gfi1DZF6 line. However, more data is necessary for comparison before drawing concrete comparative conclusions between these two Gfi1 cell lines. On the other hand, Dcx expression levels are higher showing clear differences from the controls (negative and positive). Once again, some neuronal expression levels for the wt condition were detected, which does not correspond to what we observed by immunostaining or from previous observations.

Although we observed HC markers expression to some extent, we can conclude that an intact SNAG domain is necessary for Gfi1 function, recapitulating the studies in the hematopoietic system. Again, this can be due to the way that the switch from neuronal to HC program occurs. On one hand it might not be a total switch and that is why we still detect HC markers. On the other hand taking into account the complexity of the mechanism behind it, an intact SNAG domain is not capable by itself to repress neuronal genes subsequently activating the expression of HC genes. Thus a dysfunctional SNAG domain produces these intermediary states where neuronal genes are not expressed to their full extent.

4.2. CHEMICAL INHIBITION OF THE REPRESSOR COMPLEX LSD1/COREST/HDACS1-2

In this assay we focused on the Gfi1's SNAG domain, specifically on the recruitment of the epigenetic repressor complex LSD1/CoRest/HDACs1-2. This complex includes the histone demethylase LSD1 and the histone deacetylases HDAC1 and HDAC2 [44]. They are involved in multiple biological functions [47, 48, 49, 50] and together they are associated with the silencing of neuronal genes [57, 55]. Interference with these CoRest complex components provokes a failure in the repression of the target genes [70, 57, 71]. We analyzed the mechanism behind this repressor complex recruitment by chemically inhibiting LSD1 or HDACs in the Gfi1-wt line. It was expected that the inhibition of any of these domains to partially fail in the repression of neuronal genes and in the activation of HC genes.

Two different concentrations were used to test the effect of the inhibition: 0.1µM and 1µM. Because the inhibitors are diluted in DMSO, the diluent was also added in the positive control at a low dose (0.01%). We followed the same experimental setup used in the phase discussed above, where expression of HC and neuronal markers was analyzed by comparison to a Gfi1 line without inhibitor (wt), on protein (Myo7a, Myo6, Lhx3, Tuj1 and Dcx) and gene (*Myo7a*, *Myo6*, *Lhx3*, *Otof*, *Cdh23*, *Espn*, *Tuj1* and *Dcx*) expression, by immunostaining and qPCR.

4.2.1. Problems and limitations to the interpretation

Two different concentrations of the inhibitors were used to analyze the gradient effect. Besides previous bibliography regarding to the inhibitors used, each *in vitro* system has its particularities and the concentrations used had to be optimized. It was clear during the EBs development that the samples treated with the inhibitors were generating fewer and smaller EBs. Specifically in the samples where the 1µM of the HDACs inhibitor was applied, the EBs exhibited unhealthy features which may have compromised the analysis. In addition to inhibitors' concentration optimization, extra plates had to be produced in order to overcome the lower number of EBs. We also stopped the assay at day 8 of development, given the effects of the treatment.

Regarding the variability within samples, the images shown in the Results section are chosen samples that best represent what was observed for each condition. Although the GFP expression described was generally observed in all Dox samples, there are a few differences between replicates that should be taken into account. These differences seem to be inherent to the clones used, since the variability is comparatively smaller within the same clone and larger between clones. One way of addressing this limitation is performing more replicates with different clones, thus mitigating some of the variability within samples.

Another fact worth mentioning is the obstacles during qPCR analysis. We faced discrepancies during transcript quantitative readings. Since the PCR reaction efficiency is dependent on the master mix performance, the specificity of the primers, the primer annealing temperature and the sample quality, to overcome this we repeated all the steps including the isolation of total RNA, synthesis of cDNA and qPCR. New kits were used, as well as new dilutions of primers and new pipettes, which normalized the readings. However, the variabilities between experiments were maintained. One approach to improve the qPCR results is to use more than one housekeeping gene (we used Sdha) to normalize the expression of the transcripts.

Concerning to the positive control (Gfi1-wt), there were some differences between the results obtained at this phase and the characterization of the knock-in lines phase. One possibility is that the addition of DMSO is affecting the differentiation [72], although the dose added was low (0.01%).

Due to time constraints, we gave more emphasis to qPCR analysis that allows us to look at the expression of more markers.

4.2.2. HDACs inhibition

HDACs1 and 2 are class I HDACs that remove acetyl groups on the target genes functioning as transcriptional repressors [58, 59]. In the HDACs inhibition, the drug used was TSA that has been shown to block all class I HDACs [60], in order to induce deficiencies in the HC differentiation program.

Our analyses show that HDACi treatment is affecting the activity of HC differentiation. We can see an intensification of the effect by the lower presence of HC markers with the increment of the inhibitor. While the samples treated with 0.1µM of HDACi showed at an early time point the expression of all the HC markers examined, 1µM HDACi samples only showed expression of Espn, with significant

differences from the negative control (P<0.001 at day 6 and P=0.034 at day 8). Again, it suggests that the mechanism for the formation of the hair bundle is different from HC mechanism.

Interestingly, the clear effect of the inhibitor observed for HC markers was not observed for neuronal markers. In general no neuronal markers were expressed, except in the case of EBs treated with the 1µM of HDACi, which expressed Tuj1 at day 6.

The inhibition of HDACs was previously studied [63] and, like our results suggest, it is affecting the cell cycle of the cultured cells, after 24h of treatment. The flow cytometry and immunostaining with Casp3 did not reveal a higher degree of apoptosis in these samples. Although, it cannot be ruled out that another type of cell death, than apoptosis (necrosis), or reduced cell proliferation is happening.

Altogether, we can conclude that the inhibition of HDACs affects the differentiation of HCs. Besides the low presence of Tuj1 expression, we can infer that neuronal repression is occurring, contrarily to what was expected. This can be explained by the fact that the concentration of the inhibitor is not sufficient to block the repressive function of HDACs.

4.2.3. LSD1 inhibition

LSD1 acts as a transcriptional inhibitor by demethylation of H3-K4 [53, 54], silencing neuronal genes in non-neuronal tissues and during neuronal differentiation [56]. The inhibitor used was SP2509 that acts by attenuating the binding of LSD1 to CoRest [62] and therefore we were aiming to activate neuronal differentiation.

Regarding neuronal expression, LSD1i treated samples express Tuj1, detected by immunostaining analysis, however it is not detectable by quantitative analysis. On the other hand, Dcx is detected by qPCR, but no expression is observed by immunostaining analysis. The problems associated with Dcx PCR readings (described in 4.2.1. section) leads us to believe that Dcx is not expressed.

In general, our results show that a higher concentration of LSD1 inhibitor results in a lower expression of HC markers, except for Lhx3, Cdh23 and Espn. In fact, 1µM LSD1i samples do not present significant differences with Gfi1-wt in relation to the expression of these three HC markers. Besides, the immunostaining analysis with Lhx3 showed that this marker is greatly expressed in cell of all treated conditions (Dox, 0.1µM LSD1i and 1µM LSD1i). Regarding Espn, 0.1µM LSD1i cells present a higher level of expression by comparison to the other conditions. Additionally, no significant differences were found between 1µM LSD1i, 0.1µM LSD1i and positive control (Gfi1-wt) samples.

According to studies in zebrafish, where LSD1 was inhibited [49, 50], our results suggest that LSD1 inhibition induced a reduction of the number of EBs produced, possibly caused by the inhibition of cell proliferation. Yet, the effect was not as drastic a reduction as observed with HDACs inhibition. The immunostaining against Casp3 was negative, which suggests that a cell proliferation mechanism is behind this result.

In summary, comparing previous findings and our data, there is a reduction in the expression of HC markers. Nevertheless, there was repression of neuronal genes, which can be explained by insufficient concentration of the inhibitor.

4.3. FUTURE PERSPECTIVES

Concerning the limitations in the utility of the general characterization of Gfi1 cell lines, one future aim is to produce replicates of each cell line for more confidence in our data. Another method to strengthen our data would be the use of flow cytometry for HC/neuronal markers in each of our cell lines (Gfi1b-PA, Gfi1DZF6-PA, and Gfi1P2A-PA), where by comparison with GFP could corroborate our findings. Furthermore, it would be interesting to test whether Gfi1-wt or other forms of Gfi1 bind directly to Atoh1, Pou4f3 or candidate co-regulators, by performing Gfi1 co-immunoprecipitation (Co-IP) followed by Western Blotting.

Another pressing future aim is to optimize the protocols used for the application of inhibitors so we can eliminate the variable of unhealthy EBs. We could also address this limitation through immunostaining against proliferating markers like bromodeoxyuridine [73] (BrdU) or cell cycle inhibitors such as CIP/KIP family [50]. It would also be of great interest to identify the specific genes targeted by HDACs and LSD1 inhibition. It would elucidate the role of these genes in the differentiation of HCs. In addition, identifying the cell cycle regulators should give insights into the development of mechanisms to initiate regeneration of HCs. Thus, Co-IPs analysis followed by Western Blotting [44, 74] would be a very useful step towards this objective. Moreover, ChIP-sequencing analysis [44] should reinforce the power of this ongoing work.

Given the evidence that HDACs inhibition has a more preeminent effect on the reduction of HC differentiation than LSD1 inhibition, it would be interesting to analyze the levels of methylation and acetylation in order to study the mechanistic dynamic behind it. One way to address this would be by performing Co-IP followed by Western Blotting, as previously shown using nucleosomes as substrates [61].

RNA-sequencing is being performed in the lab, and these data could reveal the continually changing cellular transcriptome which should be a valuable step to answer the question if repression of neuronal genes by Gfi1 towards the activation of HC differentiation program. Furthermore, this analysis should be considered using the cell line Gfi1P2A-PA, since it reveals expression of both neuronal and HC markers, especially hair bundle specific markers. It would give more confidence and power to the hypothesis that hair bundle formation occurs by a different mechanism.

4.4. CONCLUSION

The use of knock-in cell lines of Gfi1 proved to be a useful approach to characterize the role of Gfi1 regions involved in HC differentiation. Despite the limitations inherent to the assays and consequently limitation of the interpretation of the observed HC and neuronal expression, we believe we could identify, with some confidence, several interesting findings

Our results show that intact zinc finger and SNAG domains are required for HC markers expression. However, the suspicion remains about the first domain: does Gfi1 require binding to DNA in order to activate the transcription of HC genes? Also, the recruitment of the epigenetic repressor complex LSD1/CoRest/HDACs1-2 showed to be necessary for HC differentiation. In addition, our results suggest that HDACs inhibition causes a greater decrease in HC markers expression levels than LSD1 inhibition, which confirms the suggestion by *Lee et al., 2005* [55] that is likely that HDACs represent the first step of

the transcriptional repression by deacetylation of neuronal genes, followed by LSD1 demethylation of H3-K4, silencing the target genes.

Interestingly, HC markers expression could occur in the presence of neuronal markers. Furthermore, the expression of specific hair bundle markers (Cdh23 and Espn) in samples where the expression of other HC markers was reduced or inexistent, lead us to believe that there is a distinct mechanism behind hair bundle formation. These evidence support the idea that there is complexity associated with the differentiation and regeneration of HCs.

Moreover, we consider that our work may be used to contribute to future experiments to determine novel factors and their functions during HC fate determination, in addition to providing insights that can also be applied to basic research to improve *in vitro* differentiation protocols, thus facilitating the identification of potential therapeutic targets.

5. BIBLIOGRAPHY

1. Bermingham, N. A. *et al.* Math1: an essential gene for the generation of inner ear hair cells. *Science* **284,** 1837–41 (1999).

2. Costa, A. *et al.* Generation of sensory hair cells by genetic programming with a combination of transcription factors. *Development* **142,** 1948–1959 (2015).

3. Costa, A., Powell, L. M., Lowell, S. & Jarman, A. P. Atoh1 in sensory hair cell development: constraints and cofactors. *Semin. Cell Dev. Biol.* **65,** 60–68 (2017).

4. Frolenkov, G. I., Belyantseva, I. A., Friedman, T. B. & Griffith, A. J. Genetic insights into the morphogenesis of inner ear hair cells. *Nature Reviews Genetics* (2004). doi:10.1038/nrg1377

5. Corey, D. P. & Hudspeth, A. J. Ionic basis of the receptor potential in a vertebrate hair cell. *Nature* **281,** 675–677 (1979).

6. Russell, I. ., Richardson, G. . & Kössl, M. The responses of cochlear hair cells to tonic displacements of the sensory hair bundle. *Hear. Res.* **43,** 55–69 (1989).

7. Sand, O., Ozawa, S. & Hagiwara, S. Electrical and mechanical stimulation of hair cells in the mudpuppy. *J. Comp. Physiol.* **102,** 13–26 (1975).

8. Donaudy, F. *et al.* Espin gene (ESPN) mutations associated with autosomal dominant hearing loss cause defects in microvillar elongation or organisation. *J. Med. Genet.* **43,** 157–61 (2006).

9. Pan, L., Yan, J., Wu, L. & Zhang, M. Assembling stable hair cell tip link complex via multidentate interactions between harmonin and cadherin 23. *Proc. Natl. Acad. Sci. U. S. A.* **106,** 5575–80 (2009).

10. Tilney, L. G., Derosier, D. J. & Mulroy, M. J. The organization of actin filaments in the stereocilia of cochlear hair cells. *J. Cell Biol.* **86,** 244–59 (1980).

11. Tilney, L. G., Egelman, E. H., DeRosier, D. J. & Saunder, J. C. Actin filaments, stereocilia, and hair cells of the bird cochlea. II. Packing of actin filaments in the stereocilia and in the cuticular plate and what happens to the organization when the stereocilia are bent. *J. Cell Biol.* **96,** 822–34 (1983).

12. Hasson, T. *et al.* Unconventional Myosins in Inner-Ear Sensory Epithelia. *J. Cell Biol.* **137,** 1287 LP-1307 (1997).

13. Grati, M. & Kachar, B. Myosin VIIa and sans localization at stereocilia upper tip-link density implicates these Usher syndrome proteins in mechanotransduction. *Proc. Natl. Acad. Sci.* **108,** 11476–11481 (2011).

14. Shotwell, S. L., Jacobs, R. & Hudspeth, A. J. Directional sensitivity of individual vertebrate hair cells to controlled deflection of their hair bundles. *Ann. N. Y. Acad. Sci.* **374,** 1–10 (1981).

15. Tanimoto, M., Ota, Y., Inoue, M. & Oda, Y. Origin of Inner Ear Hair Cells: Morphological and Functional Differentiation from Ciliary Cells into Hair Cells in Zebrafish Inner Ear. *J. Neurosci.* **31,** 3784 LP-3794 (2011).

16. Gillespie, P. G. & Müller, U. Mechanotransduction by hair cells: models, molecules, and

mechanisms. *Cell* **139,** 33–44 (2009).

17. Bolz, H. *et al.* Mutation of CDH23, encoding a new member of the cadherin gene family, causes Usher syndrome type 1D. *Nat. Genet.* **27,** 108–112 (2001).

18. Rodríguez-Ballesteros, M. *et al.* A multicenter study on the prevalence and spectrum of mutations in the otoferlin gene (OTOF) in subjects with nonsyndromic hearing impairment and auditory neuropathy. *Hum. Mutat.* **29,** 823–31 (2008).

19. Hertzano, R. *et al.* Lhx3, a LIM domain transcription factor, is regulated by Pou4f3 in the auditory but not in the vestibular system. *Eur. J. Neurosci.* **25,** 999–1005 (2007).

20. Warchol, ME. Sensory regeneration in the vertebrate inner ear: Differences at the levels of cells and species. *Hear. Res.* **273,** 72–79 (2011).

21. Corwin, Cotanche, J. T. & Douglas A. Regeneration of Sensory Hair Cells After Acoustic Trauma. *Science (80-.).* **240,** (1988).

22. Gao, W.-Q. & Zheng, J. L. Overexpression of Math1 induces robust production of extra hair cells in postnatal rat inner ears. *Nat. Neurosci.* **3,** 580–586 (2000).

23. Woods, C., Montcouquiol, M. & Kelley, M. W. Math1 regulates development of the sensory epithelium in the mammalian cochlea. *Nat. Neurosci.* **7,** 1310–1318 (2004).

24. Cai, T., Seymour, M. L., Zhang, H., Pereira, F. A. & Groves, A. K. Conditional deletion of Atoh1 reveals distinct critical periods for survival and function of hair cells in the organ of Corti. *J. Neurosci.* **33,** 10110–22 (2013).

25. Kelly, M. C., Chang, Q., Pan, A., Lin, X. & Chen, P. Atoh1 Directs the Formation of Sensory Mosaics and Induces Cell Proliferation in the Postnatal Mammalian Cochlea In Vivo. *J. Neurosci.* **32,** 6699–6710 (2012).

26. Liu, Z. *et al.* Age-Dependent In Vivo Conversion of Mouse Cochlear Pillar and Deiters' Cells to Immature Hair Cells by Atoh1 Ectopic Expression. *J. Neurosci.* **32,** 6600–6610 (2012).

27. Zoghbi, H. Y. *et al.* Math1 is essential for genesis of cerebellar granule neurons. *Nature* **390,** 169–172 (1997).

28. Bermingham, N. A. *et al.* Proprioceptor pathway development is dependent on Math1. *Neuron* **30,** 411–22 (2001).

29. Rose, M. F. *et al.* Math1 is essential for the development of hindbrain neurons critical for perinatal breathing. *Neuron* **64,** 341–54 (2009).

30. Yang, Q., Bermingham, N. A., Finegold, M. J. & Zoghbi, H. Y. Requirement of Math1 for secretory cell lineage commitment in the mouse intestine. *Science* **294,** 2155–8 (2001).

31. Maricich, S. M. *et al.* Merkel cells are essential for light-touch responses. *Science* **324,** 1580–2 (2009).

32. Spitz, F. & Furlong, E. E. M. Transcription factors: from enhancer binding to developmental control. *Nat. Rev. Genet.* **13,** 613–626 (2012).

33. Yáñez-Cuna, J. O., Dinh, H. Q., Kvon, E. Z., Shlyueva, D. & Stark, A. Uncovering cis-regulatory

sequence requirements for context-specific transcription factor binding. *Genome Res.* **22,** 2018–30 (2012).

34. Wallis, D. The zinc finger transcription factor Gfi1, implicated in lymphomagenesis, is required for inner ear hair cell differentiation and survival. *Development* **130,** 221–232 (2003).

35. Xiang, M. *et al.* Essential role of POU– domain factor Brn-3c in auditory and vestibular hair cell development. *Neurobiology* **94,** 9445–9450 (1997).

36. Jafar-Nejad, H. & Bellen, H. J. Gfi/Pag-3/senseless zinc finger proteins: a unifying theme? *Mol. Cell. Biol.* **24,** 8803–12 (2004).

37. The zinc finger transcription factor Growth factor independence 1 (Gfi1). *Int. J. Biochem. Cell Biol.* **37,** 541–546 (2005).

38. The growth factor independence-1 transcription factor: New functions and new insights. *Crit. Rev. Oncol. Hematol.* **59,** 85–97 (2006).

39. van der Meer, L. T., Jansen, J. H. & van der Reijden, B. A. Gfi1 and Gfi1b: key regulators of hematopoiesis. *Leukemia* **24,** 1834–1843 (2010).

40. Möröy, T., Khandanpour, C. Growth factor independence 1 (Gfi1) as a regulator of lymphocyte development and activation. *Semin. Immunol.* **23,** 368–378 (2011).

41. Costa, A. From Embryonic Stem Cells to Sensory Hair Cells: a Programming Approach. (2014).

42. Hertzano, R. *et al.* Transcription profiling of inner ears from Pou4f3ddl/ddl identifies Gfi1 as a target of the Pou4f3 deafness gene. *Hum. Mol. Genet.* **13,** 2143–2153 (2004).

43. Zweidler-Mckay, P. A., Grimes, H. L., Flubacher, M. M. & Tsichlis, P. N. Gfi-1 encodes a nuclear zinc finger protein that binds DNA and functions as a transcriptional repressor. *Mol. Cell. Biol.* **16,** 4024–34 (1996).

44. Saleque, S., Kim, J., Rooke, H. M. & Orkin, S. H. Epigenetic Regulation of Hematopoietic Differentiation by Gfi-1 and Gfi-1b Is Mediated by the Cofactors CoREST and LSD1. *Mol. Cell* **27,** 562–572 (2007).

45. Doan, L. L. *et al.* Targeted transcriptional repression of Gfi1 by GFI1 and GFI1B in lymphoid cells. *Nucleic Acids Res.* **32,** 2508–2519 (2004).

46. Fiolka, K. *et al.* Gfi1 and Gfi1b act equivalently in haematopoiesis, but have distinct, non-overlapping functions in inner ear development. *EMBO Rep.* **7,** 326–333 (2006).

47. de Ruijter, A. J. M., van Gennip, A. H., Caron, H. N., Kemp, S. & van Kuilenburg, A. B. P. Histone deacetylases (HDACs): characterization of the classical HDAC family. *Biochem. J.* **370,** 737–49 (2003).

48. Marks, P. A., Richon, V. M., Miller, T. & Kelly, W. K. Histone Deacetylase Inhibitors. *Adv. Cancer Res.* **91,** 137–168 (2004).

49. He, Y. *et al.* Trans-2-phenylcyclopropylamine regulates zebrafish lateral line neuromast development mediated by depression of LSD1 activity. *Int. J. Dev. Biol.* **57,** 365–73 (2013).

50. He, Y., Tang, D., Cai, C., Chai, R. & Li, H. LSD1 is Required for Hair Cell Regeneration in

Zebrafish. *Mol. Neurobiol.* **53,** 2421–2434 (2016).

51. Lakowski, B., Roelens, I. & Jacob, S. CoREST-Like Complexes Regulate Chromatin Modification and Neuronal Gene Expression. *J. Mol. Neurosci.* **29,** 227–240 (2006).

52. Dallman, J. E., Allopenna, J., Bassett, A., Travers, A. & Mandel, G. Development/Plasticity/Repair A Conserved Role But Different Partners for the Transcriptional Corepressor CoREST in Fly and Mammalian Nervous System Formation. doi:10.1523/JNEUROSCI.0238-04.2004

53. Garcia-Bassets, I. *et al.* Histone Methylation-Dependent Mechanisms Impose Ligand Dependency for Gene Activation by Nuclear Receptors. *Cell* **128,** 505–518 (2007).

54. Metzger, E. *et al.* LSD1 demethylates repressive histone marks to promote androgen-receptor-dependent transcription. *Nature* **437,** 436–439 (2005).

55. Lee, M. G., Wynder, C., Cooch, N. & Shiekhattar, R. An essential role for CoREST in nucleosomal histone 3 lysine 4 demethylation. *Nature* **437,** 432–435 (2005).

56. Ballas, N., Grunseich, C., Lu, D. D., Speh, J. C. & Mandel, G. REST and Its Corepressors Mediate Plasticity of Neuronal Gene Chromatin throughout Neurogenesis. *Cell* **121,** 645–657 (2005).

57. Forneris, F., Binda, C., Vanoni, M. A., Battaglioli, E. & Mattevi, A. Human histone demethylase LSD1 reads the histone code. *J. Biol. Chem.* **280,** 41360–5 (2005).

58. Marks, P. A. *et al.* Histone deacetylases and cancer: causes and therapies. *Nat. Rev. Cancer* **1,** 194–202 (2001).

59. Morrison, B. E. *et al.* Neuroprotection by histone deacetylase-related protein. *Mol. Cell. Biol.* **26,** 3550–64 (2006).

60. Khan, N. *et al.* Determination of the class and isoform selectivity of small-molecule histone deacetylase inhibitors. *Biochem. J.* **409,** 581–9 (2008).

61. Lee, M. G. *et al.* Functional interplay between histone demethylase and deacetylase enzymes. *Mol. Cell. Biol.* **26,** 6395–402 (2006).

62. Fiskus, W. *et al.* Pre-Clinical Efficacy of Combined Therapy with LSD1 Antagonist SP-2509 and Pan-Histone Deacetylase Inhibitor Against AML Blast Progenitor Cells. *Blood* **120,** (2012).

63. Kruh, J. Effects of sodium butyrate, a new pharmacological agent, on cells in culture. *Mol. Cell. Biochem.* **42,** 65–82 (1982).

64. Slattery, E. L., Speck, J. D. & Warchol, M. E. Epigenetic Influences on Sensory Regeneration: Histone Deacetylases Regulate Supporting Cell Proliferation in the Avian Utricle. *J. Assoc. Res. Otolaryngol.* **10,** 341–353 (2009).

65. Shi, Y. *et al.* Histone Demethylation Mediated by the Nuclear Amine Oxidase Homolog LSD1. *Cell* **119,** 941–953 (2004).

66. Iacovino, M. *et al.* Inducible cassette exchange: a rapid and efficient system enabling conditional gene expression in embryonic stem and primary cells. *Stem Cells* **29,** 1580–8 (2011).

67. Iacovino, M., Roth, M. E. & Kyba, M. in *Methods in molecular biology (Clifton, N.J.)* **1101,** 339–351 (2014).

68. Livak, K. J. & Schmittgen, T. D. Analysis of Relative Gene Expression Data Using Real-Time Quantitative PCR and the 2−ΔΔCT Method. *Methods* **25,** 402–408 (2001).

69. Hunter, C. S. & Rhodes, S. J. LIM-homeodomain genes in mammalian development and human disease. *Mol. Biol. Rep.* **32,** 67–77 (2005).

70. Ballas, N. *et al.* Regulation of Neuronal Traits by a Novel Transcriptional Complex. *Neuron* **31,** 353–365 (2001).

71. Forneris, F., Battaglioli, E., Mattevi, A. & Binda, C. New roles of flavoproteins in molecular cell biology: Histone demethylase LSD1 and chromatin. *FEBS J.* **276,** 4304–4312 (2009).

72. Pal, R., Mamidi, M. K., Das, A. K. & Bhonde, R. Diverse effects of dimethyl sulfoxide (DMSO) on the differentiation potential of human embryonic stem cells. *Arch. Toxicol.* **86,** 651–661 (2012).

73. Bradford, J. A. *et al.* Detection of s-phase cell cycle progression using 5-ethynyl-2'-deoxyuridine incorporation with click chemistry.

74. Chen, F.-Q., Schacht, J. & Sha, S.-H. Aminoglycoside-induced histone deacetylation and hair cell death in the mouse cochlea. *J. Neurochem.* **108,** 1226–1236 (2009).

6. SUPPLEMENTARY DATA

6.1. ISOLATION OF TOTAL RNA

- Addition of 350µL of 70% ethanol and vortex;
- Transfer the sample to the RNA binding spin cup (seated within a 2mL collection tube) and centrifuge for 1min at maximum speed;
- Retain the spin cup and discard the filtered;
- Add 600µL of 1x low-salt wash buffer and centrifuge for 1min at maximum speed;
- Retain the spin cup and discard the filtered;
- Add a DNase solution (50µL of DNase digestion buffer plus 5µL of reconstituted RNase-free DNase I, per sample) directly onto the matrix inside the spin cup and incubate for 1h at 37ºC.
- Add 600µL of 1x high-salt wash buffer and centrifuge for 1min at maximum speed;
- Retain the spin cup and discard the filtered;
- Add 600µL of 1x low-salt wash buffer and centrifuge for 1min at maximum speed;
- Retain the spin cup and discard the filtered;
- Add 300µL of 1x low-salt wash buffer and centrifuge for 2min at maximum speed;
- Retain the spin cup and discard the filtered;
- Transfer spin cup to a 1.5mL collection tube;
- Add 50µL of elution buffer directly onto the matrix inside the spin cup and incubate for 2min at room temperature (RT);
- Centrifuge for 1min at maximum speed.

The purified RNA is in the elution buffer in the 1.5mL collection tube.

6.2. cDNA SYNTHESIS

- 1µL of random primers, 1µL of 10mM dNTP, 200ng of template RNA and high-pure water up to 10µL;
- Vortex and briefly centrifuge the components;
- Heat the RNA-primer mix for 5min at 65ºC to anneal primer to template RNA, and incubate on ice;
- Add 4µL of 5x first strand buffer, 2µL of 0.1M DTT and 1µL of ribonuclease inhibitor, vortex and briefly centrifuge;
- Incubate the reaction mixture for 2min at 37ºC;
- Add 1µL of reverse transcriptase (M-MLVRT) to the positive control (RT+) or 1µL of high-pure water to negative control (RT-);
- Incubate for 10min at 25ºC, then for 50min at 37ºC;
- Inactivate the reaction by incubating it for 15min at 70ºC.

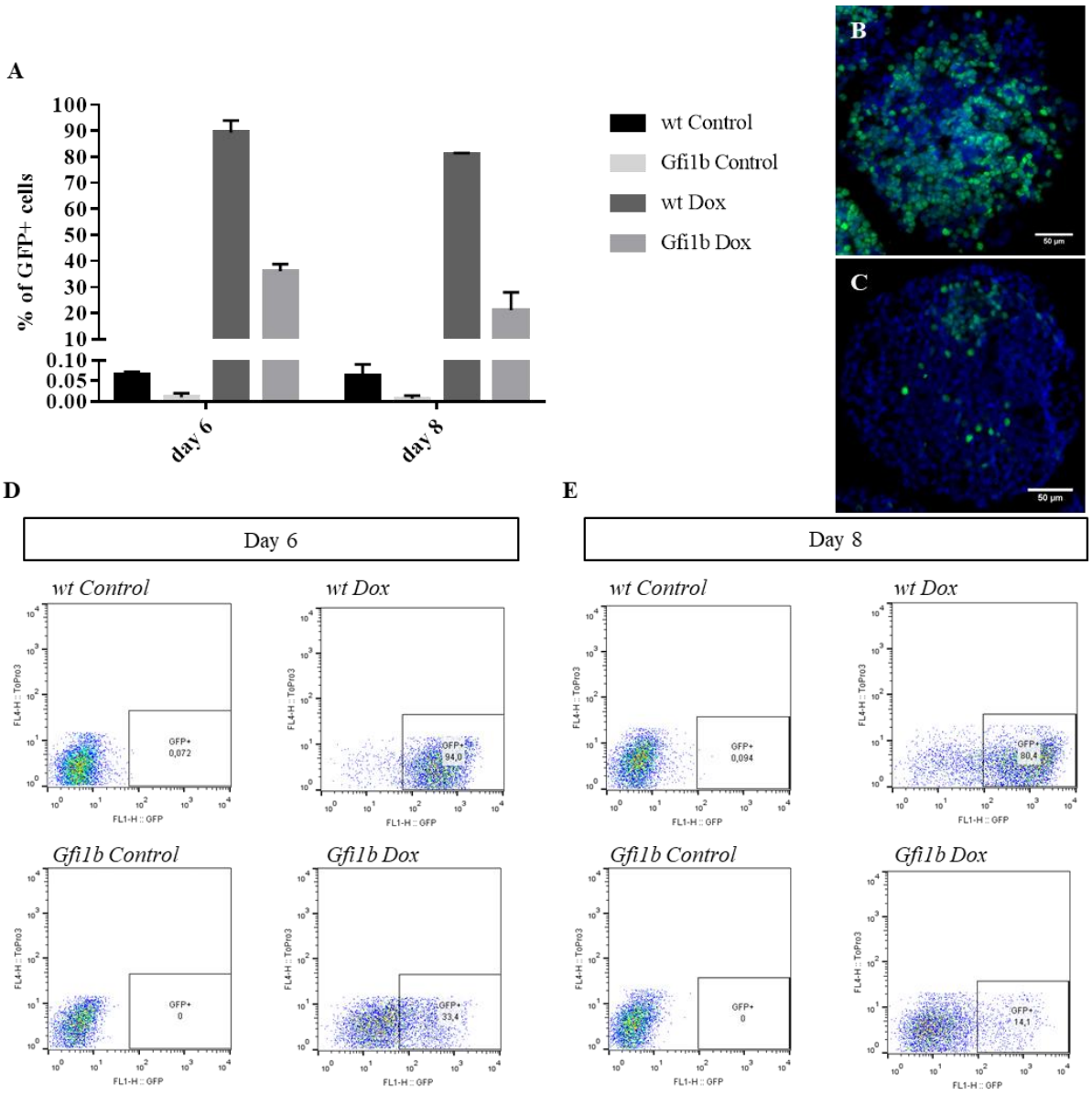

Figure 6.1 - Gfi1b-PA GFP positive cells: (A) Bar diagram showing the percentage of GFP+ cells obtained by flow cytometry analysis from EBs without Dox and EBs treated for 2 and 4 days with Dox. Percentage presented as mean±SEM (n=2). (B, C) Representative images obtained from ICC for vGFP (green) in (B) wt Dox and (C) Gfi1b Dox. Nuclei were indentified with DAPI (blue). Scale bar set to 50µm. (D,E) Representative dot plots obtained with flow analysis, showing gated GFP+ cells.

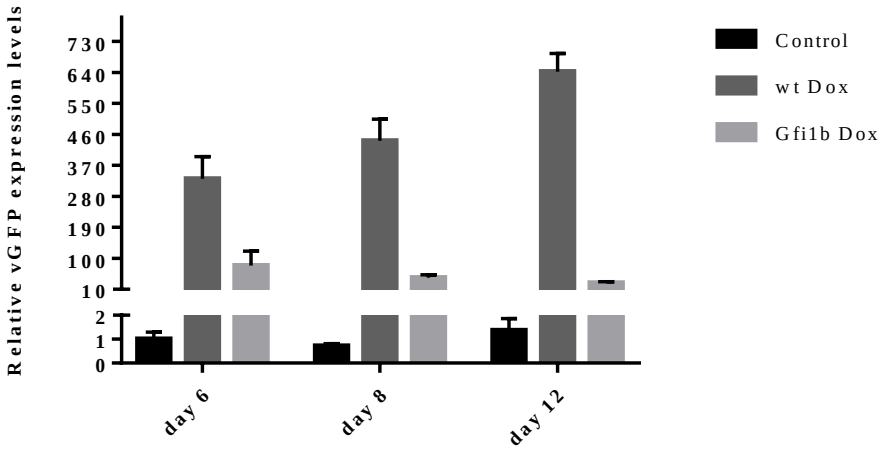

Figure 6.2 - vGFP quantification of Gfi1b-PA: Bar diagram showing the relative RNA levels of vGFP in EBs without Dox and EBs treated for 2, 4 and 8 days with Dox. Relative expression of the marker normalized to the mean of untreated EBs at day 6 (set to 1) ± SEM (n=2).

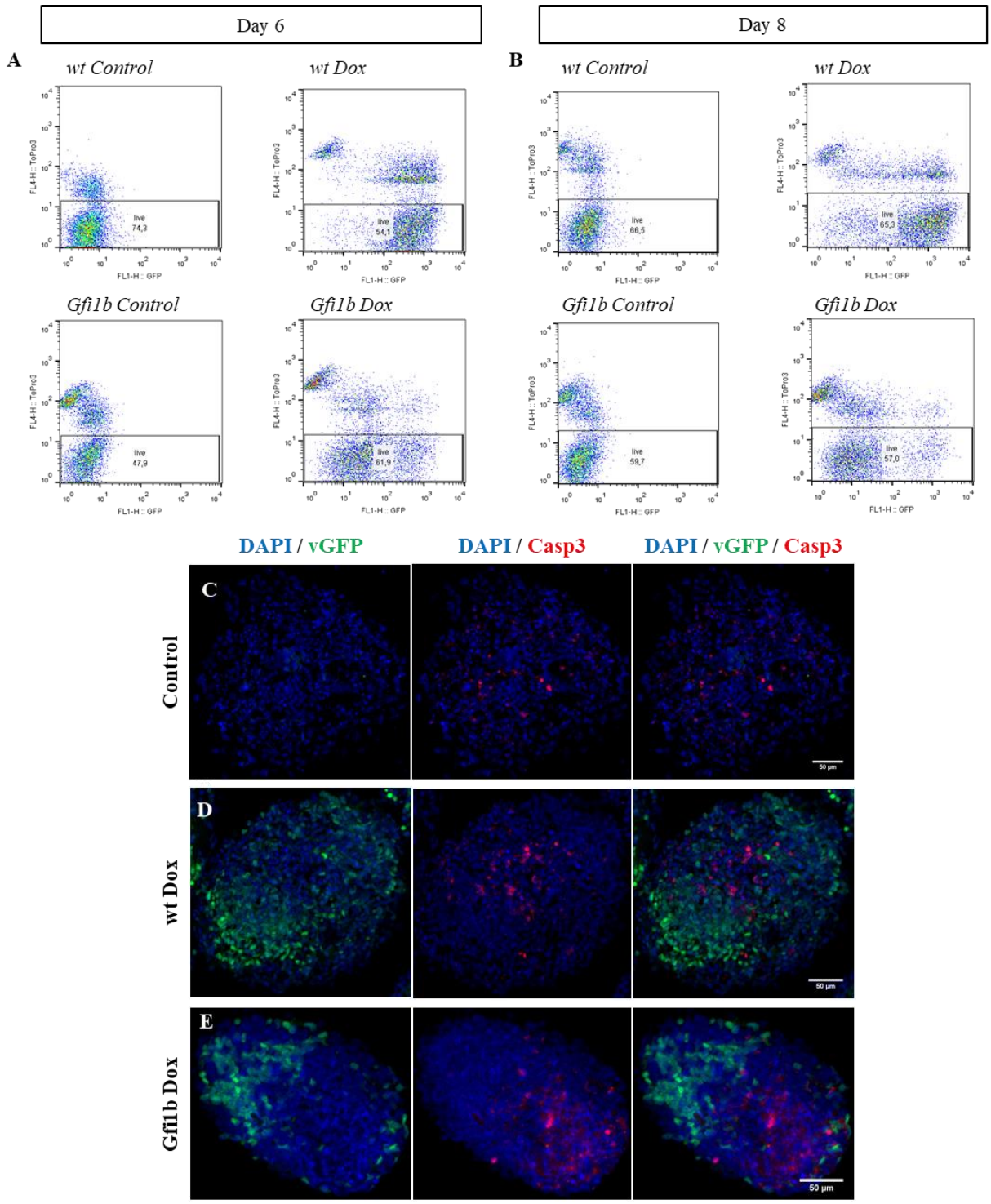

Figure 6.3 - Gfi1b-PA live cells: (A, B) Representative dot plots obtained with flow cytometry analysis showing gated life cells. Percentage of live cells presented as mean (n=2). (C, D, E) Representative images obtained from ICC for Casp3 (red) in (C) wt control, (D) wt Dox and (E) Gfi1b Dox. Overexpressing cells were identified with vGFP (green) and nuclei with DAPI (blue). Scale bar set to 50µm.

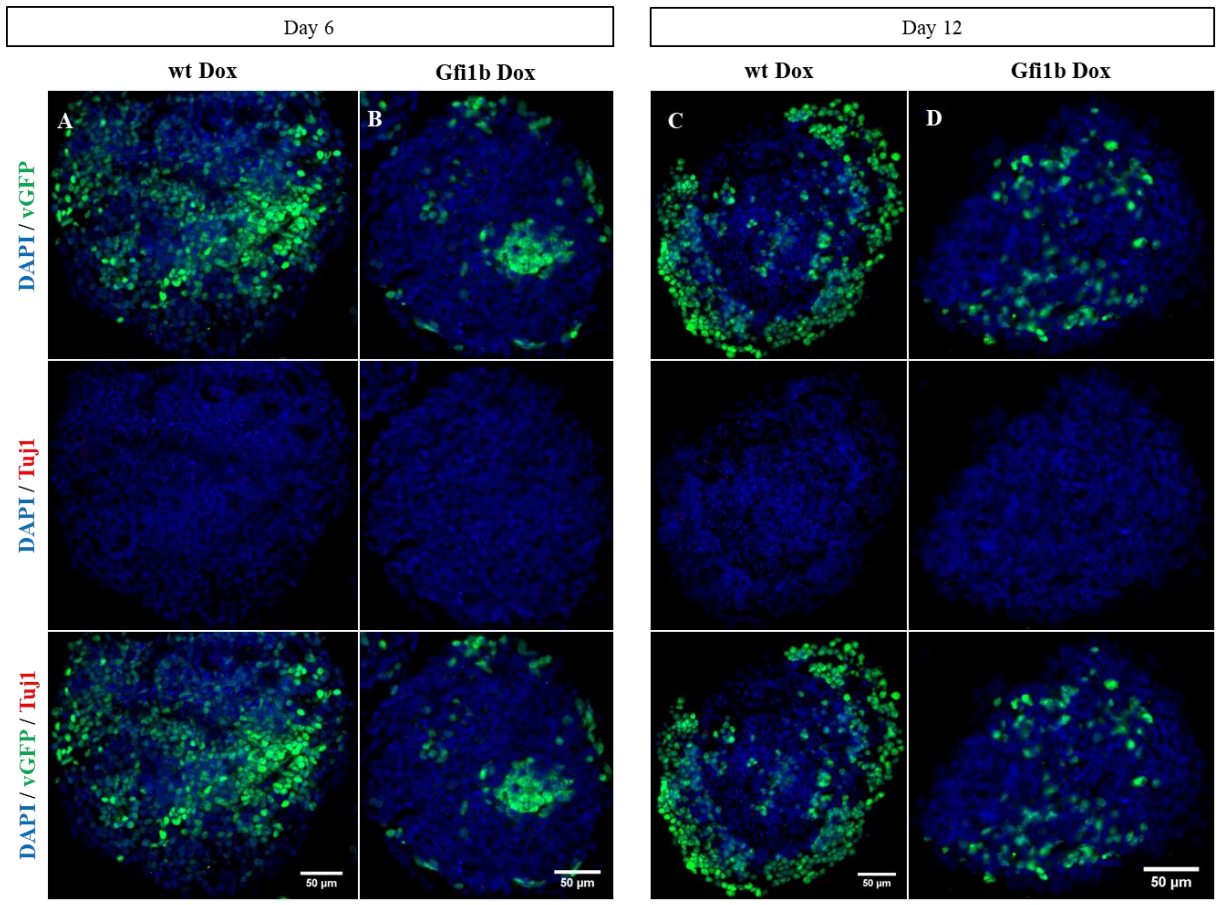

Figure 6.4 - Induction of Tuj1 in Gfi1b-PA: (A, B, C, D) Representative images of days 6 and 12 of development, obtained from ICC for Tuj1 (red). EBs were treated for 2, 4 and 8 days with Dox in (A, C) wt Dox and (B, D) Gfi1b Dox. Overexpressing cells were identified with vGFP (green) and nuclei with DAPI (blue). Scale bar set to 50µm.

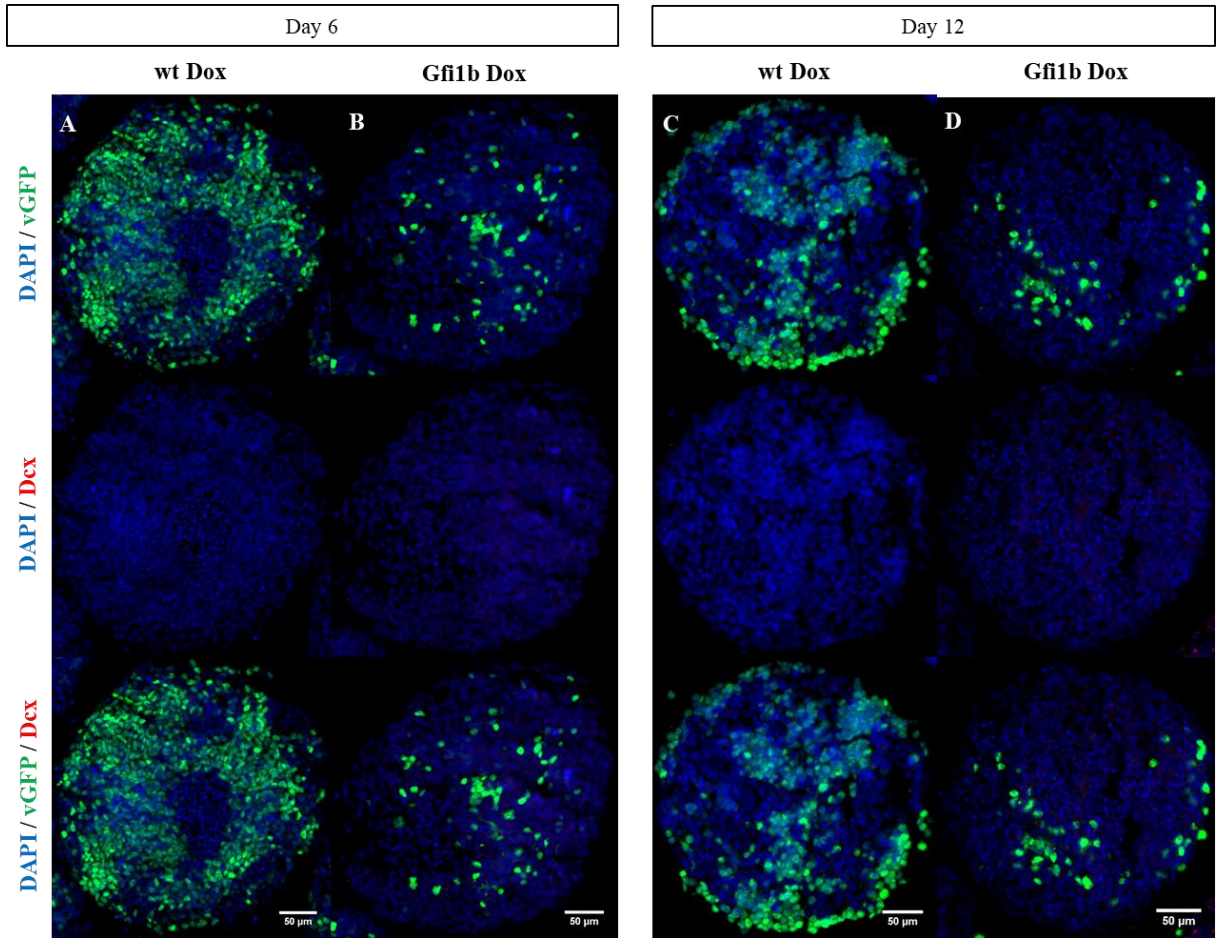

Figure 6.5 - Induction of Dcx in Gfi1b-PA: (A, B, C, D) Representative images of days 6 and 12 of development, obtained from ICC for Dcx (red). EBs were treated for 2, 4 and 8 days with Dox in (A, C) wt Dox and (B, D) Gfi1b Dox. Overexpressing cells were identified with vGFP (green) and nuclei with DAPI (blue). Scale bar set to 50µm.

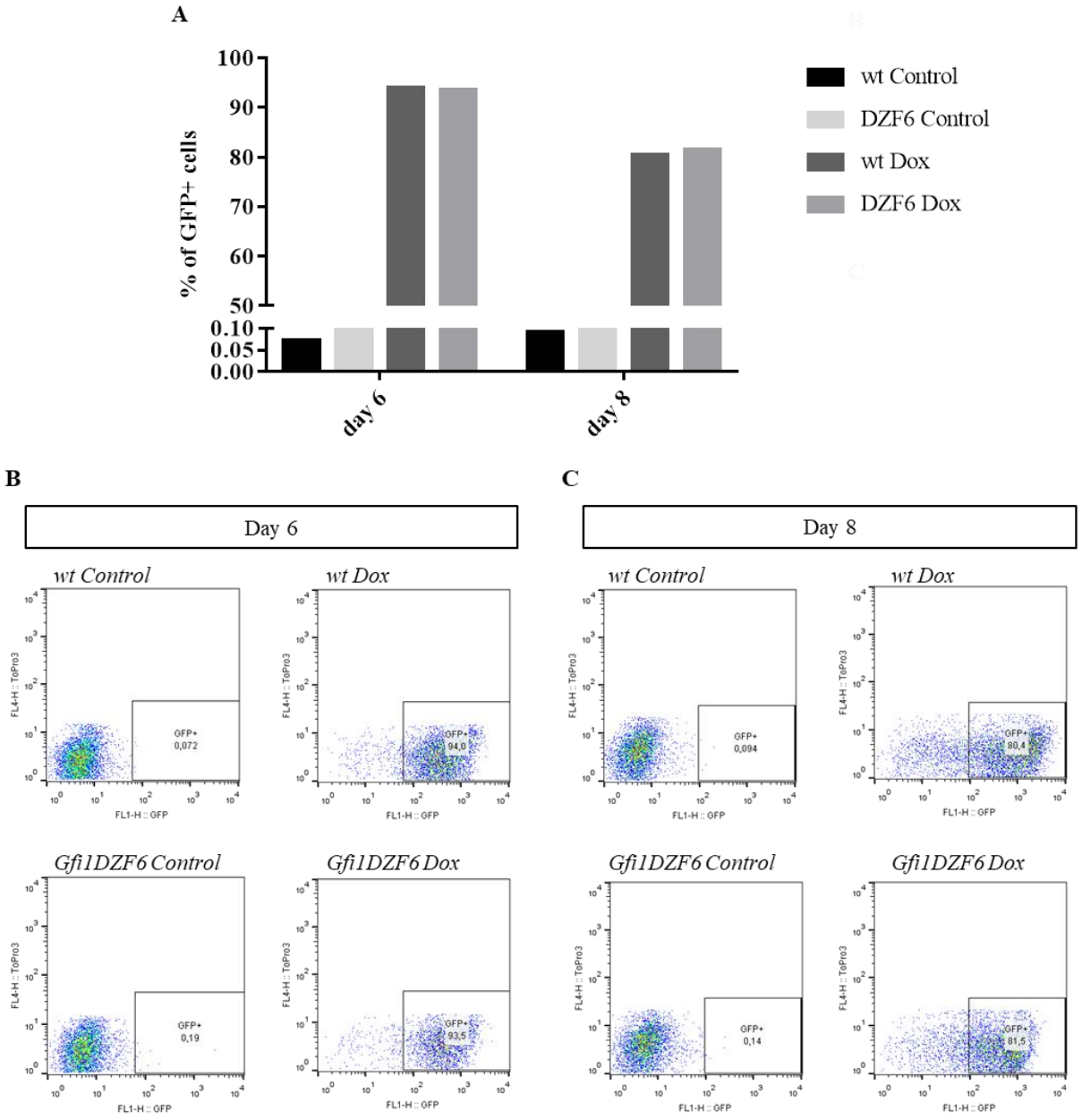

Figure 6.6 - Gfi1DZF6-PA GFP positive cells: (A) Bar diagram showing the percentage of GFP+ cells obtained by flow cytometry analysis from EBs without Dox and EBs treated for 2 and 4 days after Dox exposure (n=1). (B, C) Representative dot plots obtained with flow analysis, showing gated GFP+ cells.

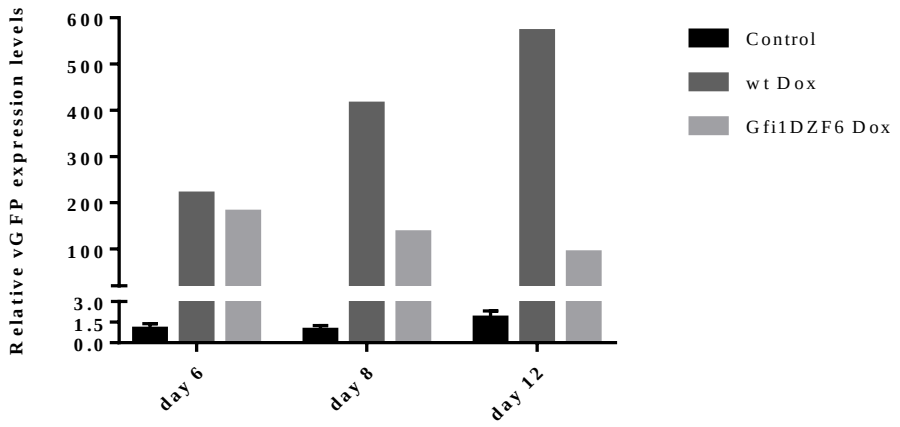

Figure 6.7 - - vGFP quantification of Gfi1DZF6-PA: Bar diagram showing the relative RNA levels of vGFP in EBs without Dox and EBs treated for 2, 4 and 8 days with Dox. Relative expression of the marker normalized to the mean of untreated EBs at day 6 (set to 1) (n=1).

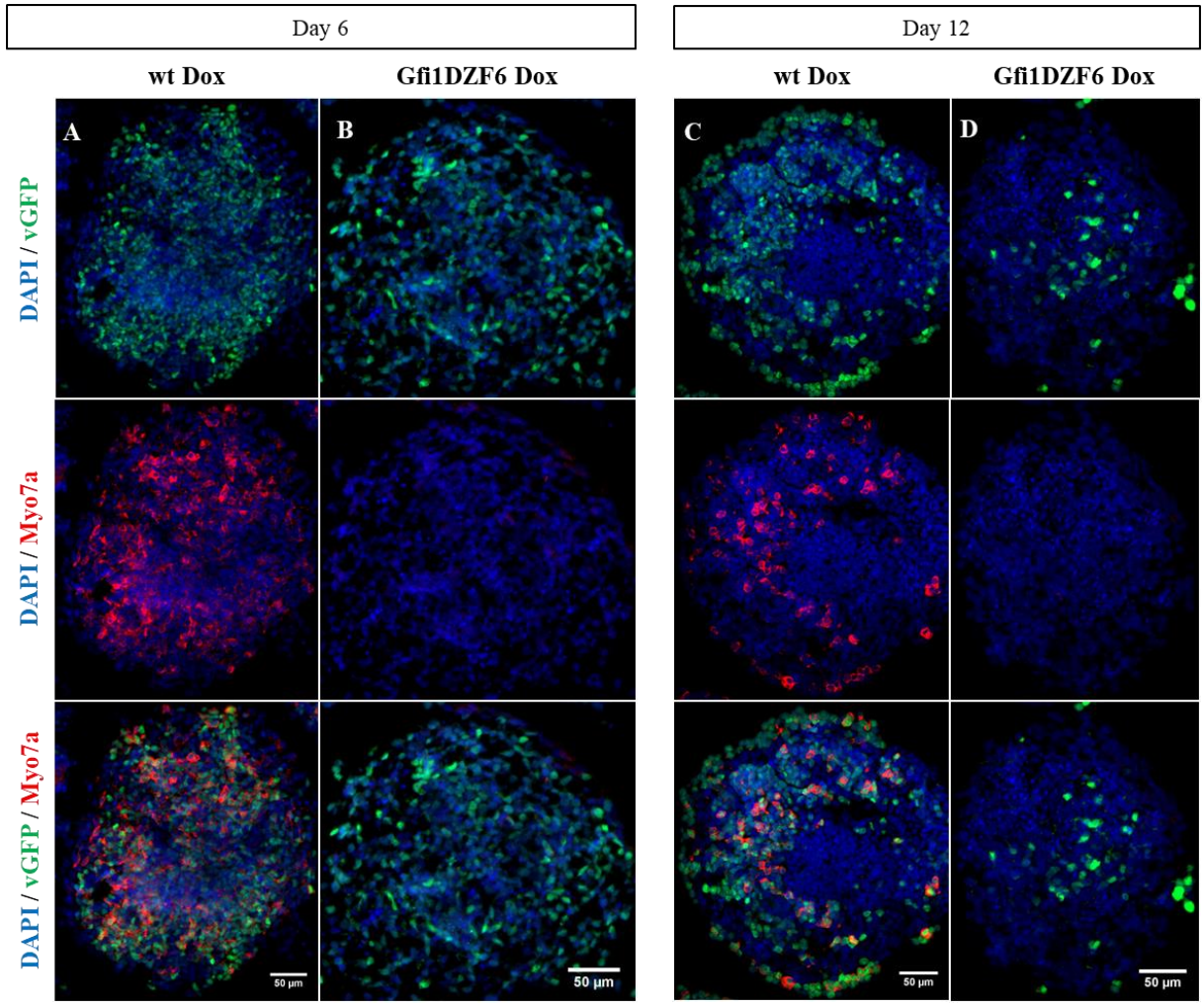

Figure 6.8 - Induction of Myo7a in Gfi1DZF6-PA: Representative images of days 6 and 12 of development, obtained from ICC for Myo7a (red). EBs were treated for 2, 4 and 8 days with Dox in (A, C) wt Dox and (B, D) Gfi1DZF6 Dox. Overexpressing cells were identified with vGFP (green) and nuclei with DAPI (blue). Scale bar set to 50µm.

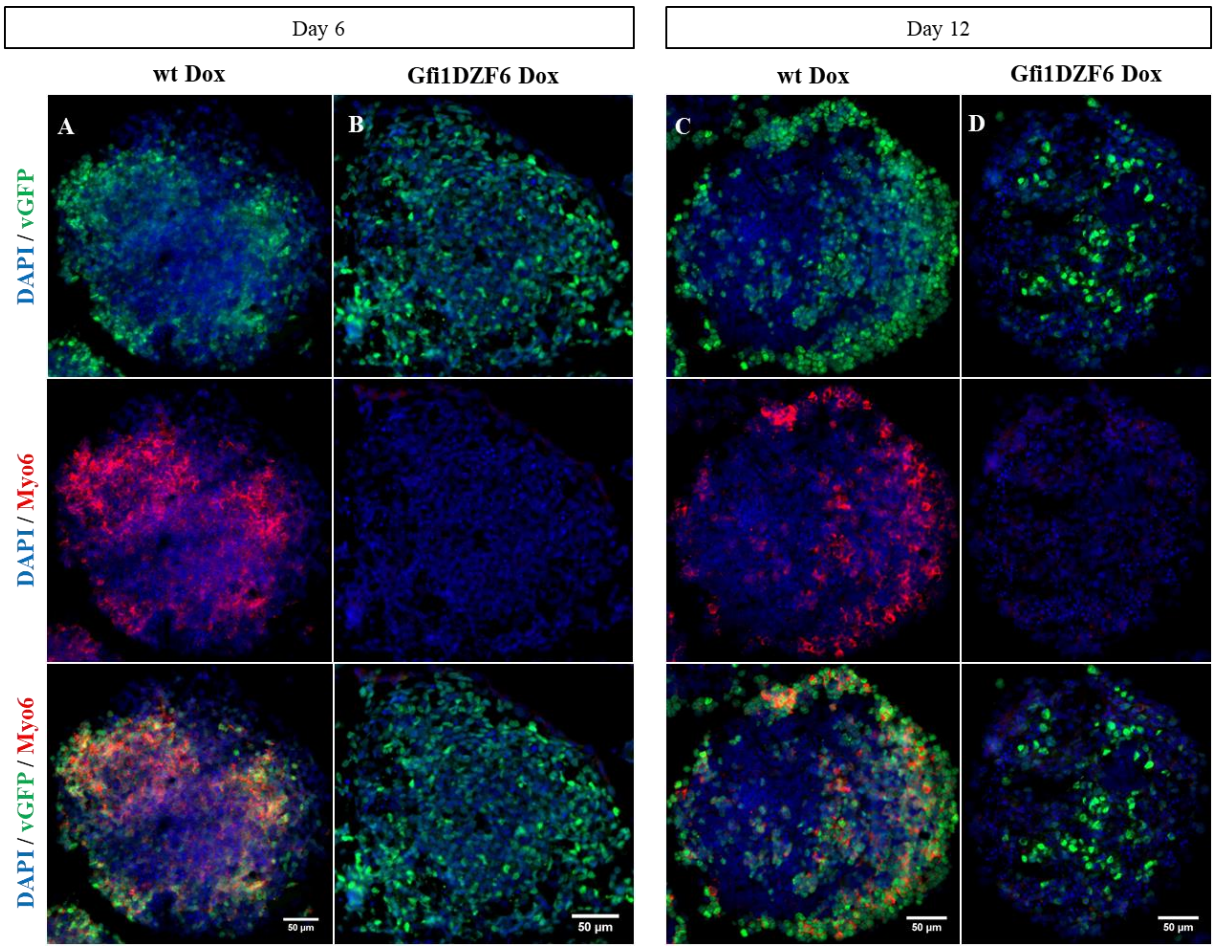

Figure 6.9 - Induction of Myo6 in Gfi1DZF6-PA: Representative images of days 6 and 12 of development, obtained from ICC for Myo6 (red). EBs were treated for 2, 4 and 8 days with Dox in (A, C) wt Dox and (B, D) Gfi1DZF6 Dox. Overexpressing cells were identified with vGFP (green) and nuclei with DAPI (blue). Scale bar set to 50µm.

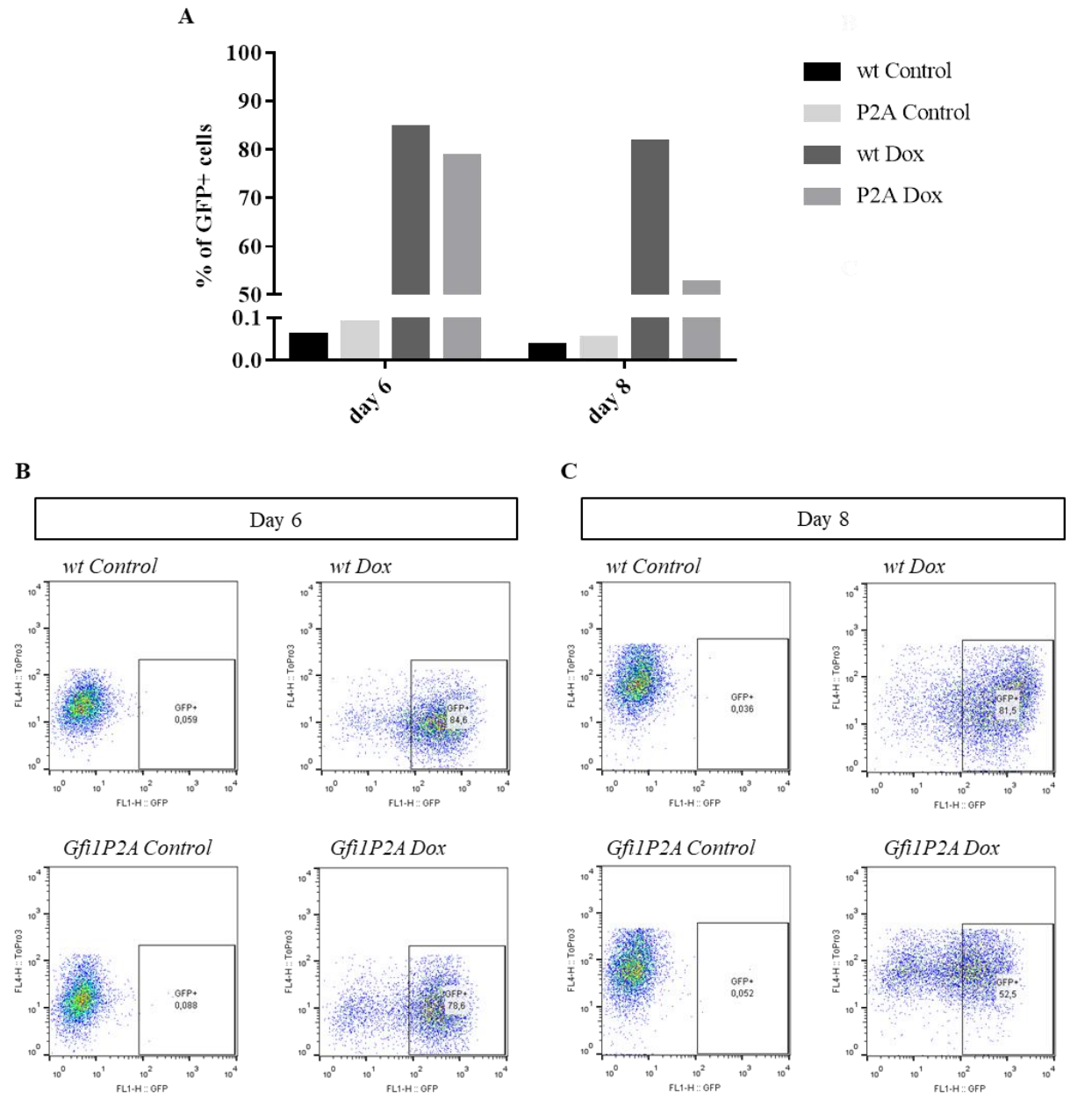

Figure 6.10 - Gfi1P2A-PA GFP positive cells: (A) Bar diagram showing the percentage of GFP+ cells obtained by flow cytometry analysis from EBs without Dox and EBs treated for 2 and 4 days with Dox (n=1). (B, C) Representative dot plots obtained with flow analysis, showing gated GFP+ cells.

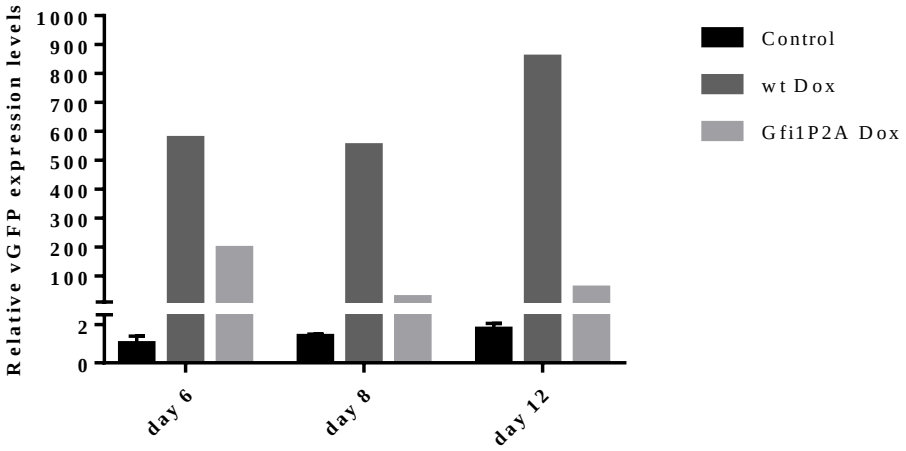

Figure 6.11 - - vGFP quantification of Gfi1P2A-PA: Bar diagram showing the relative RNA levels of vGFP in EBs without Dox and EBs treated for 2, 4 and 8 days with Dox. Relative expression of the marker normalized to the mean of untreated EBs at day 6 (set to 1) (n=1).

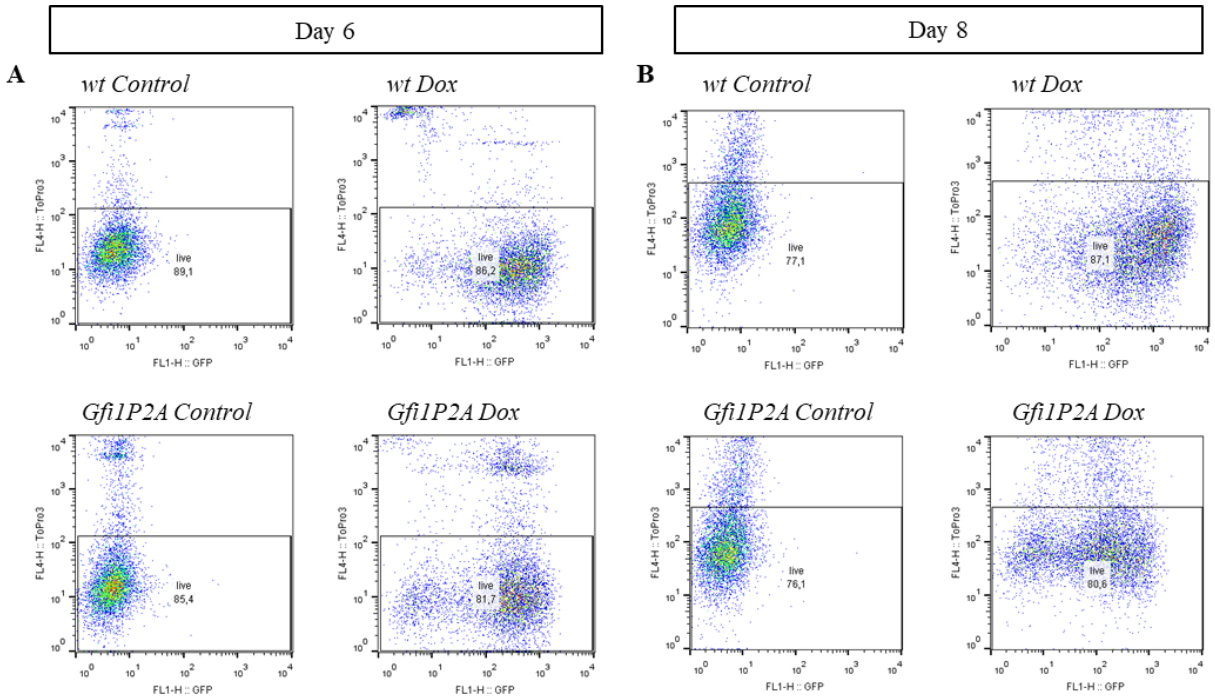

Figure 6.12 - Gfi1P2A-PA live cells: (A, B) Representative dot plots obtained with flow cytometry analysis showing gated life cells. (A) Day 6: wt control – 89.10, Gfi1P2A control – 85.40, wt Dox – 86.20, Gfi1P2A Dox – 81.70. (B) Day 8: wt control – 77.10, Gfi1P2A control – 76.10, wt Dox – 87.10, Gfi1P2A Dox – 80.60 (n=1).

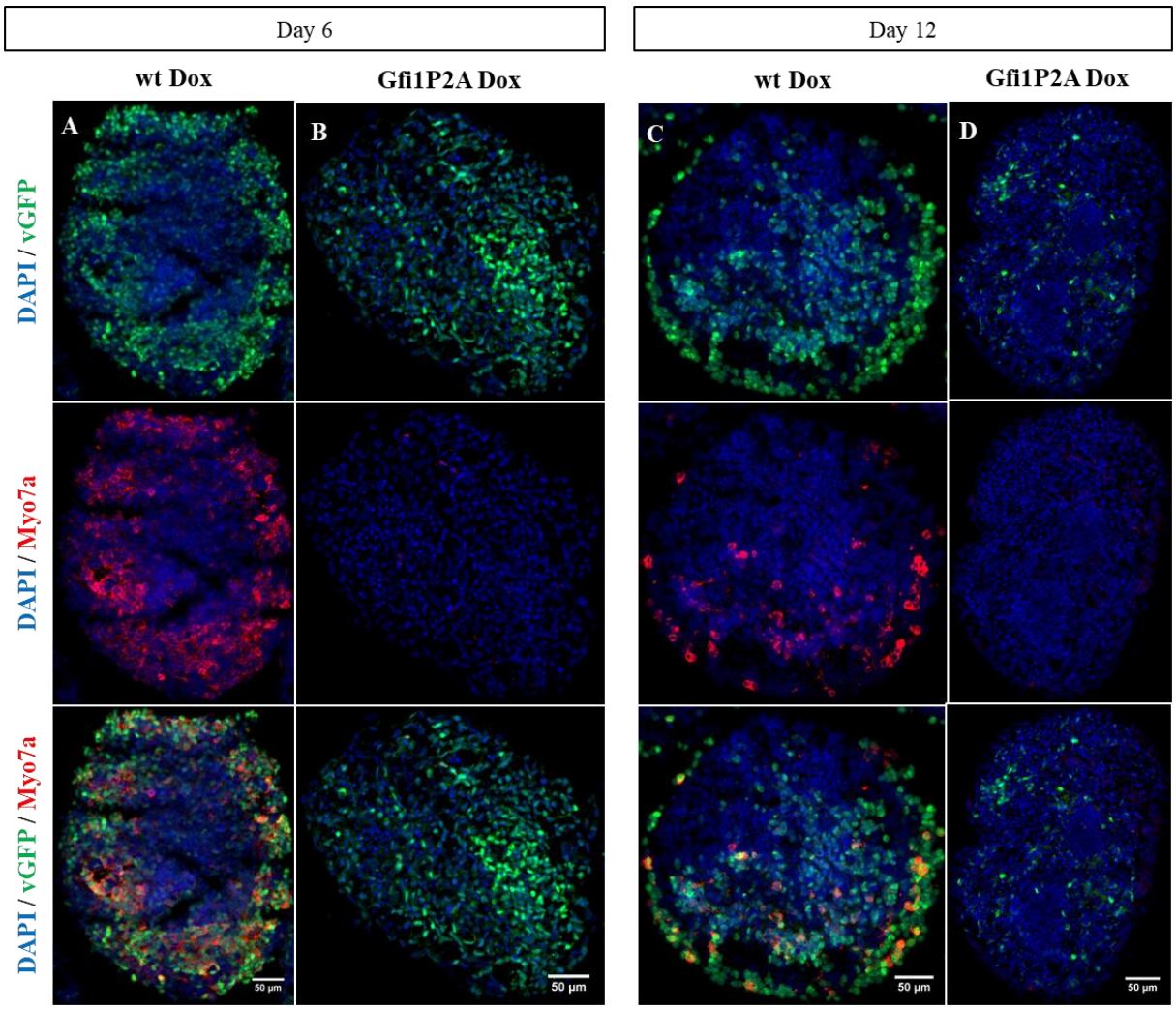

Figure 6.13 - Induction of Myo7a in Gfi1P2A-PA: Representative images of days 6 and 12 of development, obtained from ICC for Myo7a (red). EBs were treated for 2, 4 and 8 days with Dox in (A, C) wt Dox and (B, D) Gfi1DZF6 Dox. Overexpressing cells were identified with vGFP (green) and nuclei with DAPI (blue). Scale bar set to 50µm.

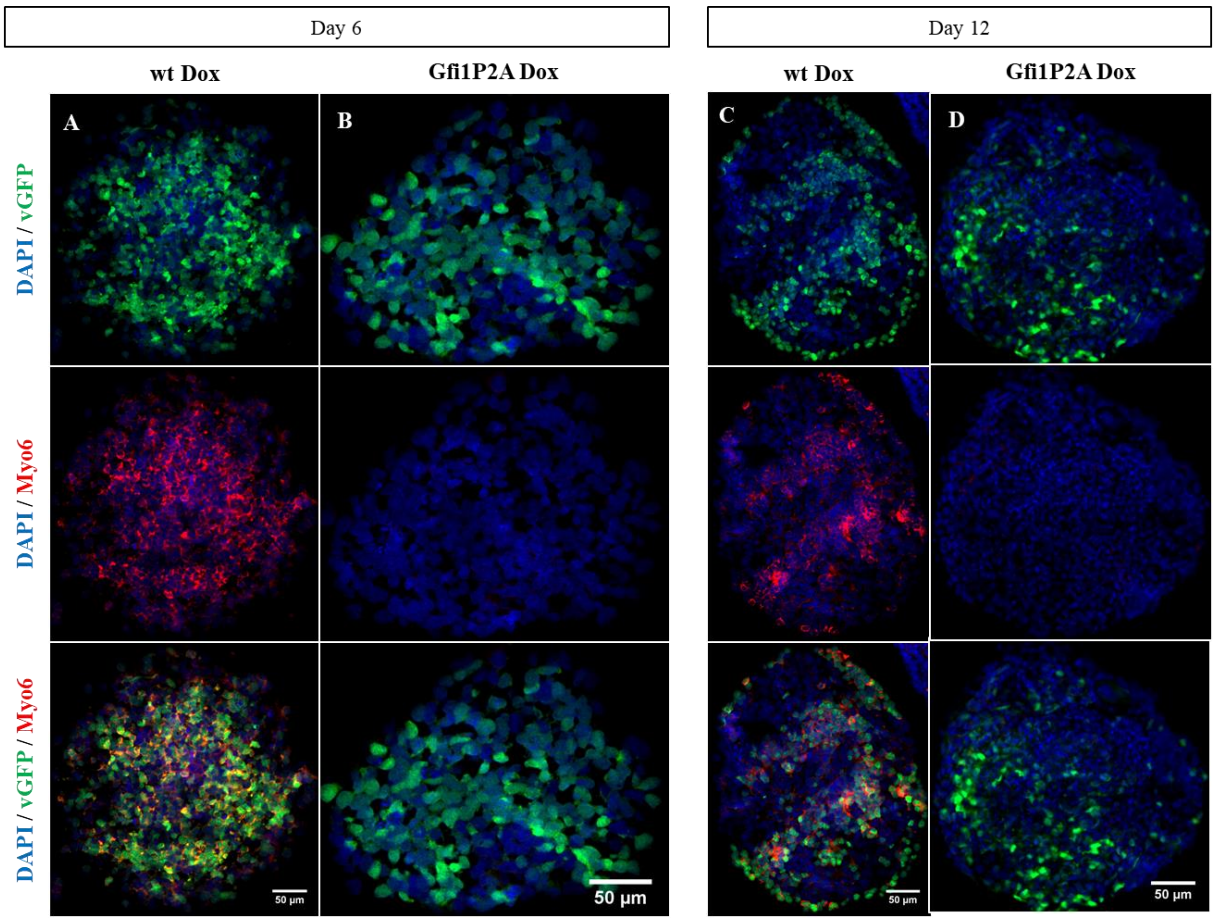

Figure 6.14 - Induction of Myo6 in Gfi1P2A-PA: Representative images of days 6 and 12 of development, obtained from ICC for Myo6 (red). EBs were treated for 2, 4 and 8 days with Dox in (A, C) wt Dox and (B, D) Gfi1DZF6 Dox. Overexpressing cells were identified with vGFP (green) and nuclei with DAPI (blue). Scale bar set to 50µm.

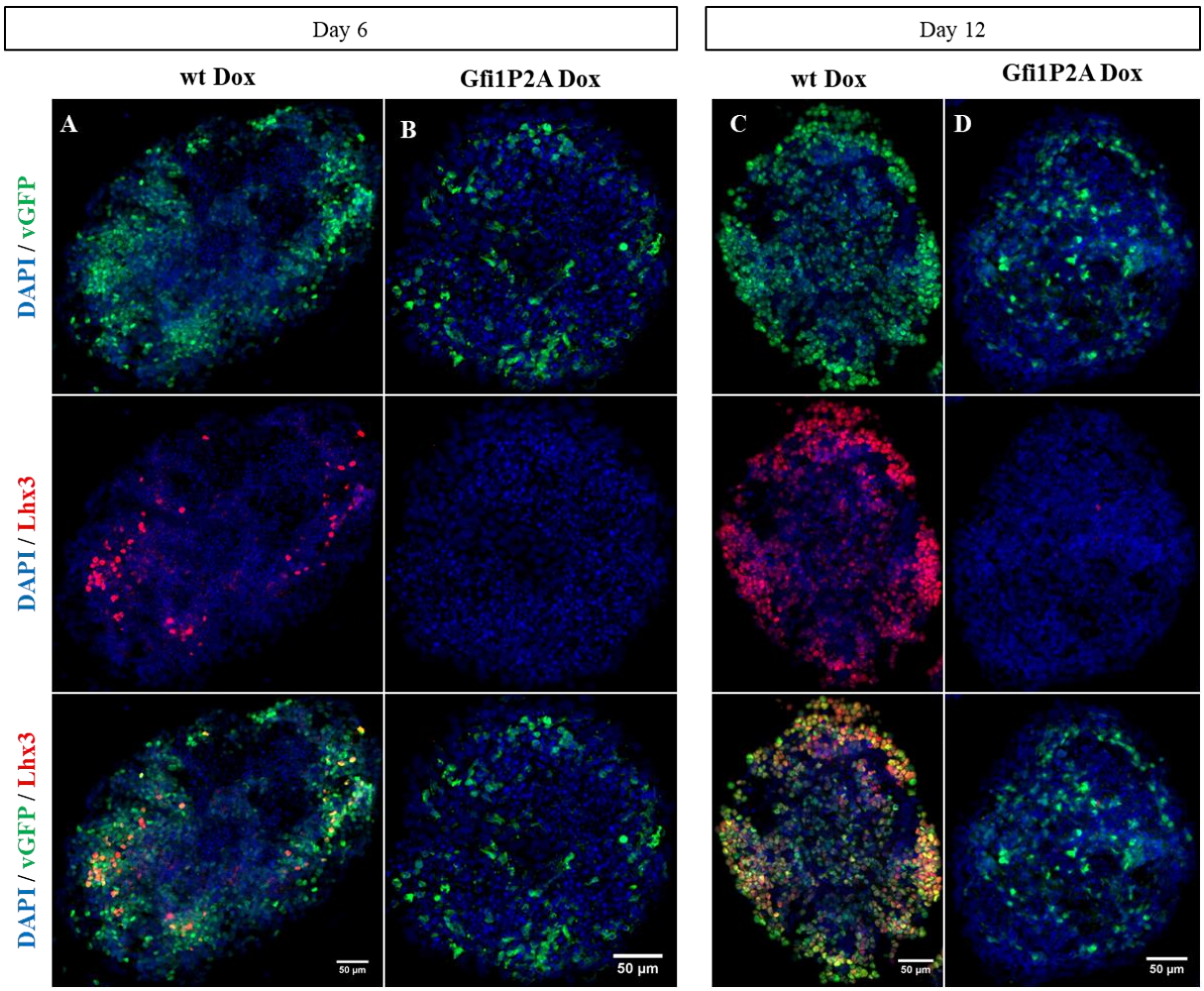

Figure 6.15 - Induction of Lhx3 in Gfi1P2A-PA: Representative images of days 6 and 12 of development, obtained from ICC for Lhx3 (red). EBs were treated for 2, 4 and 8 days with Dox in (A, C) wt Dox and (B, D) Gfi1DZF6 Dox. Overexpressing cells were identified with vGFP (green) and nuclei with DAPI (blue). Scale bar set to 50µm.

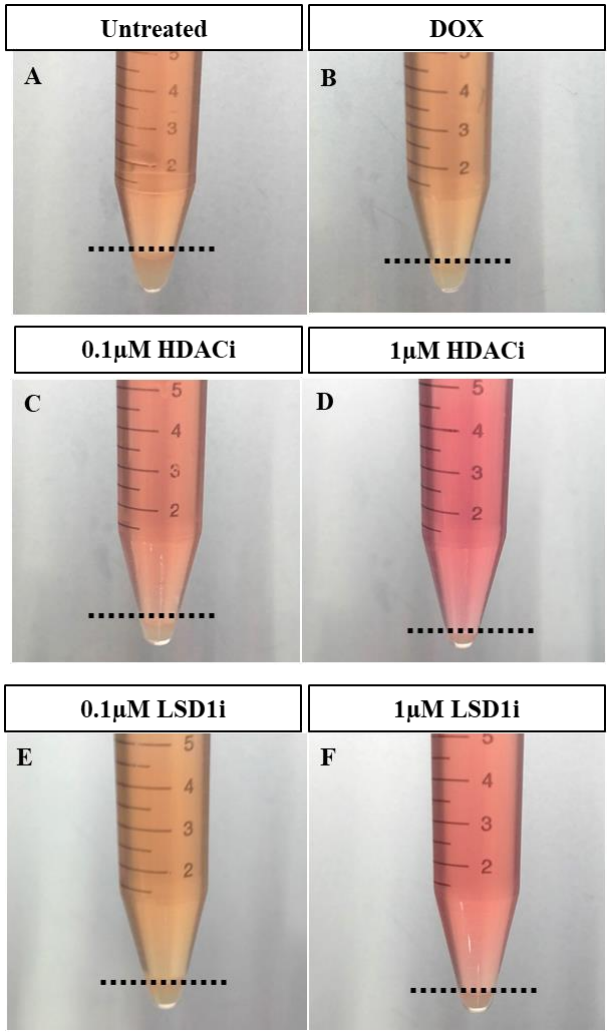

Figure 6.16 – Inhibitors effect on EBs: Representative images of sedimented EBs, marked by the dashed line, after 48h of treatment. (A) Untreated EBs (negative control) . (B) EBs treated with Dox (diluted in DMSO) (positive control). (C) EBs treated with Dox+0.1µM HDACi (diluted in DMSO). (D) EBs treated with Dox+1µM HDACi (diluted in DMSO). (E) EBs treated with Dox+0.1µM LSD1i (diluted in DMSO). (F) EBs treated with Dox+1µM LSD1i (diluted in DMSO). It is visible by the dashed line (top layer of EBs) and media color (towards pink – less concentrated in EBs; towards yellow – more concentrated in EBs) the effect on the number of EBs by adding the chemical inhibitors of HDACs and LSD1.

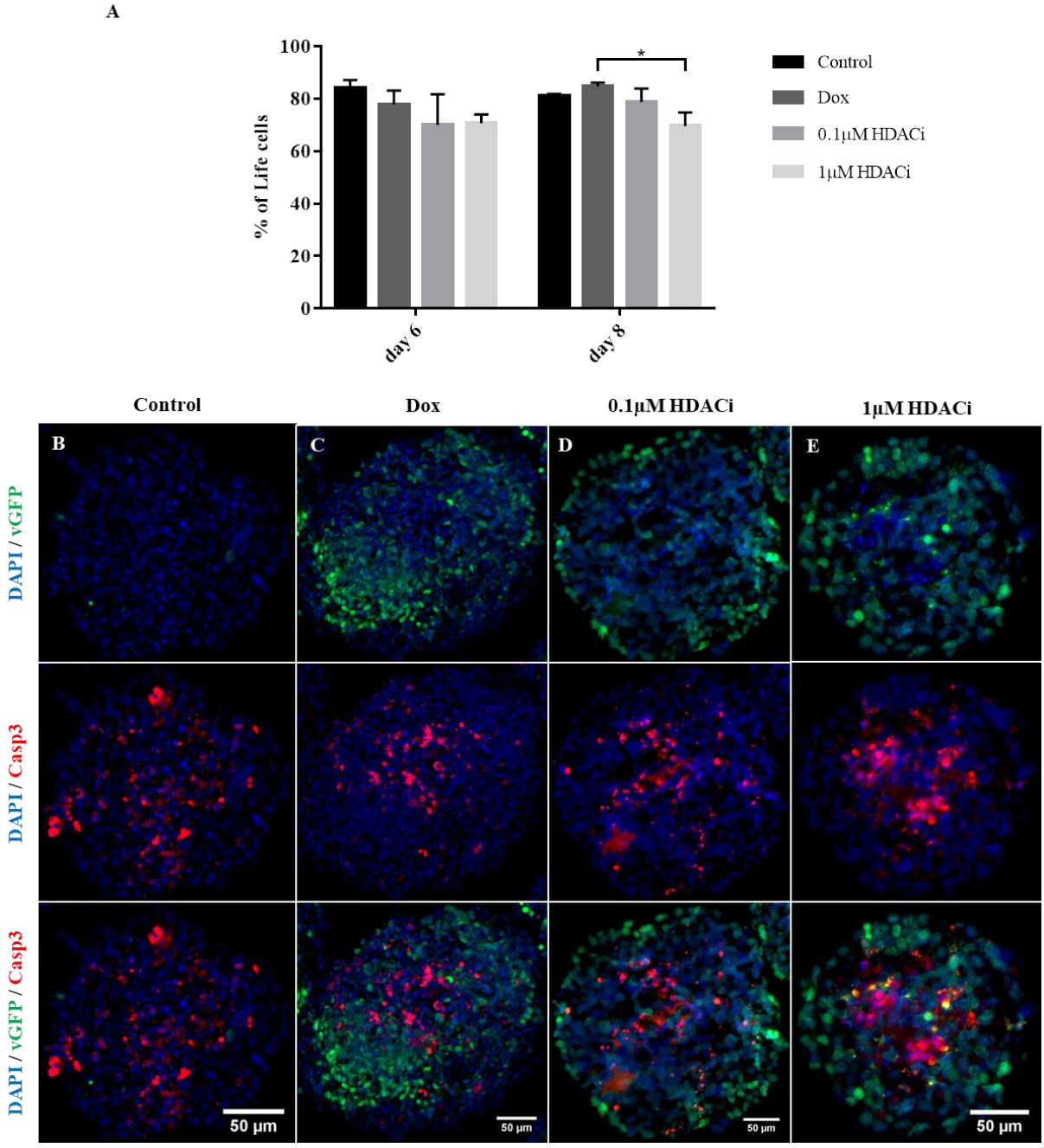

Figure 6.17 - HDACs inhibition on Gfi1's live cells: (A) Bar diagram showing the percentage of live cells obtained by flow cytometry analysis from EBs untreated and EBs treated for 2 and 4 days with Dox, Dox+0.1µM HDACi or Dox+1µM HDACi (diluted in DMSO). Percentage presented as mean±SEM (n=4). Two-way ANOVA was used for statistical analysis (*0.05>P≥0.01). (B, C, D, E) Representative images obtained from ICC for Casp3 (red) in (B) control, (C) Dox, (D) 0.1µM HDACi and (E) 1µM HDACi. Overexpressing cells were identified with vGFP (green) and nuclei with DAPI (blue). Scale bar set to 50µm.

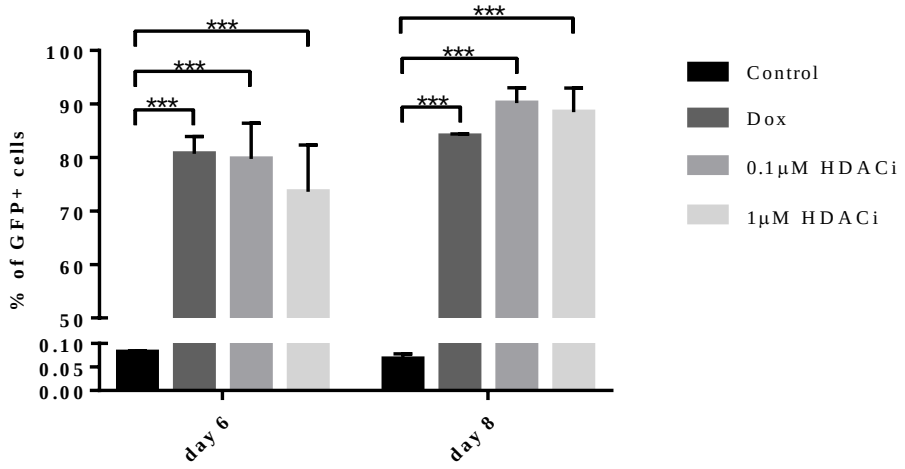

Figure 6.18 - HDACs inhibition on Gfi1's GFP positive cells: Bar diagram showing the percentage of GFP+ cells obtained by flow cytometry analysis from EBs untreated and EBs treated for 2 and 4 days with Dox, Dox+0.1µM HDACi or Dox+1µM HDACi (diluted in DMSO). Percentage presented as mean±SEM (n=4). Two-way ANOVA was used for statistical analysis (***P<0.001).

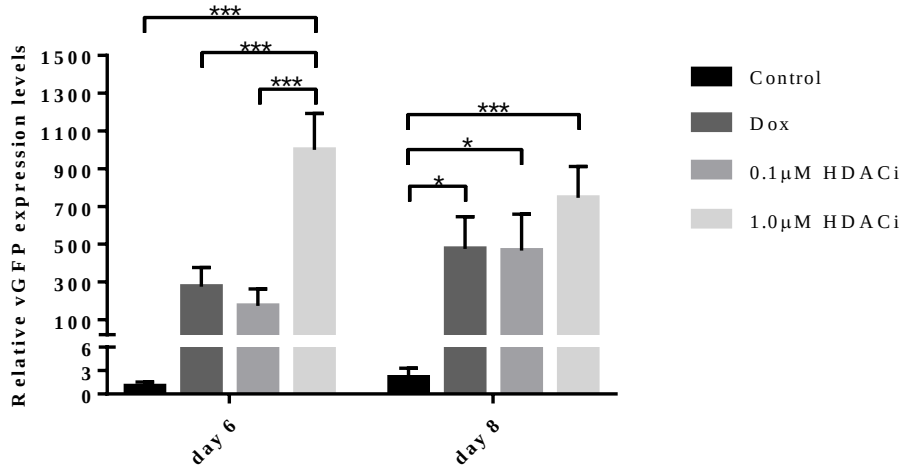

Figure 6.19 - vGFP quantification on Gfi1's HDACs inhibition: Bar diagram showing the relative RNA levels of vGFP in EBs untreated and EBs treated for 2 and 4 days with Dox, Dox+0.1µM HDACi or Dox+1µM HDACi (diluted in DMSO). Relative expression normalized to the mean of untreated EBs at day 6 (set to 1) ±SEM (n=4). Two-way ANOVA was used for statistical analysis (*0.01≤P<0.05; ***P<0.001).

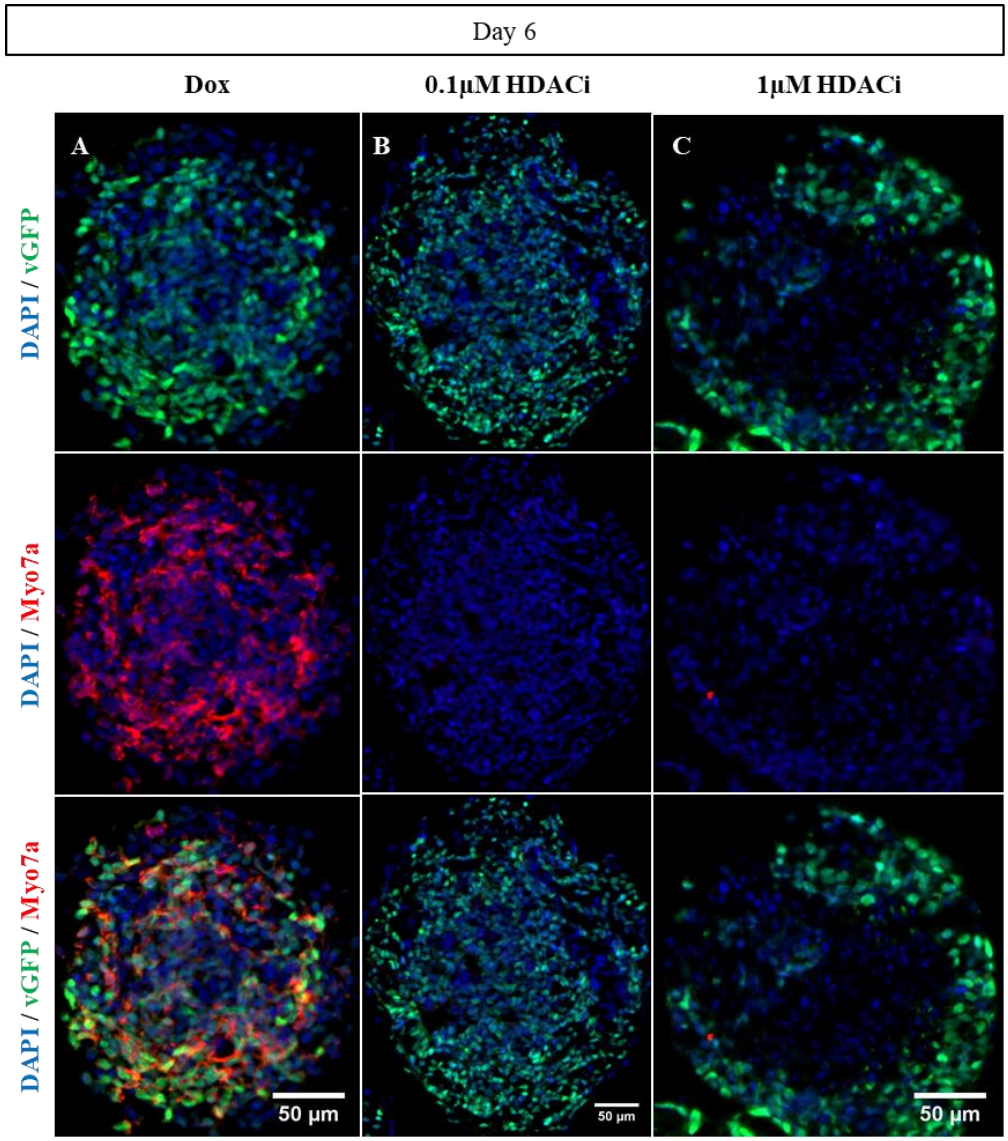

Figure 6.20 - Induction of Myo7a on Gfi1's HDACs inhibition: (A, B, C) Representative images of day 6 of development, obtained from ICC for Myo7a (red). EBs were treated for 2 and 4 days with Dox in (A) wt Dox, (B) Dox+0.1µM HDACi and (C) Dox+1µM HDACi. Overexpressing cells were identified with vGFP (green) and nuclei with DAPI (blue). Scale bar set to 50µm.

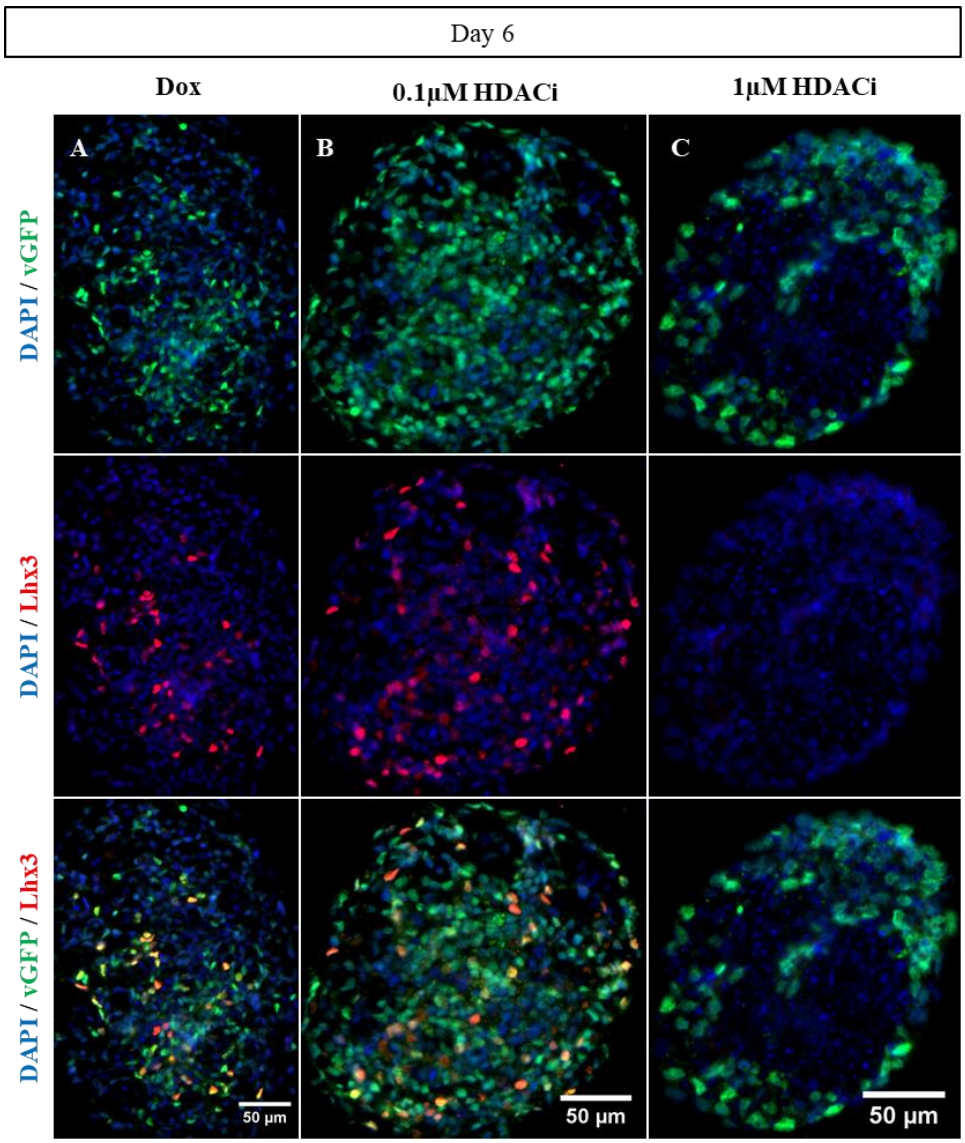

Figure 6.21 - Induction of Lhx3 on Gfi1's HDACs inhibition: (A, B, C) Representative images of day 6 of development, obtained from ICC for Lhx3 (red). EBs were treated for 2 and 4 days with Dox in (A) wt Dox, (B) Dox+0.1µM HDACi and (C) Dox+1µM HDACi. Overexpressing cells were identified with vGFP (green) and nuclei with DAPI (blue). Scale bar set to 50µm.

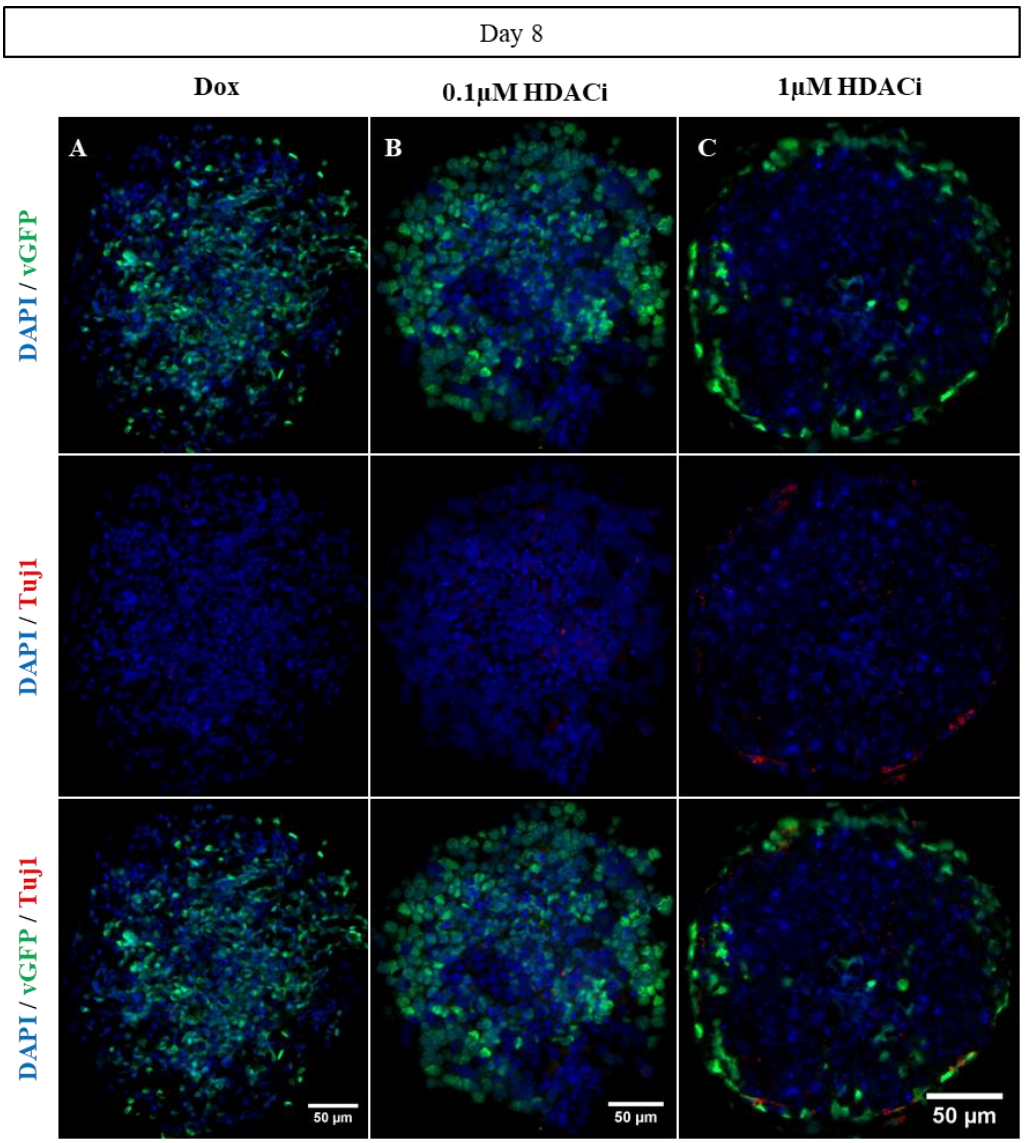

Figure 6.22 - Induction of Tuj1 on Gfi1's HDACs inhibition: (A, B, C) Representative images of day 6 of development, obtained from ICC for Tuj1 (red). EBs were treated for 2 and 4 days with Dox in (A) wt Dox, (B) Dox+0.1µM HDACi and (C) Dox+1µM HDACi. Overexpressing cells were identified with vGFP (green) and nuclei with DAPI (blue). Scale bar set to 50µm.

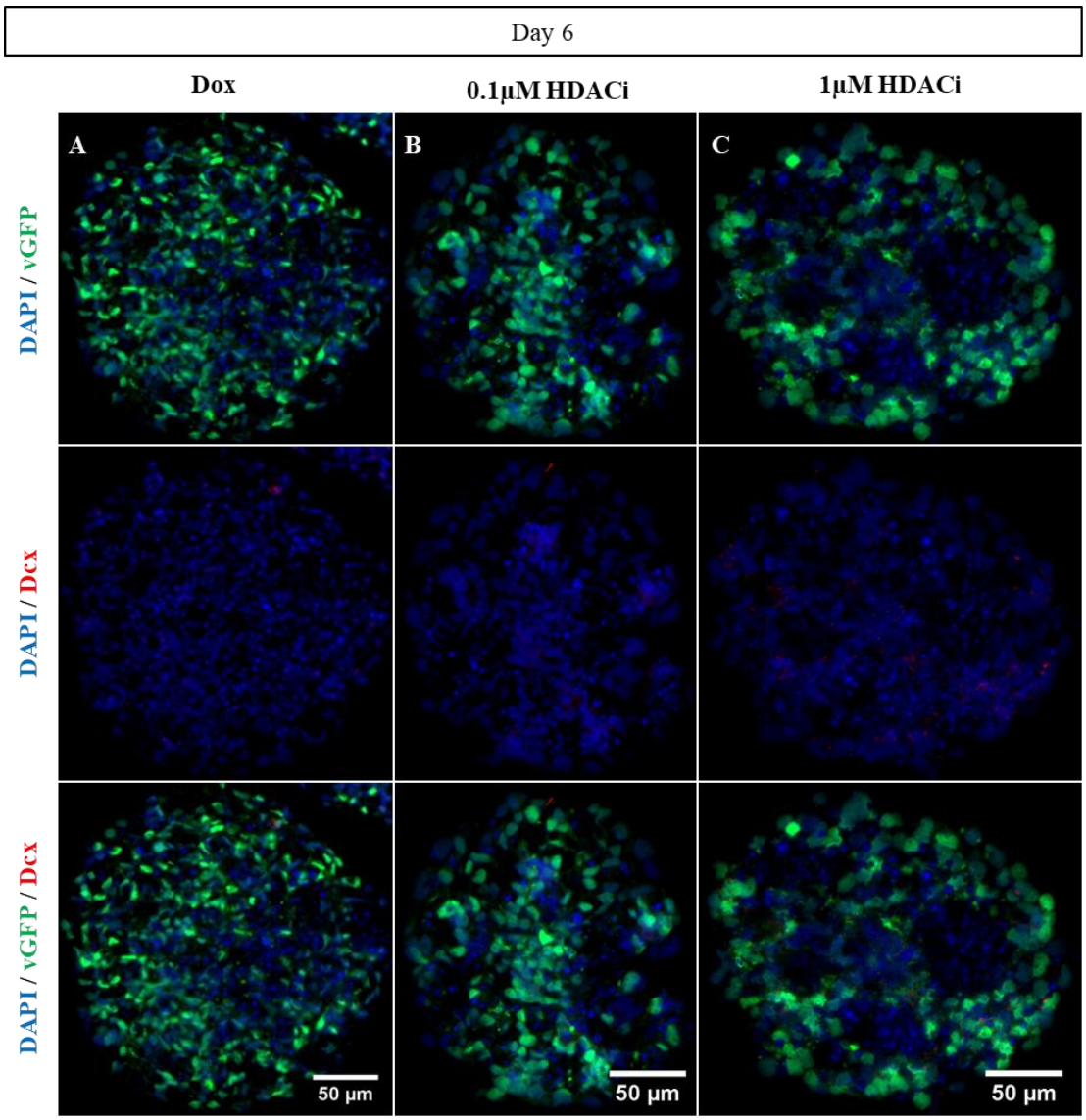

Figure 6.23 - Induction of Dcx on Gfi1's HDACs inhibition: (A, B, C) Representative images of day 6 of development, obtained from ICC for Dcx (red). EBs were treated for 2 and 4 days with Dox in (A) wt Dox, (B) Dox+0.1µM HDACi and (C) Dox+1µM HDACi. Overexpressing cells were identified with vGFP (green) and nuclei with DAPI (blue). Scale bar set to 50µm.

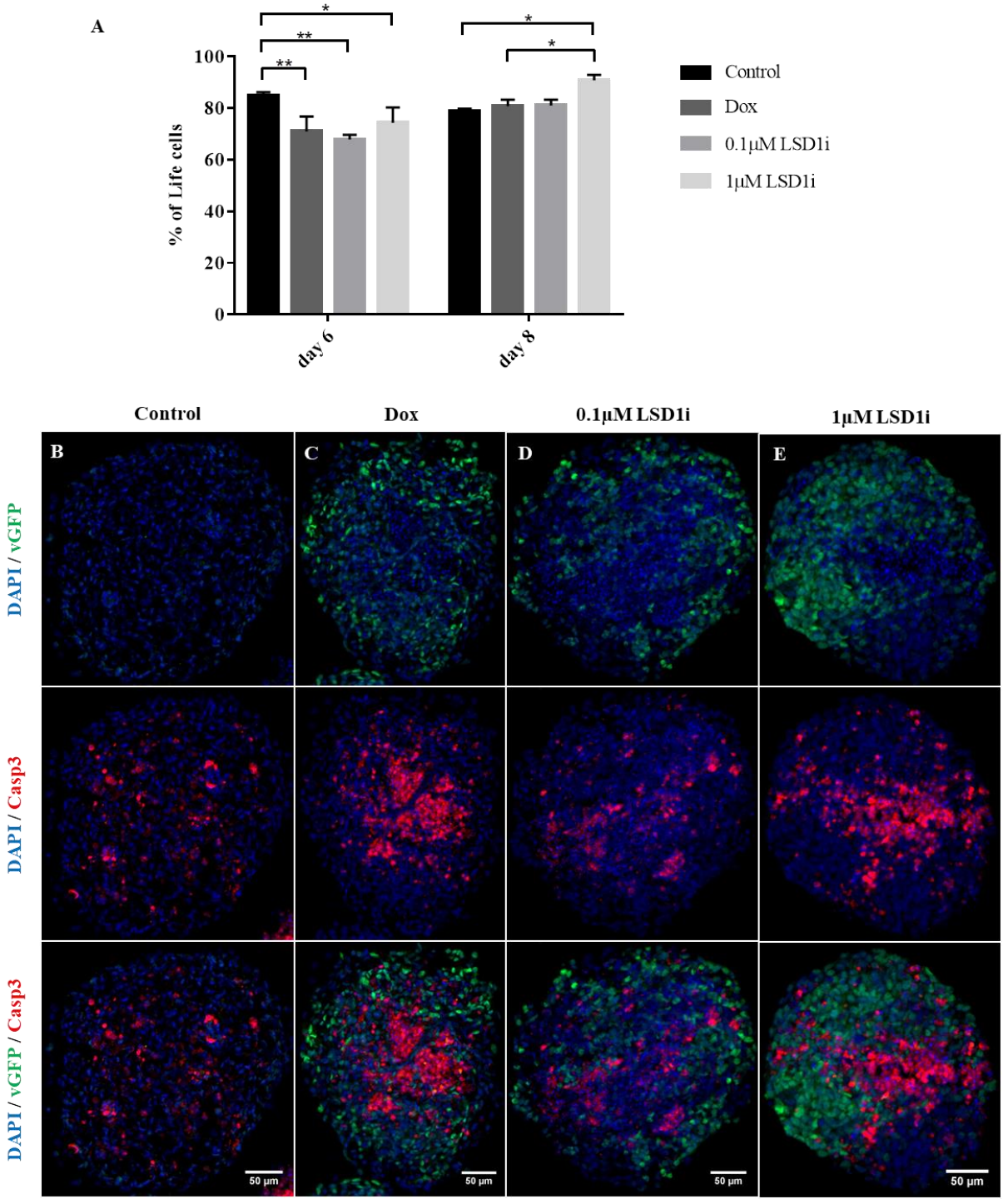

Figure 6.24 - LSD1 inhibition on Gfi1's live cells: (A) Bar diagram showing the percentage of live cells obtained by flow cytometry analysis from EBs untreated and EBs treated for 2 and 4 days with Dox, Dox+0.1µM LSD1i or Dox+1µM LSD1i (diluted in DMSO). Percentage presented as mean±SEM (n=4). Two-way ANOVA was used for statistical analysis (*0.01≤P<0.05; **0.001≤P<0.01). (B, C, D, E) Representative images obtained from ICC for Casp3 (red) in (B) control, (C) Dox, (D) 0.1µM LSD1i and (E) 1µM LSD1i. Overexpressing cells were identified with vGFP (green) and nuclei with DAPI (blue). Scale bar set to 50µm.

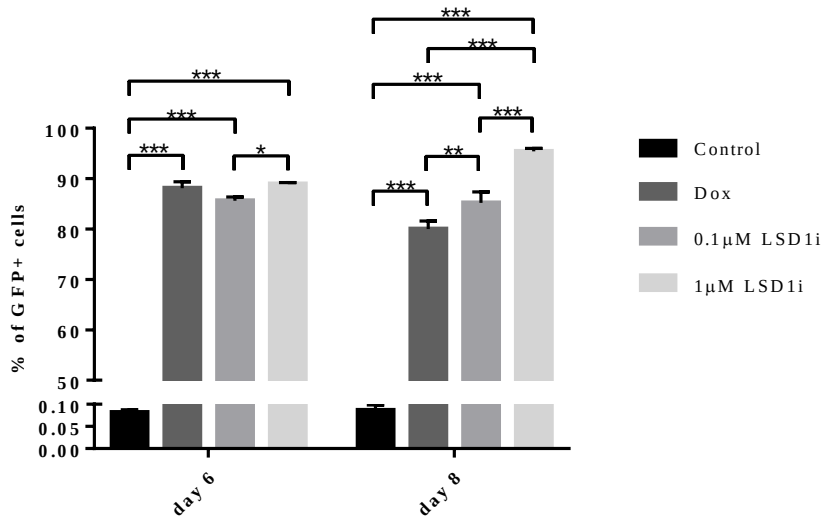

Figure 6.25 - LSD1 inhibition on Gfi1's GFP positive cells: Bar diagram showing the percentage of GFP+ cells obtained by flow cytometry analysis from EBs untreated and EBs treated for 2 and 4 days with Dox, Dox+0.1µM LSD1i or Dox+1µM LSD1i (diluted in DMSO). Percentage presented as mean±SEM (n=4). Two-way ANOVA was used for statistical analysis (*0.01≤P<0.05; **0.001≤P<0.01; ***P<0.001).

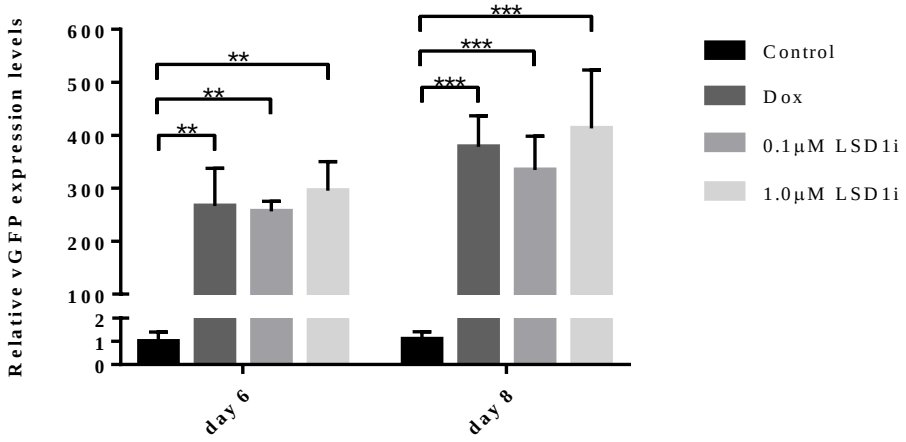

Figure 6.26 - vGFP quantification on Gfi1's LSD1 inhibition: Bar diagram showing the relative RNA levels of vGFP in EBs untreated and EBs treated for 2 and 4 days with Dox, Dox+0.1µM LSD1i or Dox+1µM LSD1i (diluted in DMSO). Relative expression normalized to the mean of untreated EBs at day 6 (set to 1) ±SEM (n=4). Two-way ANOVA was used for statistical analysis (**0.001≤P<0.01; ***P<0.001).

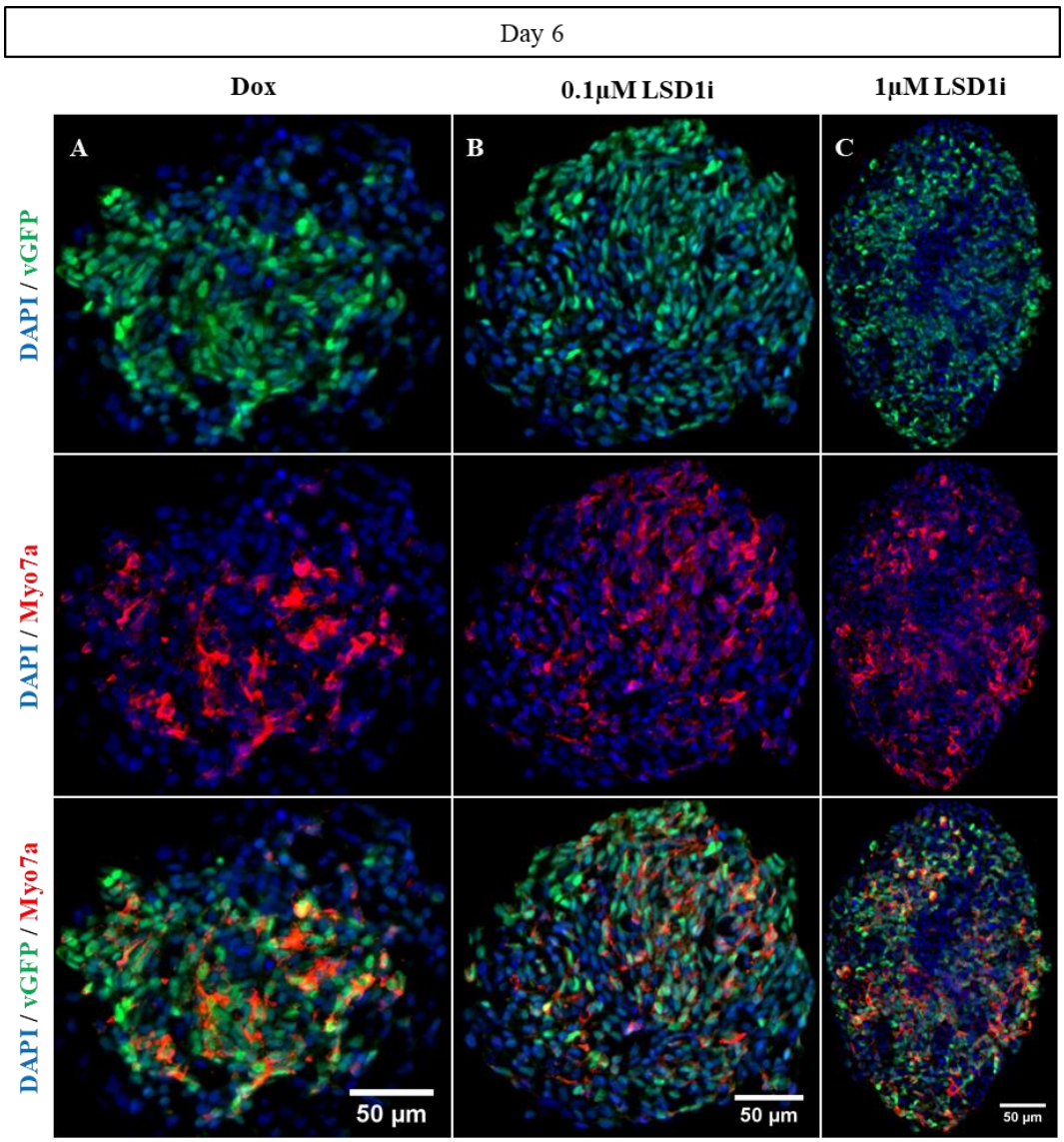

Figure 6.27 - Induction of Myo7a on Gfi1's LSD1 inhibition: (A, B, C) Representative images of day 6 of development, obtained from ICC for Myo7a (red). EBs were treated for 2 and 4 days with Dox in (B) wt Dox, (C) Dox+0.1µM LSD1i and (D) Dox+1µM LSD1i. Overexpressing cells were identified with vGFP (green) and nuclei with DAPI (blue). Scale bar set to 50µm.

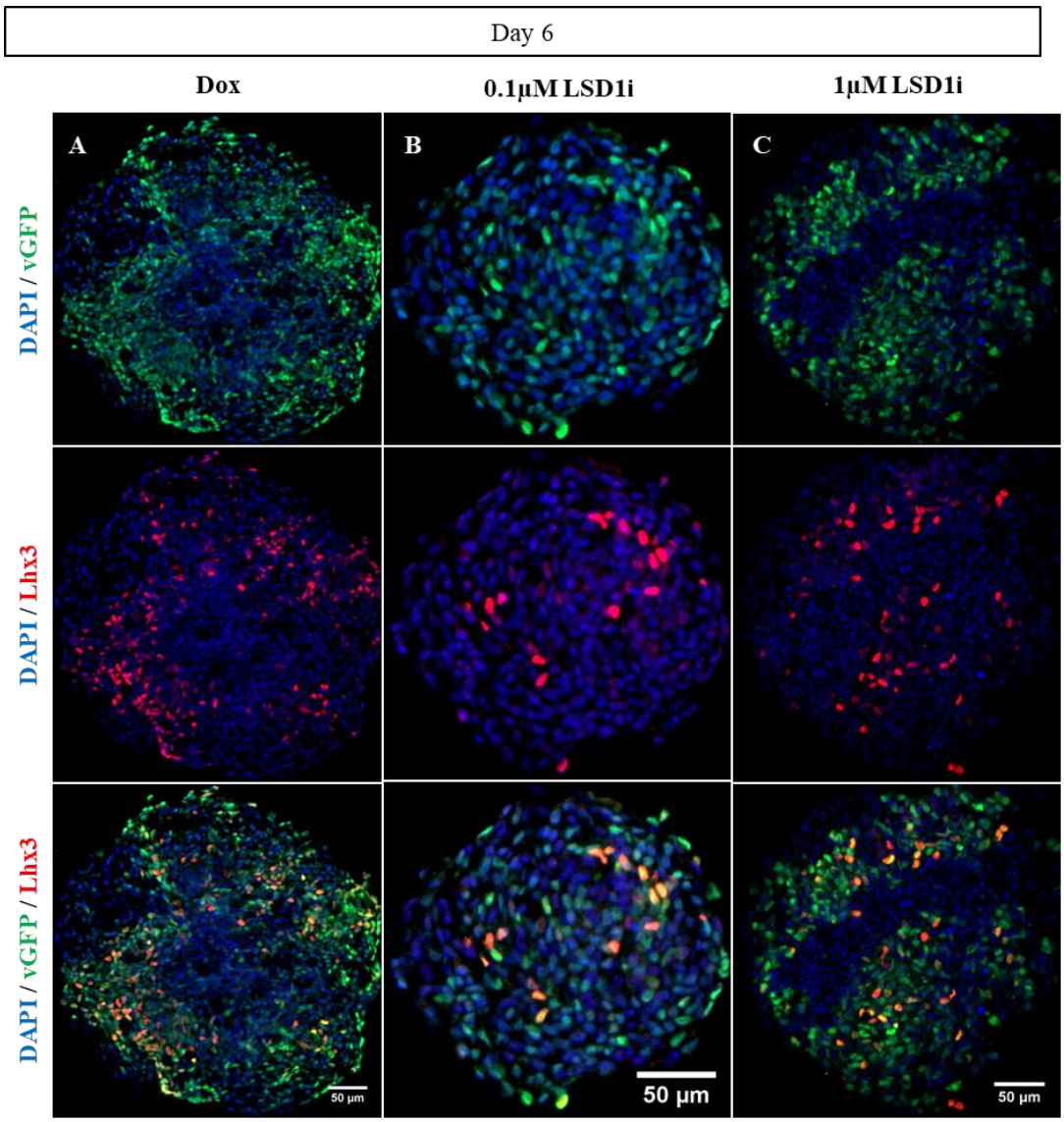

Figure 6.28 - Induction of Lhx3 on Gfi1's LSD1 inhibition: (A, B, C) Representative images of day 6 of development, obtained from ICC for Lhx3 (red). EBs were treated for 2 and 4 days with Dox in (B) wt Dox, (C) Dox+0.1µM LSD1i and (D) Dox+1µM LSD1i. Overexpressing cells were identified with vGFP (green) and nuclei with DAPI (blue). Scale bar set to 50µm.

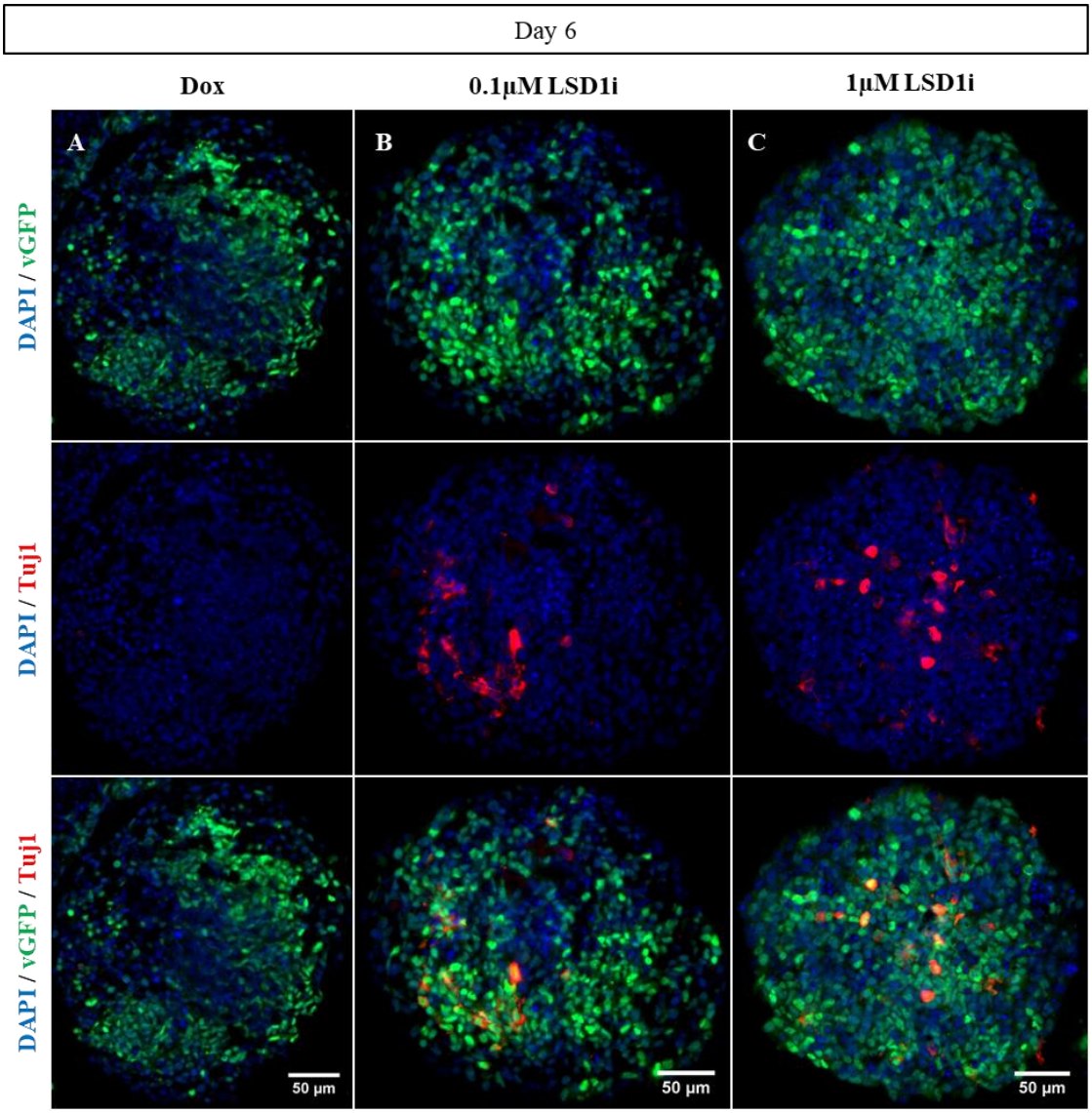

Figure 6.29 - Induction of Tuj1 on Gfi1's LSD1 inhibition: (A, B, C) Representative images of day 6 of development, obtained from ICC for Lhx3 (red). EBs were treated for 2 and 4 days with Dox in (B) wt Dox, (C) Dox+0.1µM LSD1i and (D) Dox+1µM LSD1i. Overexpressing cells were identified with vGFP (green) and nuclei with DAPI (blue). Scale bar set to 50µm.

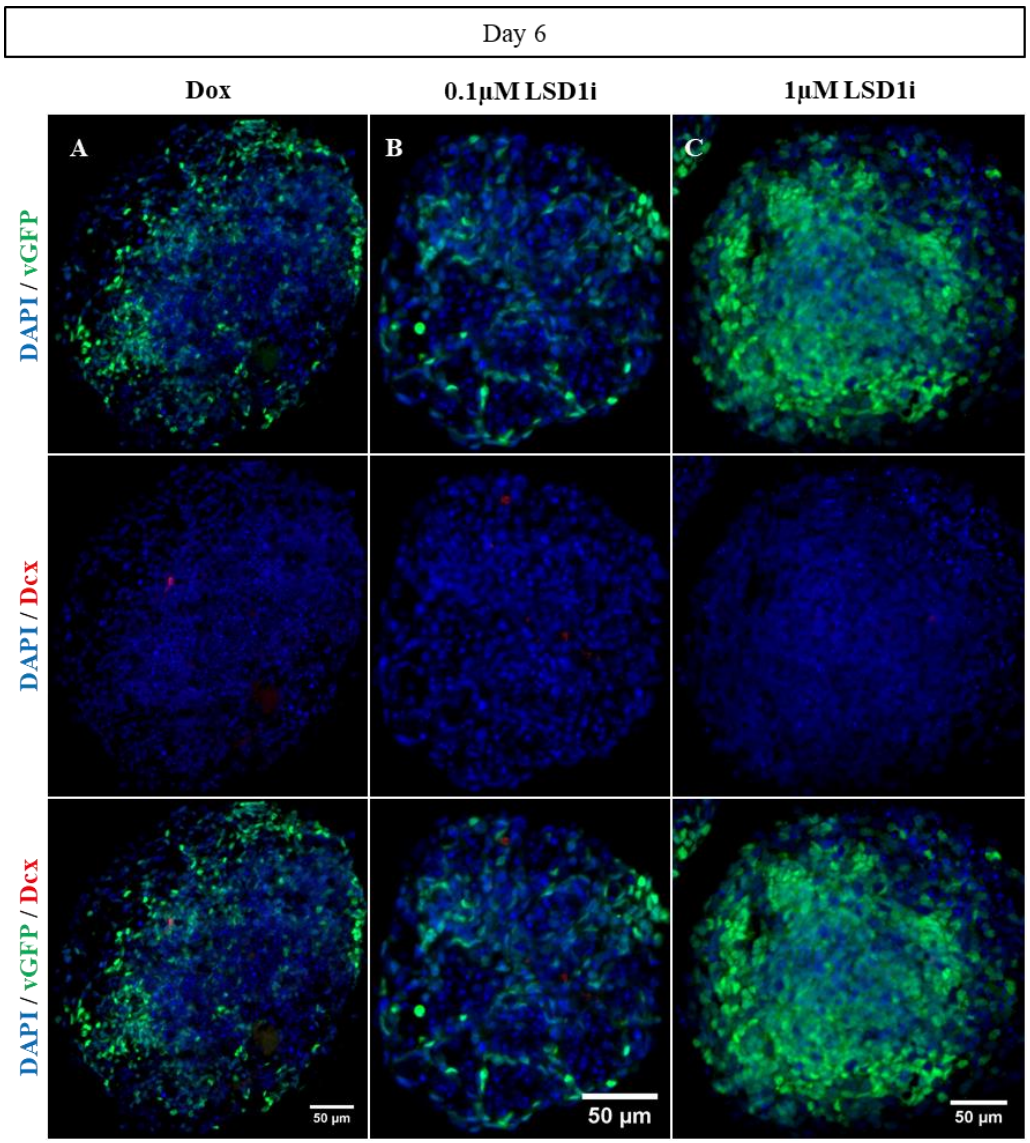

Figure 6.30 - Induction of Dcx on Gfi1's LSD1 inhibition: (A, B, C) Representative images of day 6 of development, obtained from ICC for Dcx (red). EBs were treated for 2 and 4 days with Dox in (B) wt Dox, (C) Dox+0.1µM LSD1i and (D) Dox+1µM LSD1i. Overexpressing cells were identified with vGFP (green) and nuclei with DAPI (blue). Scale bar set to 50µm.